Gersonde, R., Hodell, D.A., Blum, P., et al., 1999
Proceedings of the Ocean Drilling Program, Initial Reports Volume 177

8. Site 1093[1]

Shipboard Scientific Party[2]

BACKGROUND AND OBJECTIVES

Site 1093 (proposed site TSO-6A) is located north of Shona Ridge near the present-day position of the Polar Front (PF) but north of the average winter sea-ice edge (Fig. **F1,** p. 35, in the "Leg Summary" chapter). This area also represents the southernmost extent of North Atlantic Deep Water as it mixes with Circumpolar Deep Water (CDW) and inserts itself into the Antarctic Circumpolar Current (Fig. **F2,** p. 36, in the "Leg Summary" chapter). The water depth of 3626 m places the site within lower CDW. The region is marked by thick, moderately laminated pelagic drift deposits (Tucholke and Embley, 1984) that accumulated at very high sedimentation rates within the circum-Antarctic opal belt (Fig. **F9,** p. 43, in the "Leg Summary" chapter). The high flux of biosiliceous material to the seafloor in this region offers an unprecedented opportunity for the study of climate change at high temporal resolution. Moreover, Site 1093 is located near a sediment trap station (Mooring PF) that has monitored vertical particle fluxes to the seafloor since 1987 (Abelmann and Gersonde, 1991). This region is also known for laminated diatom mats that accumulated rapidly at very high sedimentation rates and may be important for studying past changes in the budget of dissolved silica in the global ocean. At Site 1093 cores were recovered for the first time from the circum-Antarctic opal belt using modern techniques (i.e., multiple advanced hydraulic piston corer [APC] holes and construction of a composite section).

A multichannel seismic line (AWI94090) shot across Site 1093 during *Polarstern* Cruise ANT-XI/3 shows a thick sequence of acoustically laminated sediments (Figs. **F1, F2**). Acoustic basement is estimated at 1100 meters below seafloor (mbsf) on the basis of interval velocities (Table **T1**). Basement is very smooth in the region of Site 1093 and may have formed by lava flows from the Shona Hotspot, which is

F1. Track line and shotpoints for the site surveys of Site 1093, **p. 24.**

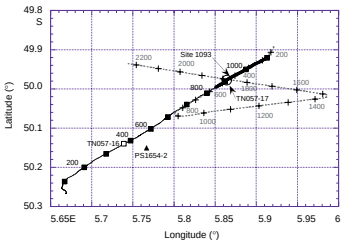

F2. Seismic line showing the location and penetration depth of Holes 1093A–1093D, **p. 25.**

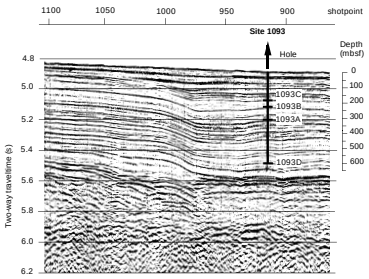

T1. Velocities used for stacking of multichannel seismic data, **p. 66.**

[1]**Examples of how to reference the whole or part of this volume.**
[2]**Shipboard Scientific Party addresses.**

Ms 177IR-108

presently thought to reside between 50° and 52.5°S near an anomalously shallow segment of the Mid-Atlantic Ridge (Hartnady and le Roex, 1985; Douglass et al., 1995). Sediment cores PS1654-2 and TTN057-17-PC1, recovered during two site-survey cruises with a piston corer near Site 1093 (Fig. F1), consist of upper Quaternary diatom ooze and diatom mud that were deposited at very high sedimentation rates (800 m/m.y.) during the Holocene. These rates decreased greatly, however, during glacial periods, when diatoms indicate that this region was covered by sea ice. Foraminifers are present throughout the cores and will be used to establish stable isotopic stratigraphies.

The drilling strategy at Site 1093 was to recover the entire Pleistocene section to the depth of APC refusal and to drill a single deep hole to obtain the older, upper Cenozoic sedimentary record. Specific objectives include the study of (1) the evolution of surface-water masses and the PF, (2) sea-ice distribution in the Southern Ocean, (3) paleoproductivity changes (e.g., biogenic silica, organic carbon export rates) and the history of the circum-Antarctic opal belt, (4) deep-water circulation including changes in the physical and chemical properties of CDW, and (5) silica diagenesis (see also "Site 1094" chapter).

Site 1093 forms part of a north-south transect of sections at 41°S (Site 1089), 47°S (Site 1091), 50°S (Site 1093), and 53°S (Site 1094) that accumulated at sedimentation rates exceeding 100 m/m.y. during the late Pliocene–Pleistocene (Fig. F15, p. 49, in the "Leg Summary" chapter). These sites will be used to reconstruct past movements of the PF and Antarctic sea-ice field and will permit correlation of millennial scale climate oscillations recorded in the marine sediments of the Southern Ocean with climate signals in ice cores from Greenland and Antarctica.

OPERATIONS

Winds were light to moderate for the 220-nmi transit to Site 1093 on the northern flank of Shona Ridge. Winds changed direction from northwesterly to southwesterly during the morning of 10 January. Thus, although the second half of the transit was slower, an average speed of 9.9 kt was achieved. The drill site was approached by Global Positioning System coordinates, and a beacon was launched at 1624 hr on 10 January.

Hole 1093A

Hole 1093A was spudded with a seafloor APC core at 2355 hr on 10 January. An 8.5-m core set the seafloor depth at 3635.0 meters below rig floor (mbrf). Continuous cores were taken with orientation beginning with Core 177-1093A-4H. Measurements with the APC temperature (APCT) tool started with Core 4H and continued through Core 16H. Core recovery was excellent, with an average of 103% achieved through APC refusal. Withdrawal of the corer required 50–60 kips beginning with Core 23H. Cores 25H and 26H failed to stroke completely in the stiffening sediments, and a severe plastic liner failure necessitated pumping Core 25H from the inner core barrel. These failures were considered to signal effective refusal depth for the APC, and coring switched to the extended core barrel (XCB) mode.

The first three XCB cores recovered low-quality core with only 38% recovery. At the request of the scientific party, an additional APC core was attempted that had incomplete stroke and recovered 3.9 m of core

of partly excellent and partly poor quality and a broken liner. An additional four XCB attempts recovered only pebbles of ice-rafted debris (IRD) in the core catchers (CCs). Though weather and motion conditions were deteriorating at the time, the inability to recover core was attributed to the properties of the diatom sediment. Coring attempts were abandoned at 309.4 mbsf after Core 34X. The bit was pulled clear of the seafloor at 1245 hr on 12 January.

Hole 1093B

In an attempt to recover the seafloor interface, the bit was positioned 4 m higher for the new spud than it had been for Core 177-1093A-1H. The first coring attempt produced no sediment, and only plastic fragments from a break at the top of the core liner were found in the CC. A second coring attempt from 9.5 m deeper recovered 7.1 m of sediment and was designated Core 1H (subsequent hole-to-hole correlation revealed that several meters apparently had been penetrated and lost from the first core barrel.)

Vessel heave, which continued to build after the earlier strong winds, died off and reached 11 ft around the time of spudding. It decreased as coring continued, however, and good results again were achieved in favorable operating conditions. Cores were oriented beginning with Core 4H. APC refusal was declared when Core 24H failed to achieve complete stroke, and the drill string was raised for the third hole.

Hole 1093C

To ensure a stratigraphic overlap, the mudline APC core was shot from 2 m deeper than the initial attempt at Hole 1093B. Again, only a trace of the soft seafloor sediment was recovered, and the interface was missed. The second core recovered 8.0 m of sediment and was designated Core 1H. Core orientation began with Core 3H.

Routine inspection of the aft coring line revealed several broken wires just above the ropesocket. The line was removed from service for reheading. During the attempt to put the forward sinker bar into the drill string, the upper wraps of line on the winch drum became fouled because the spooling of the wire was excessively loose. Efforts to correct the situation resulted in a severe kink in the wire. It was then necessary to cut and rehead the aft wire and put it back into service. A loss of 1.5 hr of operating time resulted.

Winds were light, but a moderate swell persisted as continuous cores were taken over the interval covered by the preceding two holes. The swell built rapidly in the early morning hours of 14 January and was joined by a large cross swell. Vessel heave increased to as much as 12 ft and core recovery and quality dropped concurrently. Average recovery for Cores 13H–18H was 42%. A knobby drilling joint was picked up for Core 18H, and the situation was evaluated as the operational roll limit was reached and pitch and heave limits were approached. At 169.5 mbsf, coring operations were terminated and the drill string was pulled above the seafloor to wait out the swell and weather conditions, which continued to deteriorate. Knobby drilling joints again were located at the top of the drill string to handle bending stresses at the guide horn, and the drill string was hung off with the bit suspended at 3527 mbrf.

Hole 1093D

Swell and weather conditions changed little during the afternoon and night hours, except that the cross swell gradually died out and the amount of vessel roll decreased. One set of swells of 25–30 ft persisted into the morning of 15 January. When the swell height had decreased slightly and roll and pitch were within operating limits, conditions were considered safe for rig-floor personnel to handle pipe. Heave remained too high for successful coring, but operations resumed at 0500 hr, after 15.25 hr of downtime, in the hope that conditions would continue to improve. The drill string was run back to the seafloor and Hole 1093D was spudded at 0640 hr. The hole was drilled to 136 mbsf, where continuous oriented APC coring began.

Vessel heave continued to have an adverse effect on core recovery into the afternoon of the first day. Recovery improved with environmental conditions, only to decrease as an incomplete stroke occurred with Core 12H at ~245 mbsf. Because of the inability to recover that material with the XCB system in Hole 1093A, coring continued with the APC and 9.5-m advance between cores through Core 18H (307 mbsf). Core recovery was mostly insignificant and severe liner failures occurred.

The coring mode then was switched to XCB and recovery was nil, as expected. Only pebbles of ice-rafted material were retained in the CCs of the next three cores. As the seismic record and drilling parameters suggested that a different, softer sedimentary unit might have been reached, another APC core (Core 22H) was attempted. An additional 1.2 m of soft sediment was recovered from 329 mbsf, which was sufficient for age dating. XCB coring continued, without recovery, through Core 26X. During that period, recurrent high circulating pressures indicated that jets in the main bit were becoming plugged with the small pebbles that were plentiful at the bottom of the hole (as evidenced by recovery on the top of each core). Most of the jets apparently were cleared by pumping core barrel 27X into place at a very high rate (100 strokes per minute [spm]), and near-normal circulating pressure was regained. Core 27X recovered 6 m, but a total of only 4.3 m was recovered from the next five cores despite normal operating parameters.

The nature of the sediment then changed to a clay-rich material, and high recovery rates were achieved over the next 70 m to a depth of 492 mbsf. A return to diatom ooze, however, brought the return of recovery problems, and clay-rich streaks were recovered selectively to 557 mbsf with an average recovery of only ~11%. At that depth, streaks of hard material interbedded with softer material were encountered, slowing the rate of penetration sharply with no significant increase in core recovery.

In addition to increasing signs of incomplete hole cleaning, bit plugging problems returned. Extremely high circulating pressure upon the landing of core barrel 49X indicated nearly complete blockage of the bit jet channels. Torque and weight indications also showed about 1.5 m of hard fill in the hole. Pressure was too high to attempt cutting a core and the core barrel was retrieved. A mud pill was pumped, followed by a fresh core barrel at 100 spm. The effort was successful in reducing circulating pressure to an acceptable level and another slow core was cut. The landing of core barrel 50X was a repeat of the previous attempt. The bit again was plugged when the barrel landed. As preparations were being made to retrieve the barrel, partial circulation was regained. Low rate of penetration (ROP) and core recovery had prompted the decision

to terminate coring, but Core 50X was cut while a 50-bbl mud sweep was circulated to clean the hole for logging. The ROP was slightly higher, but only 50 cm of hard cherty mudstone was recovered.

A go-devil was pumped through the drill string to latch open the lockable float valve, and the drill string was pulled to logging depth. No drag was encountered on the up-trip, so a wiper trip was not considered necessary. Knobby joints were picked up, and the bit was placed at 3722 mbrf for the logging operation.

The triple combination logging tool was the first deployed. The tool went to within 7.5 m of total depth (TD) after meeting minor resistance in the upper section of the hole. Weather and sea conditions were excellent, and a technically valid log was recorded. Its quality and usefulness were degraded by the large, washed-out hole diameter and extremely high porosity of the sediments.

The second logging run was made with the geological high-sensitivity magnetic tool (GHMT) string. The light-weight tool reached 581 mbsf, and a good magnetic susceptibility log was obtained over the entire hole interval. Because of the unfavorable hole conditions, the planned Formation MicroScanner log was not run. Logging operations were completed and the wireline sheaves rigged down by 2145 hr on 18 January.

The knobby joints were laid down, and the drill string was pulled clear of the seafloor for the final coring attempts at the site.

Hole 1093E

An additional attempt to obtain a seafloor interface core had been requested, as the uppermost sediments apparently had not yet been recovered at the site. The vessel was offset back to the coordinates of Hole 1093B, and the bit was positioned at 3629.5 mbrf. As vessel motion conditions were minimal, a single APC shearpin was used to reduce the impact of actuation. The APC appeared to fire at a relatively low pressure, as expected, but was recovered with the shearpin intact. The APC assembly was sent down for a second attempt at the same depth. Again there was difficulty in actuating the APC, with anomalous pressure indications. The corer was recovered in the stroked out condition, but with a broken liner and no trace of sediment (a "water core"), indicating a seafloor depth below 3639 mbrf and well below the 3635 mbrf indicated by Core 177-1093A-1H. A third attempt was made from 4 m deeper. The results were a broken core liner and traces of mud on the CC. Efforts to recover a mudline core were abandoned.

Hole 1093E was then officially spudded as the bit was "washed" to 4 m below the apparent seafloor depth of Hole 1093A, and an APC core was taken to fill a gap in the composite section of the site. A split liner with 6.6 m of sediment was recovered. After an additional washdown to 33 mbsf, a second core was taken to fill another gap and to end the coring program at Hole 1093E. During recovery of the core, the coring line was coated for preservation, as the remaining site was in much shallower water. Core recovery was only 5.0 m, and the liner again had failed.

The drill string was pulled above the seafloor and preparations began for a scheduled slip and cut of the drilling line.

Hole 1093F

Review of the coring results by the scientific party resulted in concerns that a gap still existed in the section, but this could not be con-

firmed without results from the multisensor track (MST) core logging. The rig operation was halted for half an hour while it was confirmed that one additional core was needed.

Hole 1093F was spudded at 0640 hr on 19 January and was drilled to 34 mbsf (inferred from Hole 1093A). A final APC core was shot from that depth and 6.2 m of sediment was recovered. The coring line was coated again on the retrieval trip.

When the bit had been pulled to ~75 m above the seafloor, the cut-and-slip operation was completed. During the ensuing pipe trip, both wind and swell had increased greatly, and most of the trip was made in steady rain with a windchill factor of 8°F. The *JOIDES Resolution* departed the site at 1800 hr on 19 January.

LITHOSTRATIGRAPHY

Overview

Site 1093 was drilled to a TD of 597.7 mbsf, corresponding to 623.8 meters composite depth (mcd). The recovered sediments are diatom-rich pelagic deposits of Quaternary (0–1.8 Ma) to early Pliocene (~3.6 Ma) age, and late Miocene (~6–7 Ma) mud rocks and diatomites in the two deepest cores of Hole 1093D, below a hiatus at 563.9 mbsf (590 mcd). The Pliocene/Pleistocene boundary is probably also marked by a hiatus (434.40 mbsf, 460.51 mcd) representing a gap of ~200 k.y. The thick Quaternary section was deposited at extremely high average sedimentation rates of ~250 m/m.y. A distinctive feature of the diatom-rich Quaternary sediments are intervals of *Thalassiothrix* diatom mats up to several meters thick, which also appear in sediment cores of Site 1091 located further north in the northern part of the circum-Antarctic opal belt. The probable Pliocene/Pleistocene hiatus is associated with a downhole increase in relative mud content deposited under lower sedimentation rates of 80 m/m.y.

Two lithostratigraphic units are present. The upper unit was further subdivided into two subunits (Fig. **F3**), on the basis of downhole compositional variations and the degree of sediment consolidation. Lithostratigraphic units and subunits are in accordance with chronostratigraphic subdivisions. Lithostratigraphic Subunit IA (Holocene–Pleistocene) consists of diatom ooze with varying proportions of mud, foraminifers, and nannofossils. Subunit IB (Pliocene) is represented by consolidated muddy diatom ooze, including several carbonate-rich intervals and few unconsolidated diatom ooze layers. Diatomites and mud rocks constitute lithostratigraphic Unit II (Miocene).

Diatoms are the most prominent sedimentary component of this site with varying abundances of foraminifers, nannofossils, and siliciclastic mud. Radiolarians and silicoflagellates are present in trace amounts. A minor but ubiquitous component is dispersed sand- to gravel-sized siliciclastic material, mainly of volcanogenic origin, that probably represents IRD.

Sediment composition was estimated from smear-slide analysis (see **"Site 1093 Smear Slides,"** p. 116). In addition, weight proportions of carbonate, opal, and siliciclastics were inferred from coulometric bulk carbonate determination (see **"Geochemistry,"** p. 15) and by quantitative X-ray diffraction (XRD) analysis of opal concentrations in the carbonate-free fraction (Table **T2**, also in ASCII format in the **TABLES** directory). Downhole compositional variations deduced from visual

F3. Lithologic summary of Site 1093, **p. 26.**

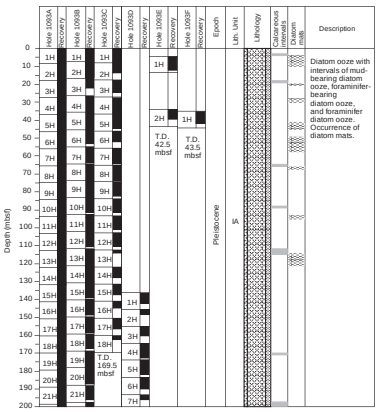

T2. X-ray diffraction data for Site 1093, **p. 67.**

smear-slide analysis do not correlate well with compositional data obtained from coulometry and XRD measurements (Fig. F4). Total carbonate concentrations in smear slides are usually 10%–20% higher than weight percentages of carbonate determined by coulometry, but relative downhole carbonate variations are in good agreement. Concentrations of siliciclastics in smear slides are generally underestimated because the fine-grained mud particles are often masked by larger biogenic particles. Hence, fluctuations of opal and siliciclastics are not well represented by smear-slide data. For the description of the lithostratigraphic units we refer to compositional data inferred from coulometry and XRD (given in average values ± standard deviations).

Recovery in Holes 1093A–1093C was good and penetrated the upper 200 to 250 m of the Quaternary sediments (Fig. F3). Recovery in the deeper interval of Hole 1093D between 250 and 420 mbsf was low to nil, probably because of problems associated with coring extensive diatom-mat sequences. An almost complete recovery marks the upper Pliocene interval between 430 and 500 mbsf. Recovery was low again in the lowermost part of Hole 1093D, yielding only remnants of lower Pliocene and uppermost Miocene mud rocks and diatomites. Holes 1093E and 1093F were drilled to fill recovery gaps in Holes 1093A, 1093B, and 1093C.

F4. Carbonate, opal, and siliciclastic contents at Site 1093, p. 29.

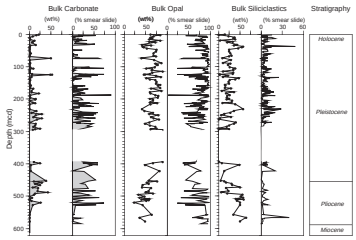

Description of Lithostratigraphic Units

Unit I

Subunit IA

Intervals: 177-1093A-1H through 34X (0–309.4 mbsf; 0–330.24 mcd); 177-1093B-1H through 24H (0–221.8 mbsf; 5.28–252.11 mcd); 177-1093C-1H through 18H (0–169.5 mbsf; 7.06–196.49 mcd); 177-1093D-1H through 34X (136.0–434.4 mbsf; 152.49–460.51 mcd); 177-1093E-1H through 2H (4.0–42.5 mbsf; 4.59–48.98 mcd); 177-1093F-1H (34.0–43.5 mbsf; 36.92–46.42 mcd). Note: 0–136.0 mbsf in Hole 1093D, 0–4.0 mbsf in Hole 1093E, and 0–34.0 mbsf in Hole 1093F were drilled ("washed") without coring.

Age: Holocene to Pleistocene

Subunit IA consists of diatom-rich sediments and is made up of alternations of four sediment types: (1) dark olive mud-bearing diatom ooze, (2) olive foraminifer-bearing diatom ooze, (3) olive gray or tan to pale tan diatom ooze (diatom mats), and (4) pale gray foraminifer diatom ooze. Subunit IA comprises the upper 460.51 mcd and extends down to the Pliocene/Pleistocene hiatus. Total carbonate concentrations vary between 0 and 53 wt%, opal averages 66 ± 13 wt%, and siliciclastics average 18 ± 12 wt%. Porcellanite fragments were found in the top sections of Cores 177-1093D-28X, 46X, and 50X. However, they are probably not in place and indicate the presence of porcellanite horizons higher in the section.

Downhole distribution patterns of sediment types were used for interhole correlations (Fig. F5). Dark olive mud-bearing diatom ooze contains 1 ± 1 wt% carbonate, 67 ± 12 wt% opal, and 32 ± 13 wt% siliciclastics. These relatively mud-rich sediments also contain high relative concentrations of IRD that mainly consists of volcanic particles including basalt and dolerite, brownish green glass shards, pumice, lappilli tuff, and welded ash fragments. Volcanic clasts consisting of feldspar and pyrox-

F5. Core correlation diagram for Site 1093, p. 30.

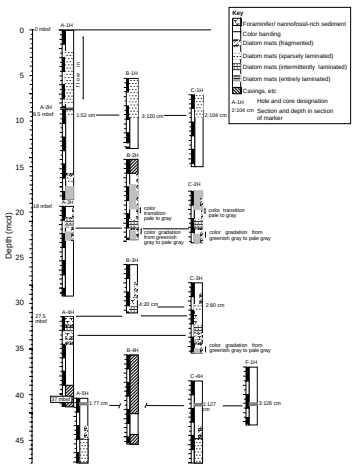

ene phenocrysts, together with garnet grains embedded in a hyaline ground mass, were also identified. Other subordinate IRD components are quartz grains, gneiss fragments, and metaquartzites. In Section 177-1093C-11H-5, a 30-cm-thick residual layer of gritty IRD was encountered (Fig. F6).

The mud-bearing diatom ooze is overlain either by foraminifer-bearing diatom ooze with 9 ± 3 wt% carbonate, 67 ± 3 wt% opal, and 24 ± 13 wt% siliciclastics, or by diatom mats. The average composition of the diatom mats is 10 ± 7 wt% carbonate, 73 ± 10 wt% opal, and 14 ± 10 wt% siliciclastics. The diatom mats include the highest opal contents of the four different sedimentary types, are characterized by a rough spongy surface texture that was observed after scraping the split cores (Fig. F7), and show sparsely to well-developed color laminations and mottles (Fig. F8). They often contain a near-monospecific diatom assemblage of *Thalassiothrix* sp. Individual intervals of diatom mats range between 1 and 10 m in thickness and are widely distributed in the upper 120 m of lithostratigraphic Subunit IA. Another dense cluster of *Thalassiothrix* sp. diatom mats appears between 200 and 300 mcd and probably below 300 mcd, throughout the remaining lower part of Subunit IA. These mats likely caused technical problems in core recovery.

In many core intervals the diatom mats grade into pale gray foraminifer diatom ooze that also contains minor quantities of nannofossils. The average composition is 29 ± 12 wt% carbonate, 57 ± 10 wt% opal, and 14 ± 10 wt% siliciclastics. The carbonate-rich units rarely exceed thicknesses >1 m and become more common below 100 mcd. Diatom mats and foraminifer-bearing diatom ooze are usually thinner above the carbonate-rich sediments than in the intervals below the carbonate-rich sediments and grade upward into olive mud-bearing diatom ooze.

Subunit IB

Intervals: 177-1093D-34X through 47X (434.4–563.5 mbsf; 461.10–589.60 mcd)
Age: late to latest early Pliocene

This subunit consists of mud diatom ooze with highly variable carbonate concentrations between 0 and 60 wt%, average opal concentrations of 43 ± 14 wt%, and high average siliciclastic mud contents of 49 ± 10 wt%. Compared to lithostratigraphic Subunit IA, the sediments of lithostratigraphic Subunit IB, apart from pure diatom ooze layers, show a higher degree of consolidation. Condensed and compacted diatom mats are not abundant but are still present as intercalations (Fig. F9). Because sediment recovery was <20% in the lowermost 60 m of the subunit, we are unable to determine possible lithologic changes in Cores 177-1093D-40X through 47X.

Unit II

Intervals: 177-1093D-49X through 50X (578.4–597.7 mbsf; 604.50–623.80 mcd)
Age: late Miocene

Recovery was poor in lithostratigraphic Unit II below the Pliocene/Miocene hiatus, which represents a time gap of ~3–4 m.y. Only lithified remnants of uppermost Miocene laminated mudrocks and diatomites were recovered in the uppermost sections of Cores 177-1093D-49X and 50X, respectively.

F6. Ice-rafted debris layer (interval 177-1093C-11H-5, 65–110 cm), p. 37.

F7. Diatom mat (interval 177-1093A-4H-2, 10–35 cm), p. 38.

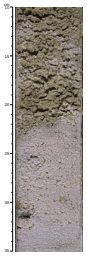

F8. Color-laminated diatom mat (interval 177-1093A-23H-4, 78–120 cm), p. 39.

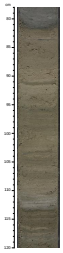

F9. Compacted color-laminated diatom mat (interval 177-1093D-38X-4, 110–136 cm), p. 40.

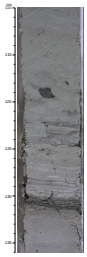

Interpretation

Site 1093 is located in the central circum-Antarctic opal belt and was dominated by high diatom export production with terrigenous background sedimentation through bottom-water current transport, ice rafting, and eolian sediment supply. Assuming that the observed alternations of distinct sedimentary types represent glacial–interglacial cycles, interglacial maxima were characterized by high biogenic carbonate accumulation that was preceded and followed by extensive deposition of diatom mats during interglacial–glacial and glacial–interglacial transitions. Deposition of diatom mats accounts for the high sedimentation rates at this site.

The composition of IRD suggests provenance from the volcanic island provinces of the Scotia Arc and the Bransfield Strait rather than a major supply from Antarctic crystalline rocks. Rare volcanic clasts, including garnet xenoliths that have an earth mantle origin, indicate ice-rafted delivery from regions with hotspot volcanism such as Bouvet Island. However, we have no clear indications of provenance and modes of ice rafting (sea ice vs. icebergs) so far.

Sedimentation rates were lower during the Pliocene. Increased concentration of siliciclastic mud may be the result of a higher supply of terrigenous matter or decreased dilution by biogenic components. Calculation of biogenic and siliciclastic accumulation rates may elucidate the controlling factor after establishing a precise chronostratigraphy.

CHRONOSTRATIGRAPHY

Composite Depths

MST and color reflectance data (650–750 nm) collected from Holes 1093A–1093F were used to determine depth offsets in the composite section. Gamma-ray attenuation (GRA) bulk density and magnetic susceptibility data were collected at 2- to 4-cm intervals on cores recovered from Holes 1093A–1093F. Color reflectance data were collected at 4- to 6-cm intervals on cores from Holes 1093A–1093F (see **"Physical Properties,"** p. 18, for details about these MST and color reflectance data sets).

The composite data show that the cores from Site 1093 provide a continuous overlap to 252 mcd (base of Core 177-1093D-10H). The data used to construct the composite section and determine core overlaps are presented on a composite depth scale in Figures **F10, F11,** and **F12**. The depth offsets that comprise the composite section for Holes 1093A–1093F are given in Table **T3** (also in ASCII format in the **TABLES** directory).

Stretching and compression of sedimentary features in aligned cores indicate distortion of the cored sequence. Because much of the distortion occurred within individual cores on depth scales of <9 m, it was not possible to align every feature in the MST and color reflectance records accurately by simply adding a constant to the mbsf core depth. Within-core scale changes will require postcruise processing to align smaller sedimentary features. Only after allowing variable adjustments of peaks within each core can an accurate estimate of core gaps be made.

Following construction of the composite depth section for Site 1093, a single spliced record was assembled for the aligned cores within the

F10. Smoothed color reflectance data for Site 1093, **p. 41.**

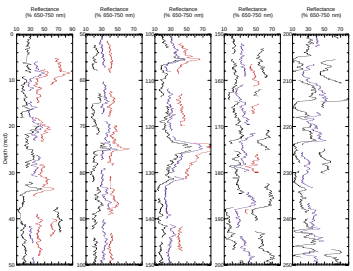

F11. Smoothed magnetic susceptibility data for Site 1093, **p. 42.**

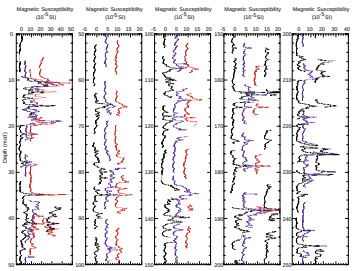

F12. Smoothed GRA bulk density data for Site 1093, **p. 43.**

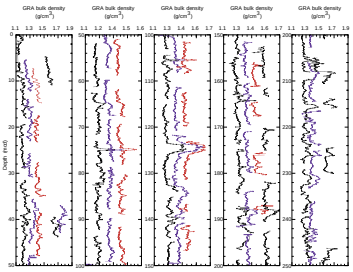

T3. Composite depths for Site 1093, **p. 69.**

upper 252 mcd by using cores from Holes 1093A–1093D and 1093F. The composite depths were aligned so that tie points between adjacent holes occurred at exactly the same depths in mcd. Intervals having significant disturbance or distortion were avoided if possible. The Site 1093 splice (Table T4, also in ASCII format in the TABLES directory) can be used as a sampling guide to recover a single sedimentary sequence between 0 and 252 mcd. Spliced records of magnetic susceptibility, GRA bulk density, and color reflectance are shown in Figure F13.

In the Site 1093 spliced record, there are eight ambiguous tie points. Ambiguities result from either insufficient overlap between adjacent cores (e.g., <1 m), lack of strong features that can be correlated across the overlapping segments of adjacent cores (e.g., diatom-mat intervals), or disagreement in magnetic susceptibility, GRA bulk density, and/or color reflectance data across the spliced interval. We have identified these ambiguous tie points with an asterisk in Table T4.

Biostratigraphy

Calcareous Nannofossils

Sediments recovered from Site 1093 provide a Pliocene–Pleistocene record. Calcareous nannofossils in this interval are abundant to rare and are characterized by low diversities and by medium to poor preservation. Some nannofossil events are poorly defined at this site because several barren intervals occur in the Pliocene–Pleistocene record (Table T5, also in ASCII format in the TABLES directory). The biostratigraphic zones of Martini (1971) and Okada and Bukry (1980), as well as some additional events defined by Raffi et al. (1993) and Wei (1993) (see "Explanatory Notes" chapter), are recognized within the Pleistocene interval. Tables T5 and T6 (both also in ASCII format in the TABLES directory) and Figure F14, summarize the main calcareous nannofossil biostratigraphic results.

The Pleistocene interval is represented from 0 to ~460 mcd at Site 1093 (Fig. F14). The base of the *Emiliania huxleyi* acme is well identified in Hole 1093A between 11.98 and 14.98 mcd, defining the base of Subzone NN21b. The first occurrence (FO) of *Emiliania huxleyi* is present from 74.43 to 75.18 mcd (base of Zone NN21). The last occurrence (LO) of *Pseudoemiliania lacunosa* is present between 152.43 and 159.16 mcd, defining the base of Zone NN20. The LO of *Reticulofenestra asanoi* is recognized from 220.79 to 227.33 mcd, although rare specimens of this species are recorded in scattered samples above 220.79 mcd and are interpreted as reworked (Table T5). The reentrance of medium *Gephyrocapsa* (4–5.5 µm) is present between 245.54 and 246.79 mcd, although the abundance of this morphotype is few to rare in this interval. The FO of *R. asanoi* is identified from 262.77 to 263.96 mcd. The LO of large *Gephyrocapsa* (>5.5 µm) is not well defined because of its scarcity above 314.53 mcd, whereas its FO is present from 323.6 to 345.1 mcd. *Calcidiscus macintyrei* is very rare at Site 1093 (Table T5) and its LO is not clearly defined.

The upper Pliocene markers are absent or few; this fact prevents an accurate identification of zonal boundaries or events in this time interval. Some fragments of calcareous sediments recovered in Sample 177-1093D-50X-CC (614.70 mcd) contain a calcareous nannofossil assemblage composed mainly of the same Reticulofenestrid species observed in the upper Miocene interval of Sites 1088 and 1092.

T4. Site 1093 splice tie points, p. 72.

F13. Spliced color reflectance, magnetic susceptibility, and GRA bulk density for Site 1093, p. 44.

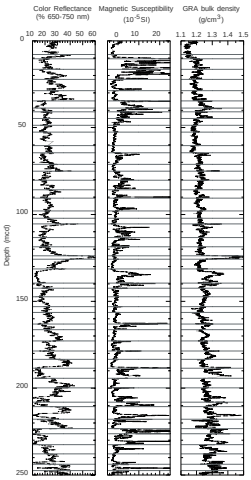

T5. Main calcareous nannofossil species in Holes 1093A, 1093B, and 1093D, p. 73.

T6. Biostratigraphic age assignments for Site 1093, p. 78.

F14. Bio- and magnetostratigraphic correlations and age designations for Site 1093, p. 45.

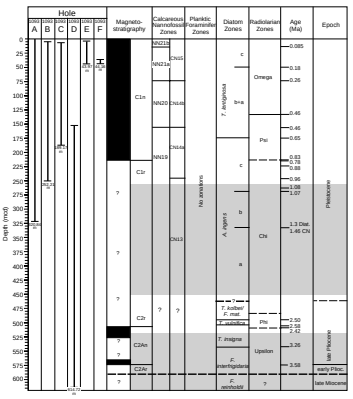

Planktic Foraminifers

The abundance of planktic foraminifers is highly variable at Site 1093. In general, abundance increases below ~200 mcd. Preservation is good to moderate in most samples. *Neogloboquadrina pachyderma* (sinistral) is by far the most abundant species (Table T7, also in ASCII format in the TABLES directory). Additional species include *Globigerina bulloides, Globigerina quinqueloba, Globigerinita uvula, Globorotalia inflata, Globorotalia puncticulata,* and *Globorotalia puncticuloides*. These species are generally present only in low abundance. Based on the examination of CC samples, it seems likely that a planktic isotopic stratigraphy may be established on *N. pachyderma* (sinistral), but it might not be continuous throughout the entire composite section of Site 1093. Low recovery between 255 and 450 mcd and below 520 mcd will also prevent the construction of a continuous record.

T7. Major planktic foraminifer species at Site 1093, p. 82.

Benthic Foraminifers

Benthic foraminifers at Site 1093 are generally not very abundant and vary considerably in their state of preservation from poor to good. Highly abundant, needle-shaped remains of the diatom genus *Thalassiothrix* in the >63-µm fraction made it necessary to wet sieve sediment samples at 150 µm.

Benthic foraminifers are highly variable, typically constituting between 5% and 100% of the total foraminifer fauna from the >150-µm fraction studied. Absolute foraminifer abundances are variable and low, reaching a maximum of 9 specimens/cm^3 in Sample 177-1093A-12H-CC, 0–10 cm. Low benthic foraminifer abundances may be explained by relatively high sedimentation rates (see below). A number of barren intervals occur, notably below 400 mcd, suggesting that a continuous benthic foraminifer isotopic record from this site may be difficult to obtain. However, *Cibicidoides wuellerstorfi* appears to be present during the Pleistocene interglacials, and a benthic stable isotopic record, albeit discontinuous, should be achievable through the late and mid-Pleistocene.

Quantitative estimates of relative species abundance were made from Holes 1093A and 1093D, with counts of up to 145 specimens/20-cm^3 sample. Species richness is variable, with a maximum of 32 taxa recorded in Sample 177-1093A-12H-CC, 0–10 cm (124.69 mcd), which corresponds to a peak in color reflectance during marine isotope stage (MIS) 11 (Fig. F13). Low values correspond to glacial intervals (e.g., the adjacent intervals to MIS 11). Samples 177-1093A-11H-CC (114.11 mcd) and 13H-CC (134.10 mcd) yield very sparse assemblages containing one and two taxa, respectively (Table T8, also in ASCII format in the TABLES directory).

T8. Benthic foraminifers at Site 1093, p. 85.

The most common benthic taxa recorded at Site 1093 include *C. wuellerstorfi, Eggerella bradyi, Globocassidulina subglobosa, Melonis pompiliodes, Pullenia bulloides, Pullenia quinqueloba,* and *Pullenia subcarinata*. The assemblages are very similar to those recorded at Site 1091 and do not provide any basis for biostratigraphic subdivision.

Diatoms

For biostratigraphic age assignments we used the zonation proposed by Gersonde et al. (1998). The late Pliocene–Pleistocene zonation proposed for the northern area of the Southern Ocean by Gersonde and

Bárcena (1998) could be applied only partially because of the diachronous or scattered presence of certain marker species, which preferentially dwell in warmer waters. All diatom stratigraphic information from the six holes was combined and converted to the mcd scale Tables T6, T9, both also in ASCII format in the TABLES directory).

Diatoms are generally abundant and display good preservation in all investigated samples. During examination of the diatom assemblages, we also encountered silicoflagellates in few to trace numbers (Table T10, also in ASCII format in the TABLES directory).

T9. Control points used to calculate sedimentation rates at Site 1093, p. 87.

T10. Diatom, silicoflagellate, ebridian, *Actiniscus*, sponge spicule, and phytolith occurrence, Site 1093, p. 88.

Biostratigraphy

The LO of *Hemidicus karstenii,* which falls in the lower portion of MIS 6 and defines the boundary between *Thalassiosira lentiginosa* Subzones c and b, was noted at 49.05 mcd (Fig. F14). Downhole variations in physical properties (compare Fig. F22) allow tentative identification of MISs in the upper 220 mcd of Site 1093. On this basis, the LO of *H. karstenii* falls in the lower part of an interval interpreted to represent MIS 6. The climatic optima of MISs 7, 9, and 11 can be tentatively placed at ~76, 106, and 125 mcd, respectively. However, *H. karstenii,* which is present in the Subantarctic and northern Polar Front Zone during these intervals (compare "Biostratigraphy" sections, "Site 1089" and "Site 1091" chapters), was found only in sediments tentatively identified as MISs 7, 8, and 9. *H. karstenii* is apparently absent in sediments assigned to MIS 11. This age assignment is supported by the LO of the calcareous nannofossil *Pseudoemiliania lacunosa* at 156 mcd, which is known to disappear in MIS 12. A similar occurrence pattern of *H. karstenii* was also observed in piston cores recovered in the area south of the Polar Front (R. Gersonde, unpubl. data). For this reason, *T. lentiginosa* Subzones a and b (Gersonde and Bárcena, 1998) cannot be discerned and must be combined at Site 1093. Below 124.77 mcd, in the lower part of the interval assigned to MIS 11, we observe rare but consistently well-preserved specimens of *Actinocyclus ingens*. This taxon has its LO in the lower portion of MIS 16 (Gersonde and Bárcena, 1998). Tentative MIS identification, and recognition of the Brunhes/Matuyama boundary at ~210 mcd (see "Paleomagnetism," p. 14), indicate that the section below 124.77 mcd is not disturbed by a hiatus. We suggest that the presence of *A. ingens* is caused by reworking of diatoms from older sediments. The reworked sediments possibly originate in late Pleistocene deposits belonging to the upper portion of the *A. ingens* Zone, because no stratigraphically older taxa (e.g., *Fragilariopsis barronii,* which marks the *A. ingens* Subzone a) were identified besides *A. ingens*. Because *A. ingens* is consistently few to abundant in number only below 174.6 mcd (Table T10), we tentatively place the top of the *A. ingens* Zone at this depth. A possible source area for the reworked sediments can be identified on a multichannel seismic line crossing the location of Site 1093 (Fig. F2). This line shows erosional features in sediments possibly related to the upper *A. ingens* Zone ~4 nmi north of Site 1093. A nearby source area is also suggested by the good preservation of the reworked *A. ingens* valves, which are unlikely to have been transported very far.

Similar to the sediments of the *T. lentiginosa* Zone, the underlying sediments assigned to the *A. ingens* Zone were also deposited at average sedimentation rates as high as 250 m/m.y. The base of *A. ingens* Subzones b and a has been placed at 272.52 and 339.75 mcd, respectively. However, the lower portion of the *A. ingens* Zone is in a section with poor recovery (Fig. F14), possibly because of the presence of diatom mats (see "Lithostratigraphy," p. 6). High recovery occurred below 450 mcd, and this sedimentary interval belongs to the lowermost portion of

the *A. ingens* Subzone a of earliest Pleistocene age. Close sample spacing allowed us to establish that assemblages representing the underlying *Proboscia barboi* Zone are not present at Site 1093. This indicates a hiatus at ~460.5 mcd that separates sequences assigned to the *A. ingens* Zone and the *Thalassiosira kolbei–Fragilariopsis matuyamae* Zone, and which spans at least 0.2 m.y. Below this hiatus we note a distinct drop in sedimentation rates to average values of ~80 m/m.y. (Fig. **F15**). The top of the *Thalassiosira vulnifica* Zone, marked by the LO of the nominate species, is noted at 494.25 mcd. This zone straddles the Matuyama/Gauss boundary. The preliminary depth assignment, however, places the base of this zone, marked by the LO of the nominate species of the underlying *Thalassiosira insigna* Zone, 1 m above the Matuyama/Gauss boundary, which has been identified at 506.85 mcd (Table **T9;** Fig. **F14**). Assemblages representing the underlying *Fragilariopsis interfrigidaria* Zone, which straddles the Gauss/Gilbert boundary and thus the late/early Pliocene boundary, were observed between 543.1 and 585.5 mcd. In the lower portion of this interval, magnetic inclination data suggest the possible placement of the Gauss/Gilbert boundary at 574.2 mcd (see **"Paleomagnetism,"** p. 14). Sediments assigned to the *F. interfrigiaria* Zone occur within an interval of incomplete recovery, which continues downhole to the base of Site 1093. Sample 177-1093D-48X-CC, 8–9 cm (594.98 mcd), contains dominant *Neobrunia mirabilis*. The co-occurrence of rare *Hemidiscus triangularus* indicates a late Miocene age for the *Fragilariopsis reinholdii* Zone. A similar ooze was recovered at Ocean Drilling Program (ODP) Site 701 with a thickness of ~30 m. This ooze has been dated as latest Miocene (between 6.3 and 6.9 Ma) (Shipboard Scientific Party, 1988). For this reason, we suggest that a hiatus separates the uppermost lower Pliocene from the uppermost upper Miocene interval, spanning a time interval of ~3 m.y. The hiatus is located between Samples 177-1093D-47X-CC, 0–10 cm, and 48X-CC, 8–9 cm, and thus occurs at ~590 mcd (Fig. **F15**).

F15. Age-depth plot of biostratigraphic and paleomagnetic events at Site 1093, **p. 46.**

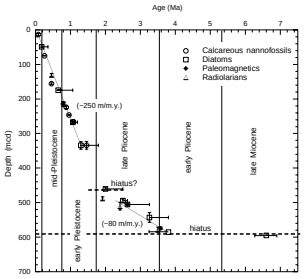

Radiolarians

Radiolarian biostratigraphy at Site 1093 is based on the examination of 58 samples (Table **T11,** also in ASCII format in the **TABLES** directory). Radiolarians at Site 1093 are generally well preserved except for the lowermost sample (177-1093D-50X-CC, 0–2 cm [614.7 mcd]), but their abundance is variable because of dilution by abundant diatoms. All the Antarctic Pleistocene to Pliocene radiolarian zones (Omega to Upsilon Zones) are recognized at Site 1093.

Stylatractus universus is persistently present below 131.47 mcd, which suggests that the boundary of the Omega and Psi Zones lies at ~130.72 mcd (Table **T9**). The boundary of the Psi and Chi Zones, marked by the LO of *Pterocanium trilobum,* is somewhat difficult to recognize because rare to few occurrences of *P. trilobum* are observed even in the Omega Zone. Judging from the continuous presence of *Pterocanium trilobum* below ~219 mcd, however, the last appearance datum of *P. trilobum* at 0.83 Ma can be placed at 213.68 mcd (Table **T9**). The boundary of the Chi and Phi Zones, defined by the LO of *Eucyrtidium carvertense* at 1.92 Ma, is tentatively placed at 484.08 mcd (Table **T9**). As for *Pterocanium trilobum,* reworked specimens of *Eucyrtidium carvertense* are observed in some horizons of the overlying Chi and Psi Zones, which makes the recognition of the boundary difficult. Moreover, the Chi/Phi boundary is apparently in the lower reversed polarity portion of the Matuyama Chron (Fig. **F14**), which suggests that the zonal age assignment by Laz-

T11. Main components of the radiolarian assemblage at Site 1093, **p. 93.**

arus (1992) cannot be applied at Site 1093. Therefore, further investigations will be necessary to clarify the details of the Chi/Phi boundary at Site 1093. The Upsilon Zone, whose top is defined by the LO of *Helotholus vema* at 2.42 Ma, is encountered within the lowermost portion of Hole 1093D, below 521.77 mcd. The lowermost sample (177-1093D-50X-CC, 0–2 cm [614.7 mcd]), yields poorly preserved *Prunopyle haysi* that has its LO in the late Miocene (Lazarus, 1992). This assemblage is quite different from that of the Upsilon Zone, which suggests the presence of a hiatus around 590 mcd as shown in Figure F14.

Paleomagnetism

Archive halves of APC and XCB cores recovered at Site 1093 were measured using the shipboard pass-through magnetometer. Measurements were made at 5-cm intervals. Sections obviously affected by drilling disturbance were not measured. The majority of core sections from Site 1093 were measured after alternating-field (AF) demagnetization at peak fields of 0 (natural remanent magnetization [NRM]), 5, 10, 15, 20, and 25 mT. The rate of cores processed through the laboratory ("core flow") at this site generally allowed this six-step measurement sequence. Shorter measurement sequences comprising four steps (0, 10, 20, and 25 mT) were used for Cores 177-1093B-1H through 9H, and for all XCB cores from Hole 1093D.

NRM intensities were about 1×10^{-2} A/m at the top of each hole, decreasing through the upper 20 mbsf to ~1×10^{-3} A/m, below which they remained fairly uniform throughout most of the APC section. After AF demagnetization at peak fields of 25 to 30 mT, intensities generally decreased to ~5×10^{-4} A/m in the APC sections (above 250 mbsf) of all holes. Magnetization intensities were slightly higher in the XCB section of Hole 1093D, particularly below 440 mbsf. NRM inclinations are typically steep down as a result of a magnetic overprint, probably largely attributable to the drill string. The drill-string remagnetization was largely removed at peak demagnetization fields in excess of 10 mT; the resulting inclination values, however, are highly scattered (Fig. F16). Magnetization directions attributed to the Matuyama Chron are particularly inconsistent, probably because of normal-polarity magnetic overprints associated with (1) drilling-related core deformation and (2) magnetite dissolution and growth of iron sulfides in a reducing diagenetic environment.

The Brunhes/Matuyama boundary is identified in the 205- to 210-mcd interval at both Holes 1093A and 1093B (Fig. F16; Table T9). The boundaries of the Gauss Chron are tentatively identified in the XCB section of Hole 1093D (Fig. F17; Table T9).

Stratigraphic Summary

At Site 1093, the sedimentary section recovered is continuous only to a depth of 252 mcd (base of Core 177-1093D-10H, early Pleistocene), and has a total thickness of ~600 mcd (base of Core 1771093D-50X, late Miocene) (Figs. F10, F11, F12, F13). Holes 1093A–1093F were cored by APC to 241.5, 221.8, 169.5, 307.0, 42.5, and 43.5 mbsf, respectively. Holes 1093A and 1093B were drilled by XCB to a TD of 309.4 and 597.7 mbsf, respectively. The offset of cores below the spliced record was arbitrarily chosen to be the same as the cumulative offset of the overlying cores. Holes 1093E and 1093F are short holes that were drilled to ensure continuous overlap in the uppermost part of the sedimentary section.

F16. Inclination of the remanent magnetization after AF demagnetization at Holes 1093A and 1093B, p. 47.

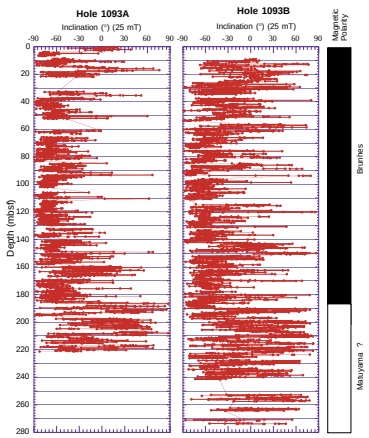

F17. Inclination of the remanent magnetization after AF demagnetization at Hole 1093D, p. 48.

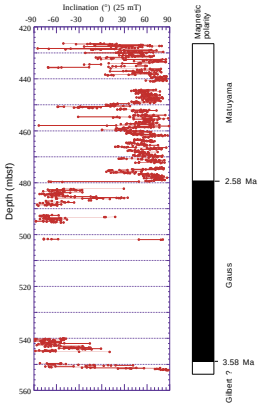

At Site 1093, an extremely expanded Holocene to mid-Pliocene section was recovered. However, this record is incomplete because of intervals of low recovery at 260–460 mcd and below 520 mcd. The lowermost biostratigraphic datum at Site 1093 was dated at 6.3–6.9 Ma as latest Miocene. The late Miocene is apparently separated by a hiatus from the overlying early Pliocene sediments. Another hiatus may be present in the late Pliocene at ~460.5 mcd (Figs. **F14, F15**).

All biostratigraphic datums, including calcareous nannofossil, diatom, and radiolarian events and available magnetostratigraphic interpretations, yield consistent age assignments throughout the record at Site 1093. The sedimentation rates in the diatom-dominated Pleistocene sequences average ~250 m/m.y. The transition between the Brunhes and Matuyama Chrons could be placed between 205 and 210 mcd. Preliminary correlation of the physical properties records with MISs during the Brunhes Chron indicates slightly higher sedimentation rates during the last 0.45 m.y., ranging between ~200 and ~720 m/m.y. In the lower portion of the Brunhes Chron, sedimentation rates are lower, ranging between ~100 and ~450 m/m.y. Because of low recovery rates (25%) in the interval between ~260 and ~460 mcd, the lower Pleistocene sedimentary record older than ~1–1.1 Ma is only sparsely documented. The top of the underlying high-recovery interval (450–520 mcd) is earliest Pleistocene in age. The absence of the *Proboscia barboi* diatom zone, which correlates with the Olduvai Subchron, may indicate that a hiatus separates the Pleistocene from the Pliocene, probably spanning at least 0.2 m.y.

Late Pliocene sedimentation rates are ~80 m/m.y. Such a distinct drop from high Pleistocene to lower late Pliocene sedimentation rates was also observed at Sites 1090, 1091, and 1092, and is probably related to the general change in biosiliceous export rates in the Southern Ocean at this time. The interval of low recovery from below 520 mcd to the bottom of Site 1093 is correlated with the Gauss Chron. The boundary between the Gauss and Gilbert Chrons is tentatively placed at 574.2 mcd. Only the uppermost early Pliocene section is present at Site 1093 because of a hiatus at ~590 mcd. Below this hiatus, which spans ~3 m.y., uppermost Miocene sediments were penetrated with low recovery.

The extremely expanded upper and mid-Pleistocene sediments provide a unique opportunity for paleoceanographic reconstructions at very high time resolution in a pelagic environment. Sedimentation rates between 100 and 700 cm/k.y. allow sample spacing with a temporal resolution of less than 100 yr. This record can be correlated in detail with paleoclimatic records from Greenland and Antarctic ice cores. On the basis of CC samples, it seems likely that a nearly continuous planktic isotopic stratigraphy (*N. pachyderma* [sinistral]) and a more or less continuous benthic isotopic record can be established for the late and mid-Pleistocene sections at Site 1093.

GEOCHEMISTRY

Volatile Hydrocarbons

As a part of the shipboard safety and pollution program, volatile hydrocarbons (methane, ethane, and propane) were measured in the sediments of Holes 1093A and 1093D using the standard ODP headspace sampling techniques (Table **T12;** Fig. **F18**). Headspace methane concentrations at Site 1093 range from 2 to 19 parts per million by vol-

T12. Concentration of methane at Site 1093, **p. 96.**

F18. Concentration of methane vs. depth at Holes 1093A and 1093D, **p. 49.**

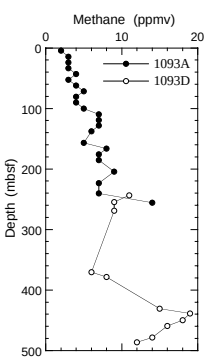

ume (ppmv), with a trend toward higher methane at depth. Ethane, propane, and other higher molecular weight hydrocarbons were not observed.

Interstitial Water Chemistry

Shipboard chemical analyses of the interstitial water from Site 1093 followed the procedures for Sites 1088–1092. A total of 64 interstitial water samples were taken from Holes 1093A and 1093D to a depth of 483 mbsf (Table T13; Fig. F19). Samples were taken from every core section (except the bottom section of each core) of the upper 63 mbsf in Hole 1093A; the first two sections of Core 177-1093A-7H were omitted because of split core liners. Sampling in Hole 1093A continued at a frequency of one sample per core to 185 mbsf, and then every other core to 255 mbsf. The sampling from Hole 1093D extends the profile to 498 mbsf, but whole-round samples were only taken where there was sufficient recovery. The depth offset between Hole 1093A and 1093D profiles at around 240–255 mbsf is ~15 m. In many cases, however, truly continuous profiles of dissolved species cannot be constructed from the combination of profiles from the two holes because of the poor recovery in Hole 1093D, and unusual values observed in some chemical species from the bottom of Hole 1093A. Porcellanite fragments were observed in the tops of Cores 177-1093D-28X, 46X, and 50X (see "Lithostratigraphy," p. 6). Although probably not in place, these fragments indicate porcellanite layers higher in the section, and these may have contributed somewhat to the poor recovery observed in the intervals from ~260 to 370 mbsf and from ~380 to 425 mbsf.

For almost all the dissolved species, the trends in Site 1093 are remarkably similar to those observed at Site 1091. The high-resolution sampling of the upper 60 mbsf created an especially detailed Cl^- profile that is identical (within analytical uncertainty) to its lower resolution counterpart from Site 1091. Both sites are characterized by a well-defined Cl^- maximum in the interval from 50 to 60 mbsf. If caused by glacial increases in whole-ocean salinity, the similarity in Cl^- peak depth implies comparable diffusivities at the two sites. As at Site 1091, the high sedimentation rate and the presence of diatom mats may be responsible for creating such a distinct Cl^- maximum.

The lack of significant carbonate deposition (except in certain specific horizons; see "Lithostratigraphy," p. 6) suggests that the major cation profiles are largely independent of carbonate dissolution and recrystallization. In the upper 190 m of the section, both dissolved Ca^{+2} and Mg^{+2} decrease very slightly, perhaps because of carbonate precipitation driven by increases in alkalinity. Between 190 and 280 mbsf, both Ca^{+2} and Mg^{+2} concentrations increase abruptly. Neither Cl^- nor salinity increase significantly over the same interval, and there is no distinct change in lithology. We, therefore, have no immediate explanation for the Ca^{+2} and Mg^{+2} trends between 190 and 280 mbsf, and the profiles must be reproduced with additional shore-based analyses before we can verify these data. However, as it stands, these trends in Ca^{+2} and Mg^{+2} are responsible for a very large excursion in the Na^+ profile, which was determined from charge balance calculations. Below ~280 mbsf, Ca^{+2} increases and Mg^{+2} decreases more unambiguously downhole, with a $\Delta Mg/\Delta Ca$ slope of about –2. This behavior is characteristic of basaltic ash alteration (Baker, 1986), and is consistent with the volcanic detritus and glass shards observed in smear slides (see "Lithostratigraphy," p. 6). Sr^{+2} concentrations increase only very slightly to ~400 mbsf, con-

T13. Interstitial water chemistry at Site 1093, p. 97.

F19. Interstitial water chemistry profiles vs. depth at Holes 1093A and 1093D, p. 50.

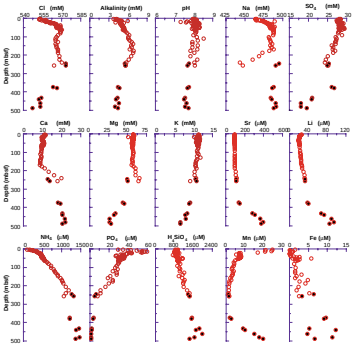

sistent with the general lack of carbonate sediments. However, there is a rather abrupt increase in Sr^{+2} below 400 mbsf that accompanies the increase in $CaCO_3$ observed in the lower part of the section at Site 1093 (see Fig. **F20,** and **"Solid Phase Analysis,"** p. 17).

Site 1093 can be classified as slightly reducing based on the consistent presence of H_2S (as judged by scent), except in the deepest part of the section below ~380 mbsf. However, as at Site 1091, sulfate concentrations decrease only gradually throughout the section. In fact, the entire redox environment and history at Site 1093 are apparently very similar to that of Site 1091. In particular, phosphate is characterized by a prominent maximum in the upper 20 mbsf, with a gradual decline below. Alkalinity shows a broad maximum from ~150 to 200 mbsf, and ammonium increases steadily to values of nearly 1500 µM at ~300 mbsf. The Mn^{+2} profile largely mimics that of phosphate, whereas Fe^{+2} shows a small maximum just below the base of the phosphate maximum. Mn^{+2} and Fe^{+2} increase in the bottom of the section.

All of these features are shared with Site 1091 (though the scale of the trends may differ between sites in some cases) and must reflect unique conditions associated with the burial of diatom organic matter (see **"Geochemistry,"** p. 13, in the "Site 1091" chapter). The presence of moderately high sulfate despite rapid sedimentation, and the relatively shallow dissolved phosphate maximum (compared with the maxima in alkalinity and ammonium at depth), suggest that at least two different organic pools are remineralized. One rapidly degradable pool may exist in the uppermost sediments, whereas a second refractory pool, perhaps internal to the opal structure, probably degrades more slowly deeper in the sedimentary column. Furthermore, the significant dissolved Mn and Fe concentrations observed downhole imply substantial mobility, which, in turn, suggests that the redox zone may be migrating and/or changing cyclically with climatically induced fluctuations in the diatom-rain rate.

F20. $CaCO_3$, TOC, TN, TS, and TOC/TN vs. depth at Holes 1093A and 1093D, **p. 51.**

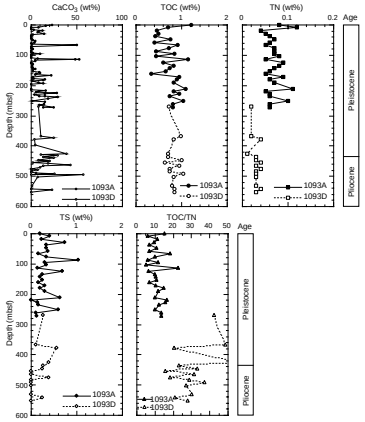

Solid Phase Analysis

The shipboard solid phase analysis at Site 1093 consisted of measurements of inorganic carbon, total carbon, total nitrogen (TN), and total sulfur (TS) throughout the section cored in Holes 1093A and 1093D (Table **T14;** Fig. **F20;** see **"Explanatory Notes"** chapter for methods). $CaCO_3$ contents at Site 1093 were generally low, ranging from 0 to 56.9 wt% and averaging ~9.2 wt% throughout the section. Slightly higher $CaCO_3$ values were observed from 400 to 480 mbsf in the late Pliocene section (Fig. **F20**).

Total organic carbon (TOC) contents vary between 0.34 and 1.21 wt%, with an average value of 0.77 wt% in the Pliocene–Pleistocene section at Site 1093. This average TOC value is slightly higher than the 0.65 wt% average observed in the sediments from the Pleistocene section at Site 1091, and the 0.43 wt% average in the Pliocene–Pleistocene section at Site 1089. TS concentrations vary between 0 and 1.04 wt%. TN contents range from 0.01 to 0.12 wt%. The lower TN contents observed in Hole 1093D (Fig. **F20**) are probably an underestimate, because the measurements of these samples were performed under poor analytical conditions (an air leak in the carbon-nitrogen-sulfur analyzer). Therefore, TOC/TN values are likely also overestimated in the sediments at Hole 1093D (Fig. **F20**). At Hole 1093A, however, TOC/TN values vary between 5.4 and 22.9 with an average of 11.3, which is a

T14. Analytical results of IC, CaCO3, TC, TOC TN, TS, and TOC/TN at Site 1093, **p. 99.**

value that is intermediate between unaltered algal organic matter (5–8) and fresh land-plant material (25–35) (e.g., Emerson and Hedges, 1988; Meyers, 1994). These higher TOC/TN values suggest that the organic materials in the sediments at Site 1093 may have been derived from both marine and terrigenous sources (Fig. F21). However, significant fluctuations in TOC/TN values covary with both organic carbon and $CaCO_3$ contents and, because of the analytical problems that are clearly apparent in Hole 1093D samples, additional shore-based analyses are required before any firm conclusions can be drawn. Pyrolysis analyses were not performed because of the relatively organic-carbon-poor nature of the sediments.

F21. TOC vs. TN at Hole 1093A, p. 52.

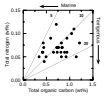

T15. Physical properties measurements conducted at Site 1093, p. 101.

PHYSICAL PROPERTIES

Gamma-ray attenuation (GRA) bulk density, magnetic susceptibility, natural gamma-ray (NGR) emission, and *P*-wave velocity were measured with the MST on whole-core sections recovered from Site 1093. Color reflectance and resistivity were measured on the working half of all split APC cores using the Oregon State University Split Core Analysis Track (OSU-SCAT) (see "Explanatory Notes" chapter). Other physical properties measurements conducted on discrete core samples included moisture, density, and *P*-wave velocity. Measured parameters were initial wet bulk mass (M_b), dry mass (M_d), and dry volume (V_d). Velocity was measured on split-core sections using the *P*-wave velocity sensor 3 (PWS3). Table T15 and Figure F22 summarize the physical properties measurements performed at Site 1093.

F22. Site 1093 NGR, magnetic susceptibility, resistivity, bulk density, and reflectance, p. 53.

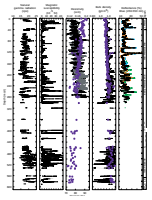

Multisensor Track and Split Core Analysis Track

At Site 1093, as with Sites 1091 and 1092, downhole variations in physical properties are controlled largely by changes in the proportion of carbonate vs. siliceous sedimentary components. Intervals rich in carbonate show (1) high GRA bulk densities that are verified by discrete-sample (moisture and density [MAD] method) bulk densities (Fig. F23); (2) lower porosity (MAD method) and higher resistivity (OSU-SCAT) values; and (3) bright reflectance with little divergence between the blue, red, or nearinfrared reflectance bands. In contrast, intervals that are rich in diatoms exhibit lower density, higher porosity, and a greater contrast between blue and red reflectance. Exceptions to the above generalization occur where terrigenous grains are a significant component of the sediment.

F23. Relationship between GRA and MAD bulk density at Site 1093, p. 54.

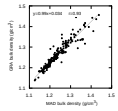

There are four major carbonate layers within the upper 140 mcd of Site 1093 that have a similar reflectance character (magnitude and red/blue values) and correlate with similar carbonate layers in the upper 60 mcd of Site 1091 (Fig. F24). These layers are also marked by high GRA bulk density intervals (Fig. F25). The preliminary shipboard age model (see "Chronostratigraphy" sections, this chapter and "Site 1091" chapter) indicates that these layers may represent the major interglacials of the late Pleistocene (MISs 5, 7, 9, and 11). At Site 1093, red/blue values, which appear to reflect the relative proportion of carbonate vs. silica, are slightly higher (lower carbonate content) than at Site 1091, probably because of lower production or preservation of carbonate at Site 1093. In ~10-m-thick intervals that occur immediately below each carbonate layer, the magnetic susceptibility signal shows high-frequency (period <1 m) oscillations (Fig. F25). One of these layers is present

F24. Preliminary correlation of reflectance between Sites 1093 and 1091, p. 55.

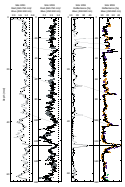

F25. Magnetic susceptibility, porosity, resistivity, bulk density, and reflectance for the upper 290 mcd, p. 56.

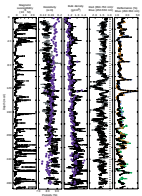

between 10 and 20 mcd. These layers appear to contain more mud, sand, and dropstones (see "Lithostratigraphy," p. 6), suggesting that intervals of greater ice rafting preceded the deposition of each carbonate layer.

In the upper 290 mcd of Site 1093, there are several maxima in the red/blue values (e.g., the two intervals between 110 and 120 mcd in Fig. F24) as a result of sediments that reflect strongly in the red (650–750 nm) band. These "red" sediments may result from the diatom *Fragilariopsis kerguelensis,* which dominates in some intervals (e.g., ~100–125, 164, and 174 mcd; see "Chronostratigraphy," p. 9), giving the sediment an orange-tan color (Fig. F25).

In the upper 280 mcd of Site 1093, GRA bulk density and resistivity show an overall increase downhole, but a similar trend is not apparent in reflectance (Fig. F22). Between 180 and 280 mcd, magnetic susceptibility shows a greater frequency of high susceptibility values than in the upper 180 mcd, suggesting an increase in terrigenous content (Fig. F25). Smear slides (see "Lithostratigraphy," p. 6) show higher sand concentrations in this interval (particularly around 240 mcd) than at any other depths in the section.

Between 290 and 460 mcd, recovery was poor, resulting in large gaps in the record (Fig. F22). With improved recovery below 460 mcd, NGR, magnetic susceptibility, and bulk density show large amplitude fluctuations. This can be attributed to a general increase in mud concentration, alternations between laminated mud rocks and diatomites (see "Lithostratigraphy," p. 6), and large amplitude fluctuations in the concentrations of these constituents.

P-wave Velocity

Figure F26 shows *P*-wave velocities measured with the PWS3 velocimeter and *P*-wave logger (PWL) at Site 1093. PWS3 velocities generally increased gradually and steadily downhole from values of 1550 m/s at the top to 1600 m/s at the bottom, reflecting the gradual increase in bulk density described above. High values around 3000 m/s were measured on clasts and mud rocks below 590 mcd (Fig. F26). The recurring problem with the PWL at previous Leg 177 sites was finally rectified (see "Explanatory Notes" chapter), resulting in much better agreement between velocity measurements obtained with the PWL and the PWS3. PWL velocities are, however, somewhat lower than PWS3 velocities by a mean difference of ~20 m/s.

Heat Flow

A total of 142 thermal conductivity measurements gave values within a narrow range of 0.54 to 0.78 W/(m·K) (Table T16, also in ASCII format in the TABLES directory; Fig. F27B). This is consistent with the results from Site 1091, where the cores are also dominantly composed of diatom ooze. Correlation with trends in bulk density is poor because the lithologic variability is small when compared to the analytical error (Fig. F27B).

At Site 1093, eight downhole temperature measurements were taken using the APCT shoe (Adara tool), one in bottom water and seven in sediment between 37 and 151 mbsf. Two additional measurements were taken in stiffer formations (251 and 482 mbsf), using the Davis-Villinger temperature probe (DVTP). Measurements were slightly to severely affected by frictional heat noise and/or cold-water flux (pre-

F26. *P*-wave velocity at Site 1093, p. 57.

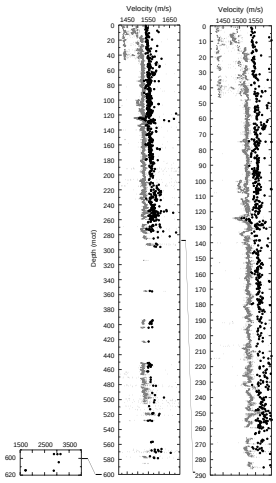

T16. Thermal conductivity measurements at Site 1093, p. 102.

F27. Thermal conductivity measurements at Site 1093, p. 58.

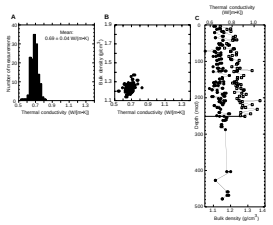

sumably pumped inadvertently from uphole down the drill pipe) during deployment at all stations (Fig. F28). The temperature-time series was evaluated using shipboard processing programs to derive equilibrium temperatures. Relatively large errors, estimated from repeated model curve fitting over different intervals, range from ±0.5° to ±1.0°C (Fig. F28).

Despite the compromised data quality, the depth-temperature relationship reveals an apparently consistent temperature gradient of 93°± 3°C/km (Fig. F29). A second-order polynomial fit yields a better correlation coefficient than the linear fit, and is more compatible with the bottom-water temperature and the deepest measurement, both of which are considered to have relatively small errors. Using an average thermal conductivity of 0.7 W/(m·K) for the sedimentary section, a moderately high average heat flow of 65 ± 4 mW/m² is calculated for the drilled interval.

F28. Downhole temperature measurements at Site 1093, p. 59.

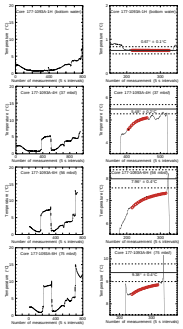

WIRELINE LOGGING

Logging Operations

Hole 1093D was logged with the GHMT and triple combination tool strings after the hole had been flushed of debris (see "Explanatory Notes" chapter for tool details). Logging was conducted between 04:30 and 21:30 on January 18, 1998. The drill pipe was initially set at 87 mbsf but was raised during the first upward log run to a depth of 68 mbsf, where it stayed for subsequent logging runs. On the processed logs provided by the Lamont-Doherty Earth Observatory (LDEO) logging contractor, the bottom-hole assembly (BHA) depth is ~65 mbsf. The discrepancy of the wireline and drill-pipe measurements may be the result of ship heave, use of the wireline heave compensator, and/or pipe/wire stretching. We ran one main pass each with the GHMT (68–568 mbsf) and the triple combination tool (68–579 mbsf) strings. A short repeat pass (477–566 mbsf) was also run with the GHMT tool near the bottom of the hole. The wireline heave compensator was used for the entire logging period.

F29. Depth-temperature curve for Site 1093, p. 62.

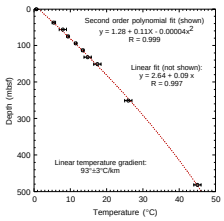

Log Quality

The diatom sediments encountered at Site 1093 were prone to washout, leading to poor core recovery in XCB sections and a large-diameter hole. The borehole caliper measurements collected during the triple combination tool string pass showed that the hole diameter was greater than the maximum extent of the caliper (18 in) for all but 150 of the 511 m logged (Fig. F30). Only 40 m of the hole had a diameter less than the 15-in necessary to run the Formation MicroScanner (FMS) and the decision was made to forego the FMS-Sonic tool run. The triple combination tool string had difficulties passing the four short intervals, located between 120 and 160 mbsf, where the hole narrowed to a minimum diameter of 7 in, and no repeat pass was attempted. The bridged intervals correspond to spikes in the density logs most likely related to good sensor contact over these sections. The porosity and density measurements, which require good contact with the borehole wall, are highly suspect over the intervals where the caliper is at maximum extension. The total magnetic field strength at Site 1093 was below the range of the GHMT string. However, the magnetic susceptibility and

F30. Site 1093 logs of caliper, natural gamma, magnetic susceptibility, bulk density, porosity, and resistivity, p. 63.

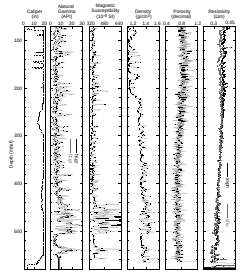

natural gamma logs show strong covariance and agree well with core data over the interval of core recovery, providing the potential for core-log integration down to the meter scale (Figs. F30, F31, and F32).

Shore-based Log Processing

Depth shift: Original logs were interactively depth shifted with reference to the hostile environment natural gamma-ray sonde (HNGS) log from the dual induction tool (DIT)/accelerator porosity sonde (APS)/hostile environment litho-density sonde (HLDS)/HNGS run and to the seafloor (–3637.5 m). This value corresponds to the seafloor depth shown on the DIT/APS/HLDS/HNGS logs and differs by 2.5 m from the "bottom-felt" depth given by the drillers. The program used is an interactive, graphical depth-match program that allows the user to visually correlate logs and to define appropriate shifts. The reference and match channels are displayed on the screen, with vectors connecting old (reference curve) and new (match curve) shift depths. The total gamma-ray curve from the natural gamma-ray spectrometry tool (NGT) or HNGS tool run on each logging string is used most often to correlate the logging runs. In general, the reference curve is chosen on the basis of constant, low cable tension and high cable speed (tools run at faster speeds are less likely to stick and are less susceptible to data degradation caused by ship heave). Other factors, however, such as the length of the logged interval, the presence of drill pipe, and the statistical quality of the collected data (better statistics are obtained at lower logging speeds) are also considered in the selection. A list of the amount of differential depth shifts applied at this hole is available upon request from LDEO.

Gamma-ray processing: The HNGS data were corrected in real time for borehole size and type of drilling fluid used during the recording. The NGT data were corrected for borehole size and type of drilling fluid used during the processing.

High-resolution data: Neutron porosity data were recorded at a sampling rate of 5.08 cm in addition to the standard 15.24-cm sampling rate.

Geological magnetic tool: The geological magnetic tool collected data at two different sampling rates, the standard 15.24-cm and a 5.08-cm rate. Both data sets have been depth shifted to the reference run and to the seafloor.

Shore-based Quality Control

During processing, quality control of the data is mainly performed by cross-correlation of all logging data. A large (>12 in) and/or irregular borehole affects most recordings, particularly those that require eccentralization (APS/HLDS) and a good contact with the borehole wall. Caliper readings show the hole to be larger than 18 in over most of the logged interval; because of the lack of proper contact with the borehole wall, both density and porosity readings are of extremely poor quality and are not presented.

Data recorded through the BHA, such as the HNGS data above 65 mbsf, should be used qualitatively only because of the attenuation on the incoming signal.

Hole diameter was recorded by the hydraulic caliper (LCAL) on the HLDS tool.

F31. Site 1093 NGR logs compared to calculated thorium, potassium, and uranium, p. 64.

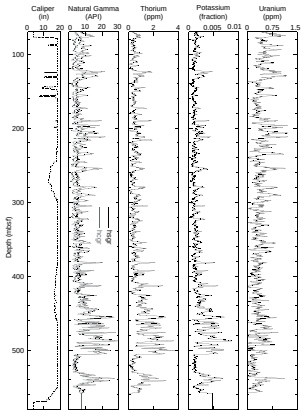

F32. Site 1093 GHMT magnetic susceptibility compared to MST magnetic susceptibility, p. 65.

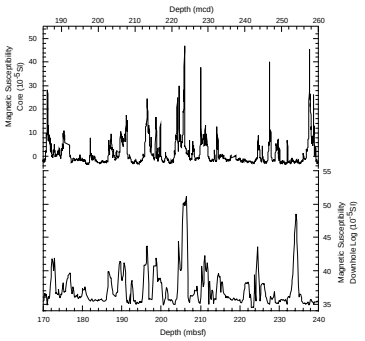

Results

The natural gamma ray and magnetic susceptibility logs both show clear and coherent downhole variability associated with lithologic changes related presumably to glacial–interglacial cyclicity. The high values of natural gamma ray and magnetic susceptibility correspond to depths where core lithology is dominated by muddy diatom oozes characterized by relatively high concentrations of IRD (see **"Lithostratigraphy,"** p. 6, and **"Physical Properties,"** p. 18). Low natural gamma ray and magnetic susceptibility values are associated with both the diatom-mat intervals and the pale gray foraminifer-diatom oozes that overlay them. This cyclicity extends downhole through the section of poor core recovery (270–435 mbsf). The low overall natural gamma ray values made it difficult to establish the mudline through the drillpipe using the NGR logs (estimated at 3637 mbrf wireline depth using NGR logs vs. 3635 mbrf driller's depth).

The interval between 435 and 530 mbsf is represented by higher amplitude variability in the natural gamma ray and magnetic susceptibility data. The XCB coring was more successful over this interval as well, and the sediments recovered were better consolidated and had higher average siliciclastic mud contents, consistent with the increased natural gamma ray and magnetic susceptibility signals. The density data also show stronger variability over this interval, with higher densities associated with highs in magnetic susceptibility and natural gamma radiation ray.

Measured porosities were very high throughout the hole and may be influenced by bad contact with the borehole wall. The presence of clay in the formation may also cause an overestimation of porosity, because the calculation assumes that the entire formation hydrogen is in the interstitial water. The porosity data show a general decrease downhole from 80%–90% in the upper portion of the hole to 70%–80% in the lower portion, which is in rough agreement with discrete measurements on core material (see **"Physical Properties,"** p. 18). Over some intervals, the tool-measured porosities are ≥100%, suggesting that the tool was measuring borehole fluid and not sediment.

The resistivity of the formation was extremely low throughout the hole with the exception of the bottom of the hole, where some clear variability (>550 mbsf) was most likely associated with the presence of diatomites and laminated mudrocks that were more consolidated than the overlying sediments.

REFERENCES

Abelmann, A., and Gersonde, R., 1991. Biosiliceous particle flux in the Southern Ocean. *Mar. Chem.*, 35:503–536.

Baker, P.A., 1986. Pore-water chemistry of carbonate-rich sediments, Lord Howe Rise, Southwest Pacific Ocean. *In* Kennett, J.P., von der Borch, C.C., et al., *Init. Repts. DSDP,* 90: Washington (U.S. Govt. Printing Office), 1249–1256.

Douglass, J., Schilling, J.-G., Kingsley, R.H., and Small, C., 1995. Influence of the Discovery and Shona mantle plumes on the southern Mid-Atlantic Ridge: Rare earth evidence. *J. Geophys. Res.*, 21:2893–2396.

Emerson, S., and Hedges, J.I., 1988. Processes controlling the organic carbon content of open ocean sediments. *Paleoceanography,* 3:621–634.

Gersonde, R., 1989. Taxonomy and morphostructure of late Neogene diatoms from the Maude Rise (Antarctic Ocean). *Polarforschung,* 59:141–171.

Gersonde, R., and Bárcena, M.A., 1998. Revision of the late Pliocene–Pleistocene diatom biostratigraphy for the northern belt of the Southern Ocean. *Micropaleontology*, 44:1–15.

Gersonde, R., Spiess, V., Flores, J. A., Hagen, R., and Kuhn, G., 1998. The sediments of Gunnerus Ridge and Kainan Maru Seamount (Indian sector of Southern Ocean). *Deep-Sea Res. Part I,* 45:1515-1540.

Hartnady, C.J.H., and le Roex, A.P., 1985. Southern ocean hotspot tracks and the Cenozoic absolute motion of the African, Antarctic, and South American plates. *Earth Planet. Sci. Lett.*, 75:245–257.

Lazarus, D., 1992. Antarctic Neogene radiolarians from the Kerguelen Plateau, Legs 119 and 120. *In* Wise, S.W., Jr., Schlich, R., et al., *Proc. ODP, Sci. Results,* 120: College Station, TX (Ocean Drilling Program), 785–809.

Martini, E., 1971. Standard Tertiary and Quaternary calcareous nannoplankton zonation. *In* Farinacci, A. (Ed.), *Proc. 2nd Int. Conf. Planktonic Microfossils Roma:* Rome (Ed. Tecnosci.), 2:739–785.

Meyers, P.A., 1994. Preservation of elemental and isotopic source identification of sedimentary organic matter. *Chem. Geol.,* 144:289–302.

Okada, H., and Bukry, D., 1980. Supplementary modification and introduction of code numbers to the low-latitude coccolith biostratigraphic zonation (Bukry, 1973; 1975). *Mar. Micropaleontol.,* 5:321–325.

Raffi, I., Backman, J., Rio, D., and Shackleton, N.J., 1993. Plio-Pleistocene nannofossil biostratigraphy and calibration to oxygen isotopes stratigraphies from Deep Sea Drilling Project Site 607 and Ocean Drilling Program Site 677. *Paleoceanography,* 8:387–408.

Shipboard Scientific Party, 1988. Site 701. *In* Ciesielski, P.F., Kristoffersen, Y., et al., *Proc. ODP, Init. Repts.,* 114: College Station, TX (Ocean Drilling Program), 363–482.

Tucholke, B.E., and Embley, R.W., 1984. Cenozoic regional erosion of the abyssal seafloor off South Africa. *In* Schlee, J.S. (Ed.), *Interregional Unconformities and Hydrocarbon Accumulation.* AAPG Mem., 36:145–164.

Wei, W., 1993. Calibration of Upper Pliocene-Lower Pleistocene nannofossil events with oxygen isotope stratigraphy. *Paleoceanography,* 8:85–99.

Figure F1. Track line and shotpoints for the site surveys of Site 1093 conducted during *Polarstern* Cruise ANT-XI/3 (Line AWI-94090; solid line, filled squares) and *Thompson* Cruise TTN057 (dashed line, pluses). The bold portion of the track line corresponds to the segment of the seismic profile displayed in Fig. **F2,** p. 25. Triangle and open square show core locations from the site survey cruises.

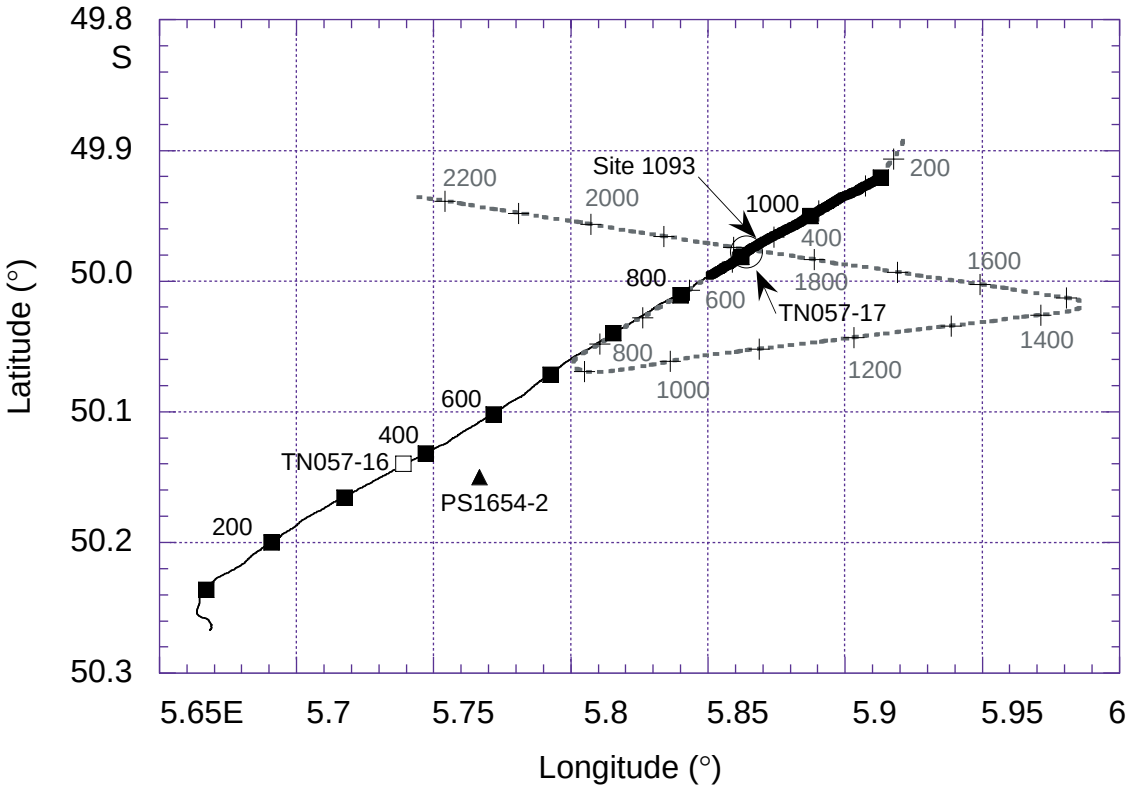

Figure F2. Segment of multichannel seismic Line AWI-94090 collected during site-survey *Polarstern* Cruise ANT-XI/3 showing the location and penetration depth of Holes 1093A–1093D. Depth was assigned according to the preliminary interval velocity estimates presented in Table T1, p. 66.

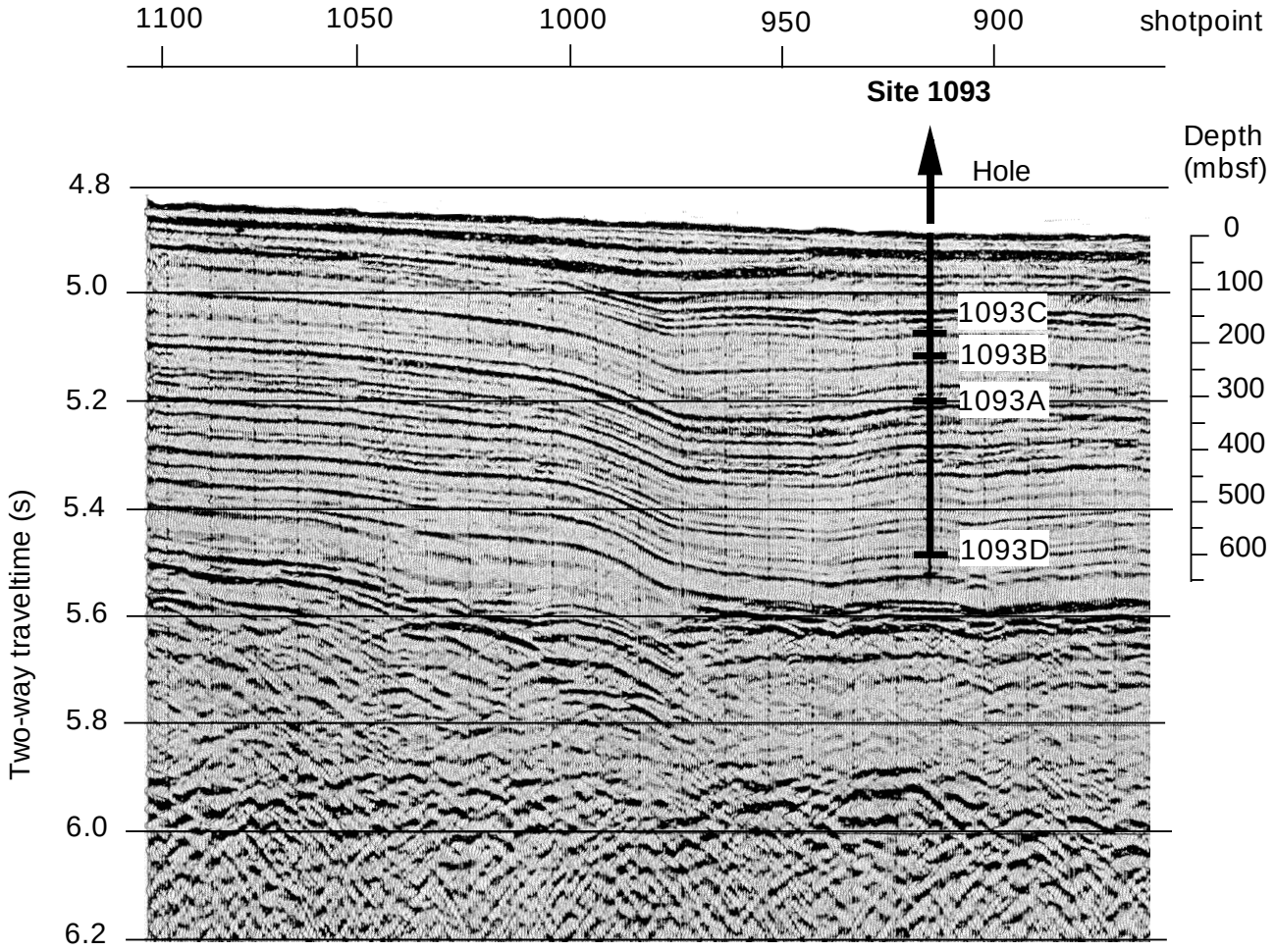

Figure F3. Lithologic summary showing core recovery, epoch, lithologic unit, graphic lithology, calcareous intervals, and diatom mats for Site 1093. Thicknesses of the calcareous intervals and diatom mats are only schematically represented, with true thicknesses and locations in each core accurately represented in the Site 1093 core correlation diagram (Fig. F5, p. 30). T.D. = total depth. (Continued on next two pages.)

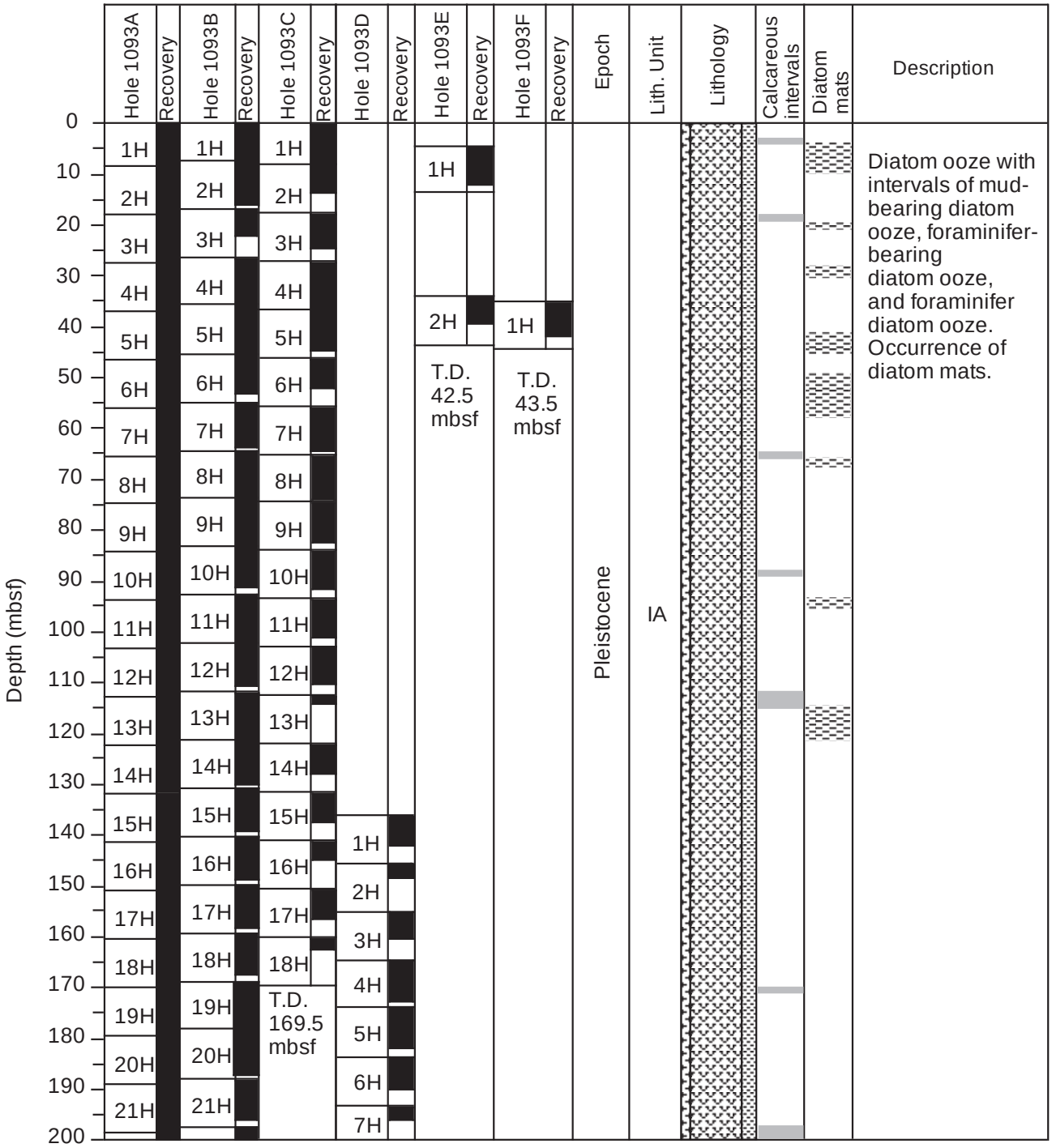

Figure F3 (continued).

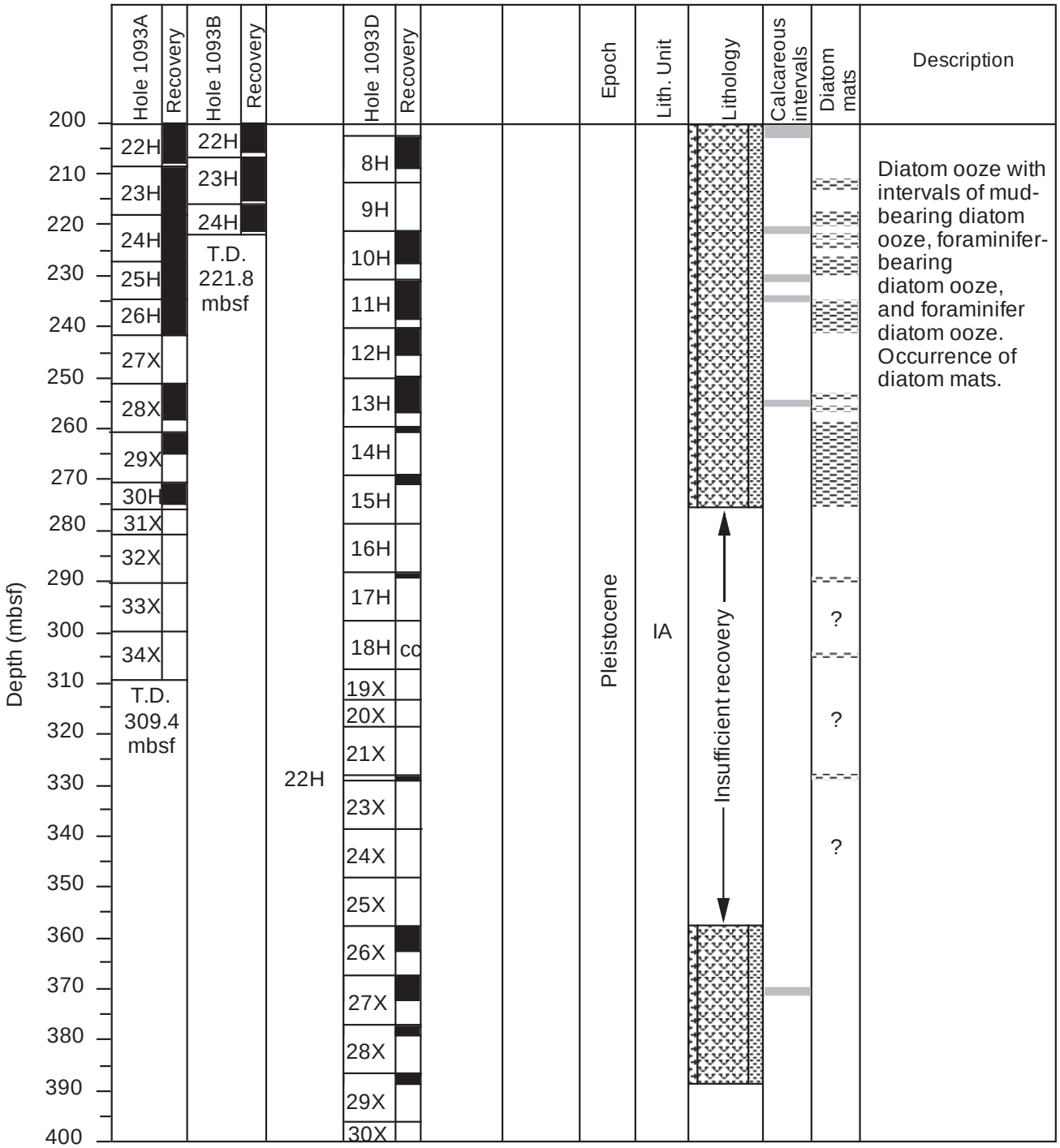

Figure F3 (continued).

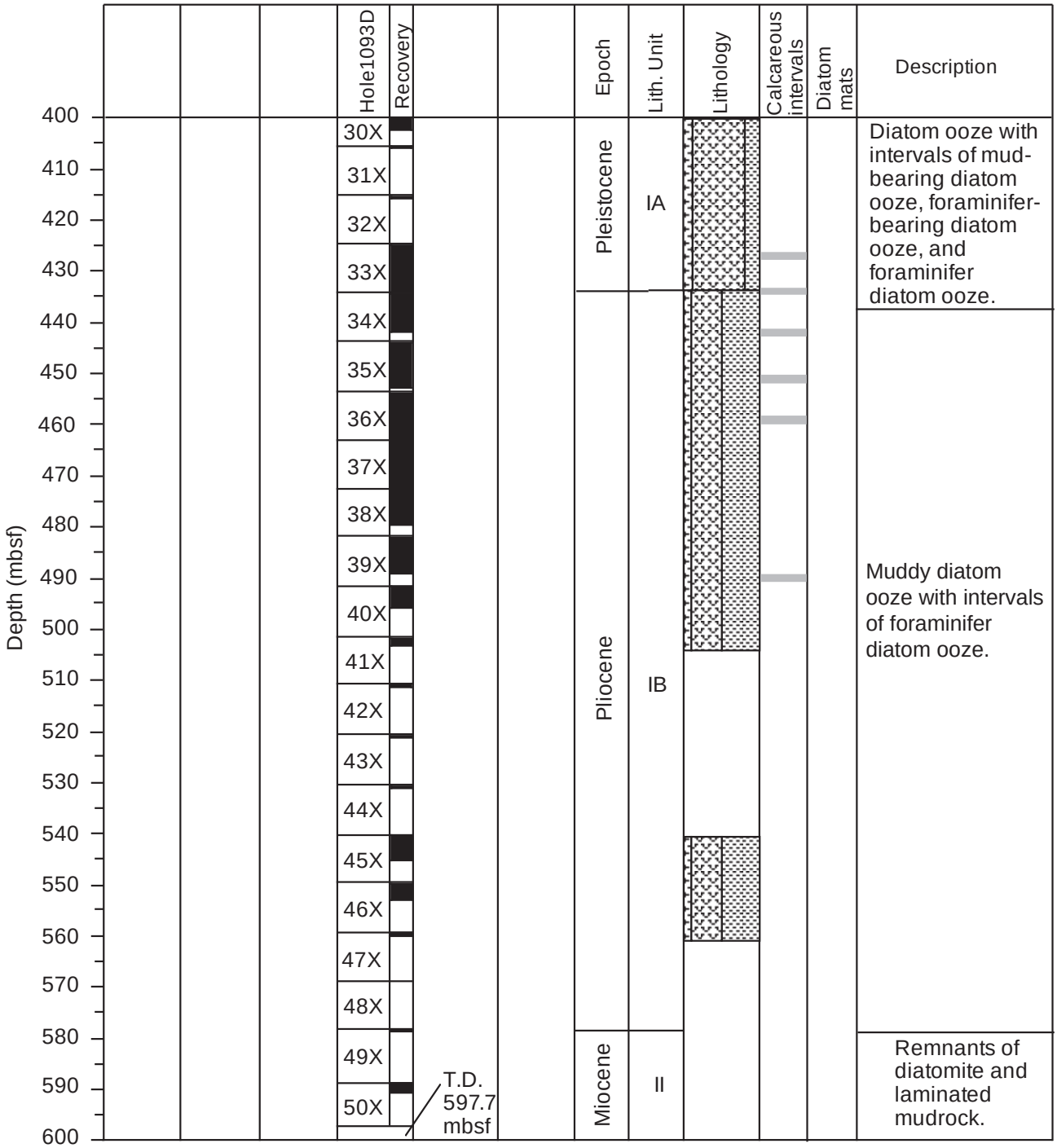

Figure F4. Downhole variations of carbonate, opal, and siliciclastic contents at Site 1093. Lithology inferred from smear-slide analysis (area percentage), coulometric carbonate determination, and quantitative XRD analysis of opal and siliciclastic concentrations.

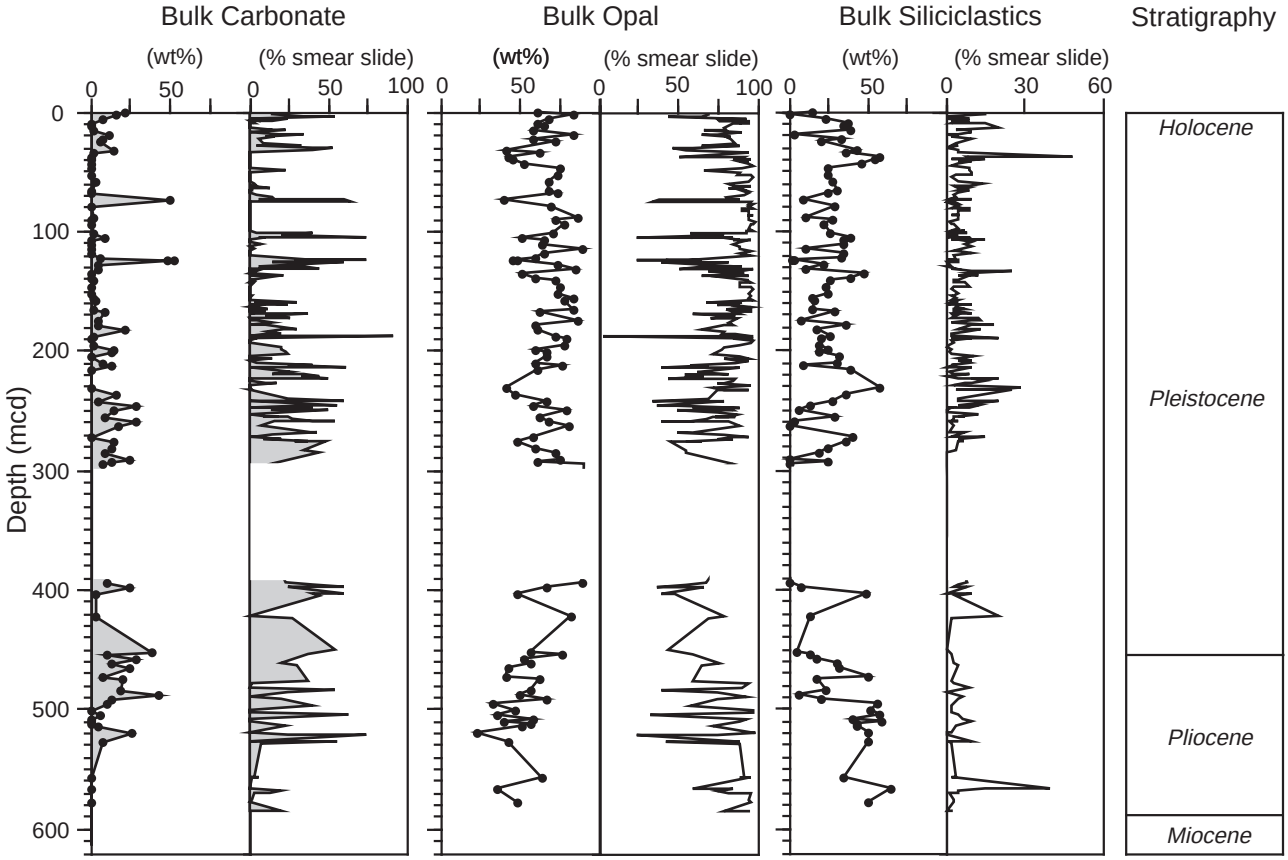

Figure F5. Core correlation diagram for Site 1093. Cores are plotted in mcd on the basis of lithologic correlation and MST data. Gray tones represent color variations from pale tan to dark grayish green. (Continued on next six pages.)

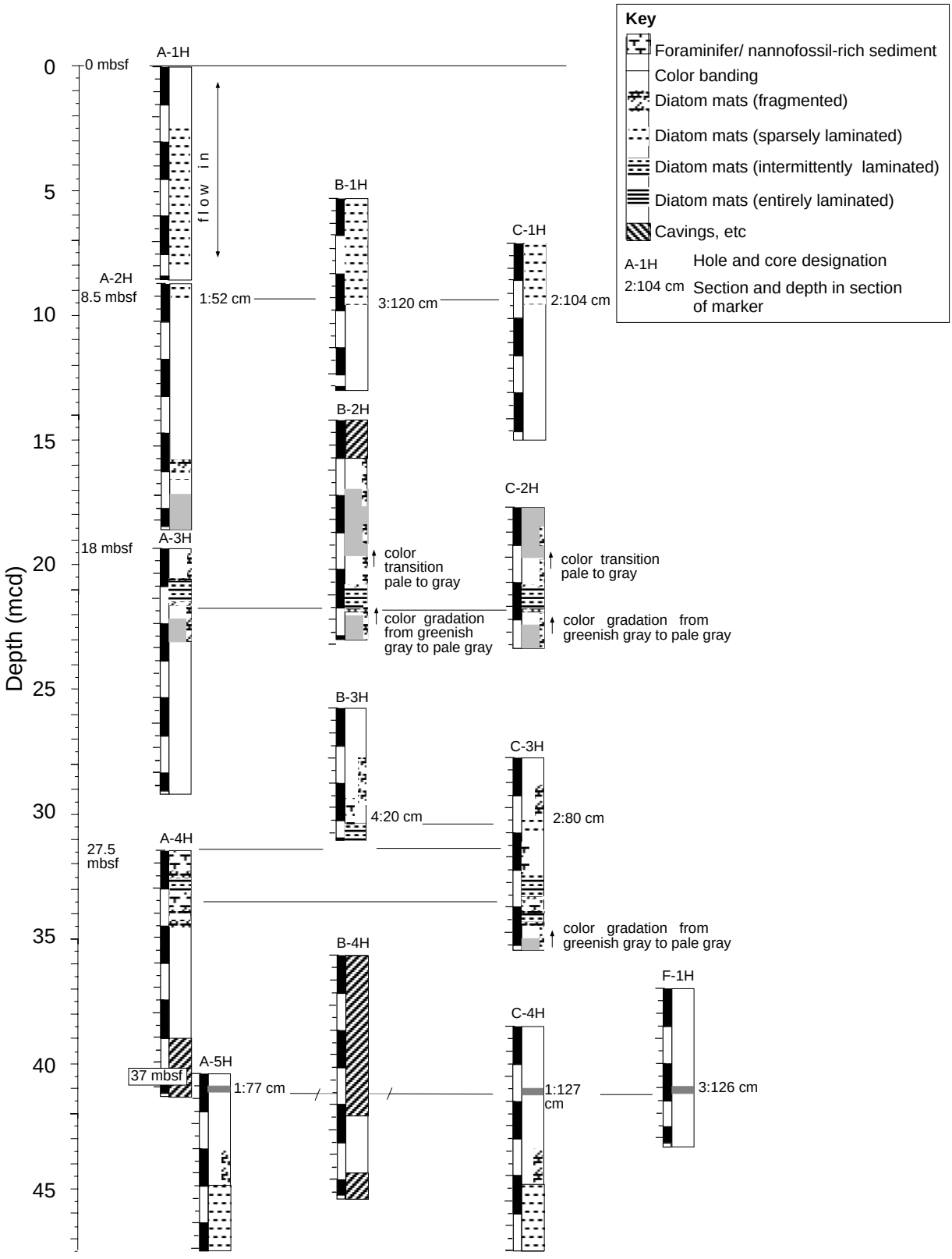

Figure F5 (continued).

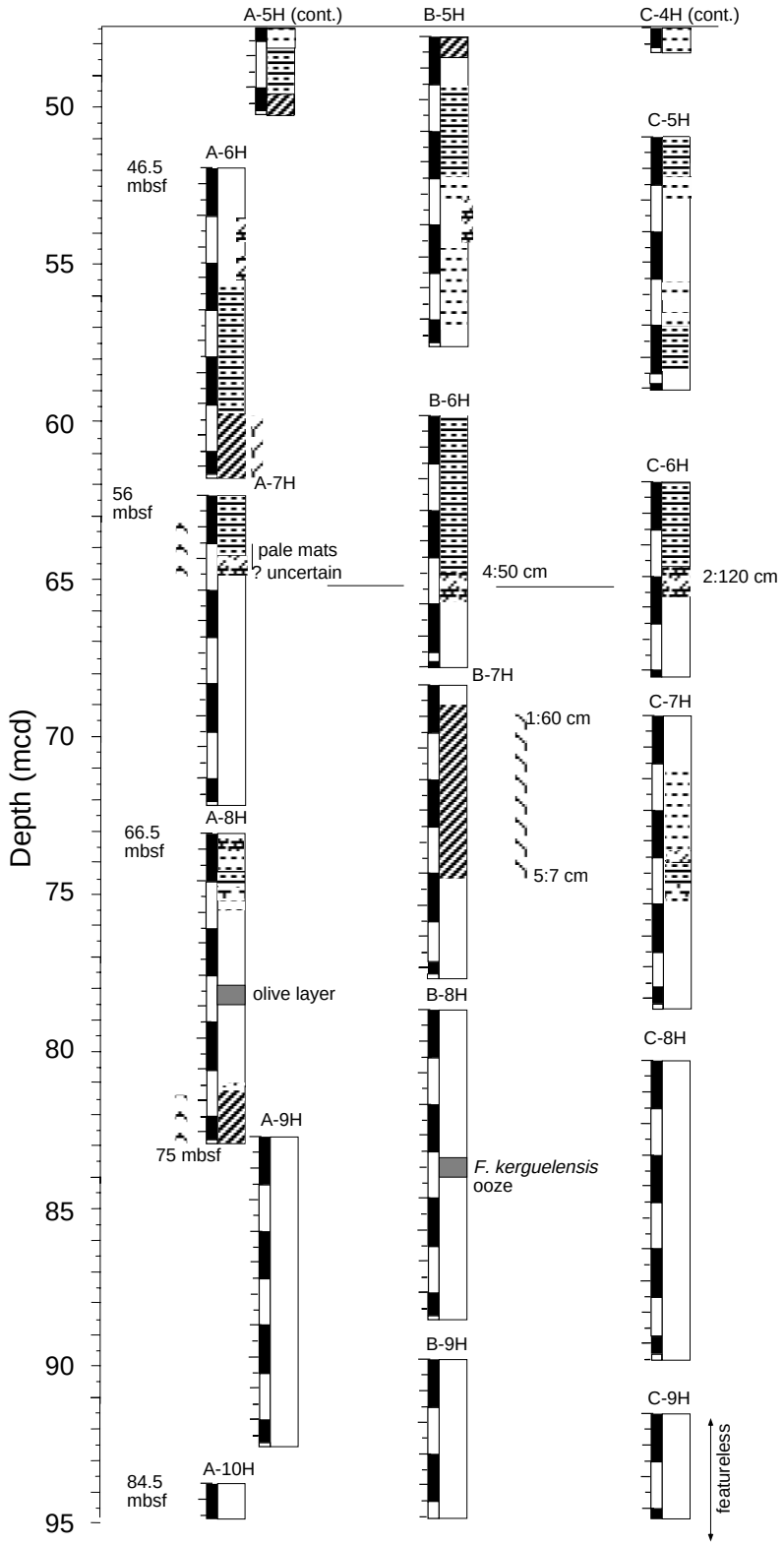

Figure F5 (continued).

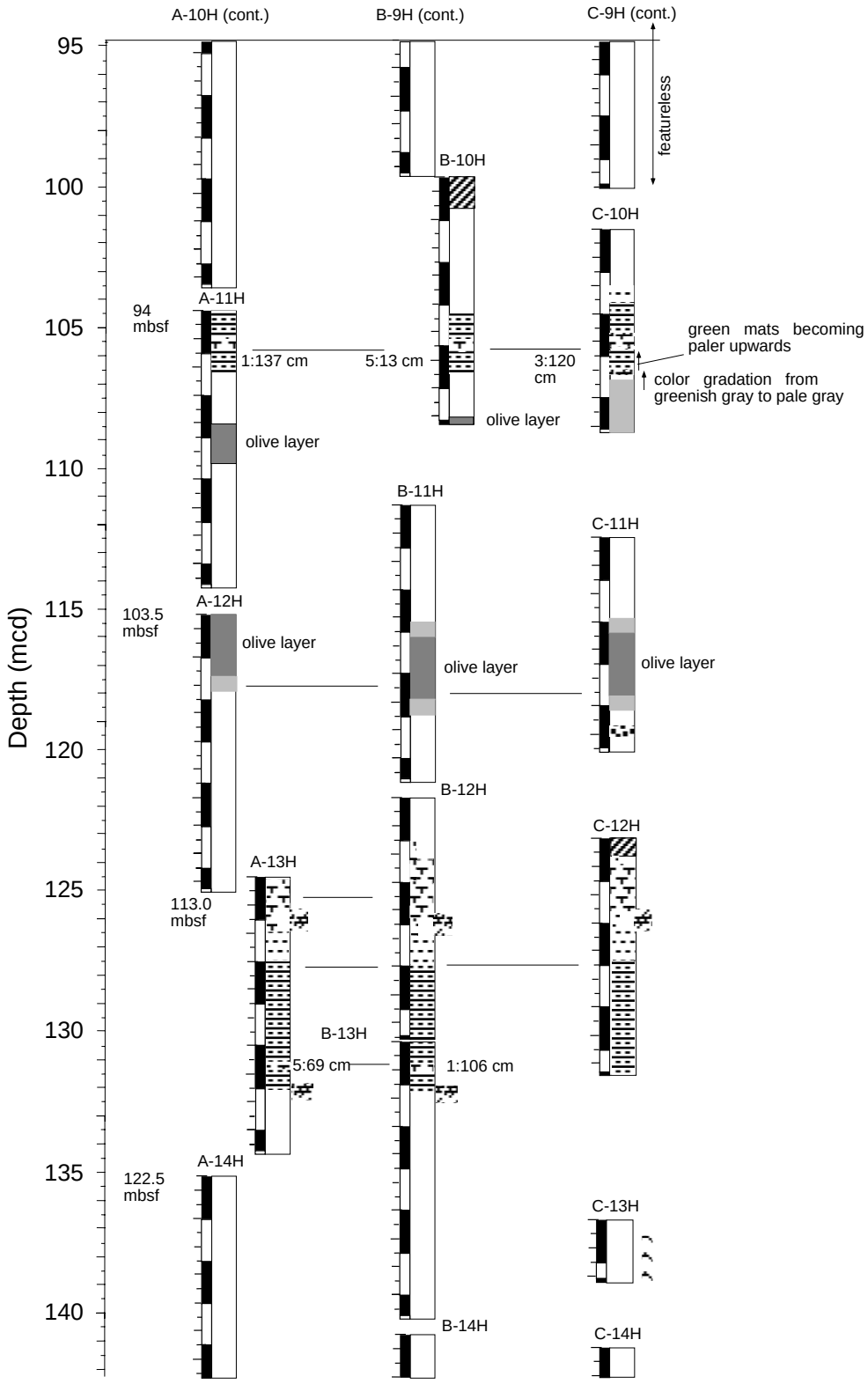

Figure F5 (continued).

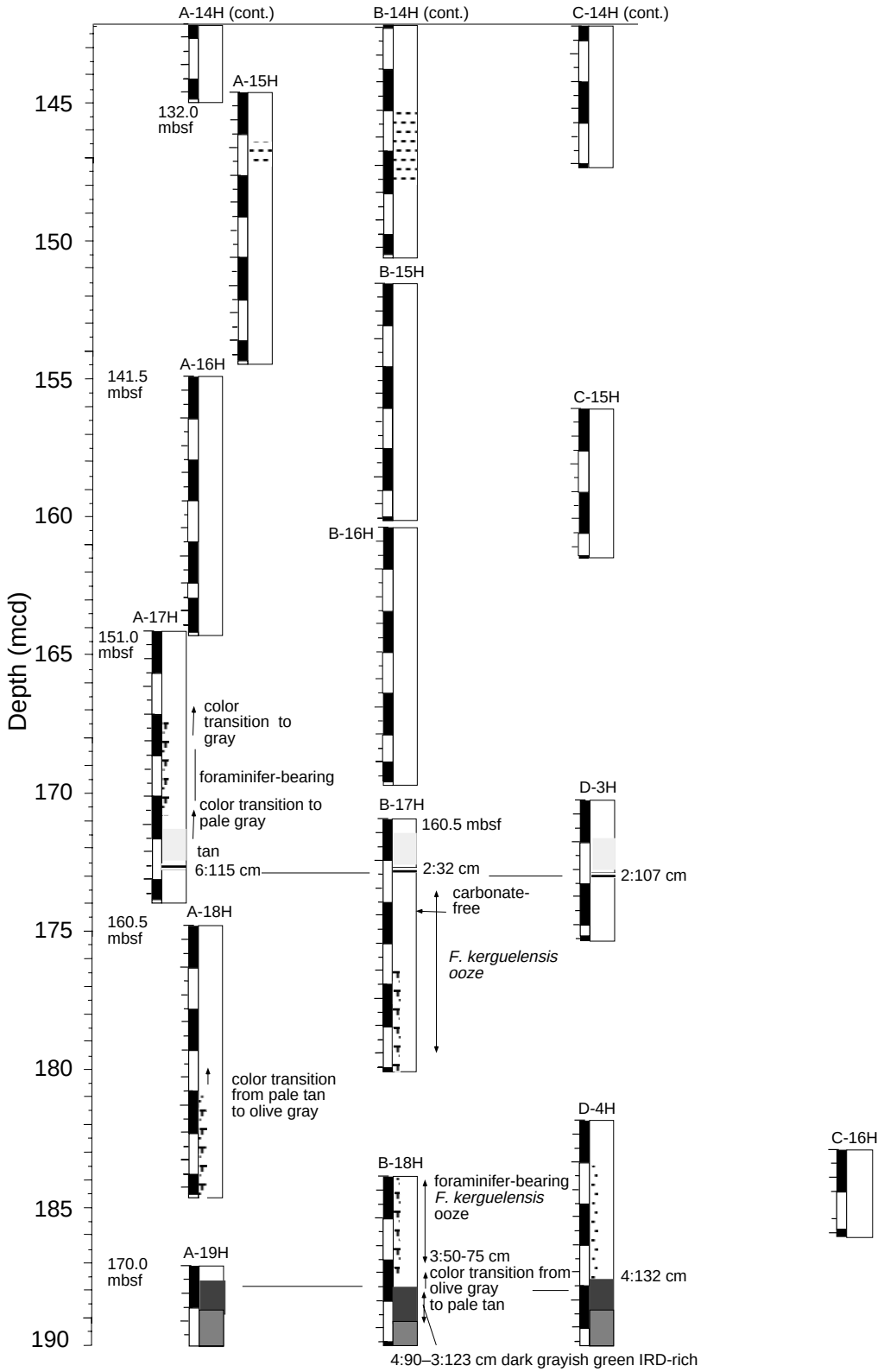

Figure F5 (continued).

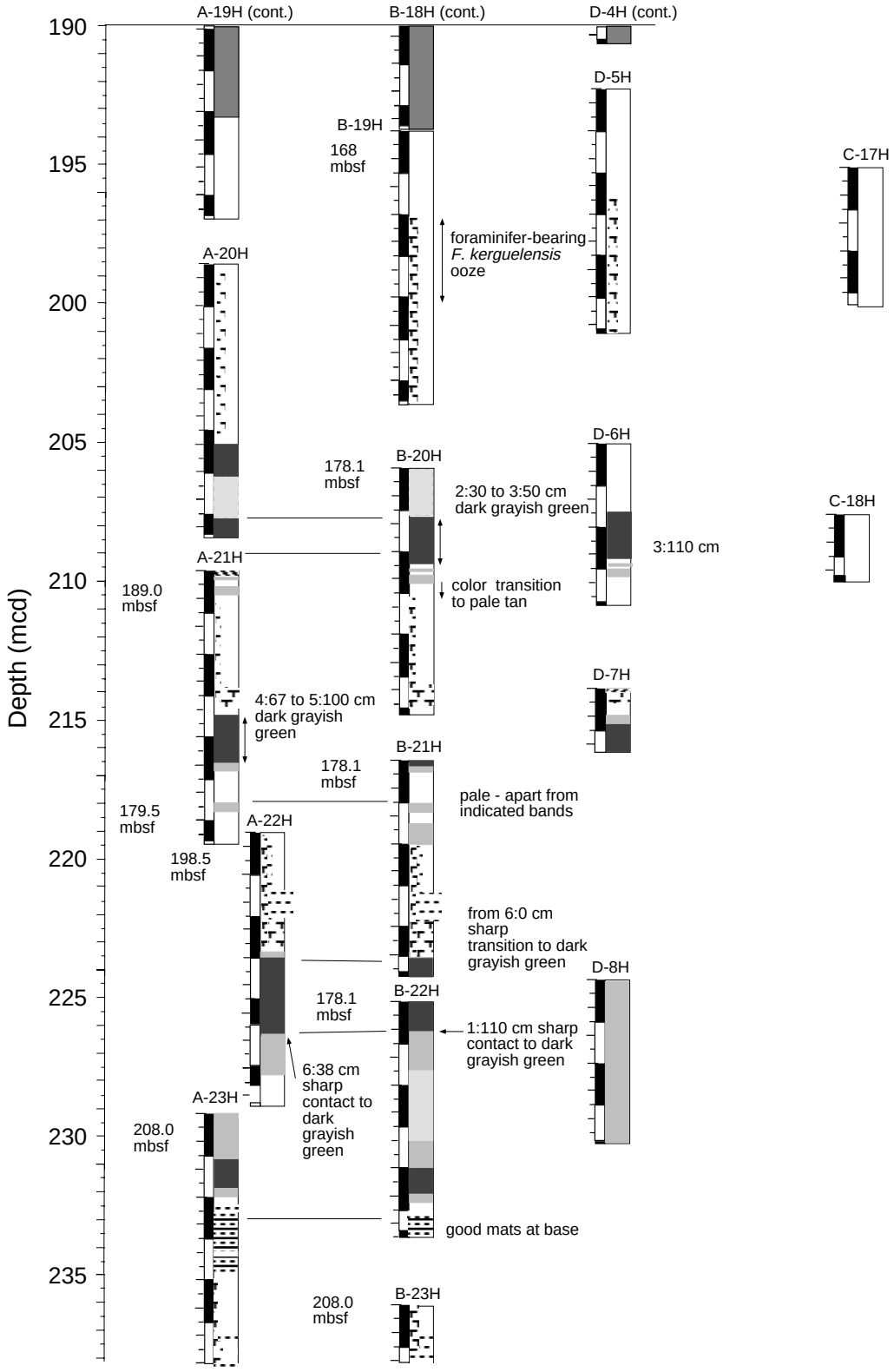

Figure F5 (continued).

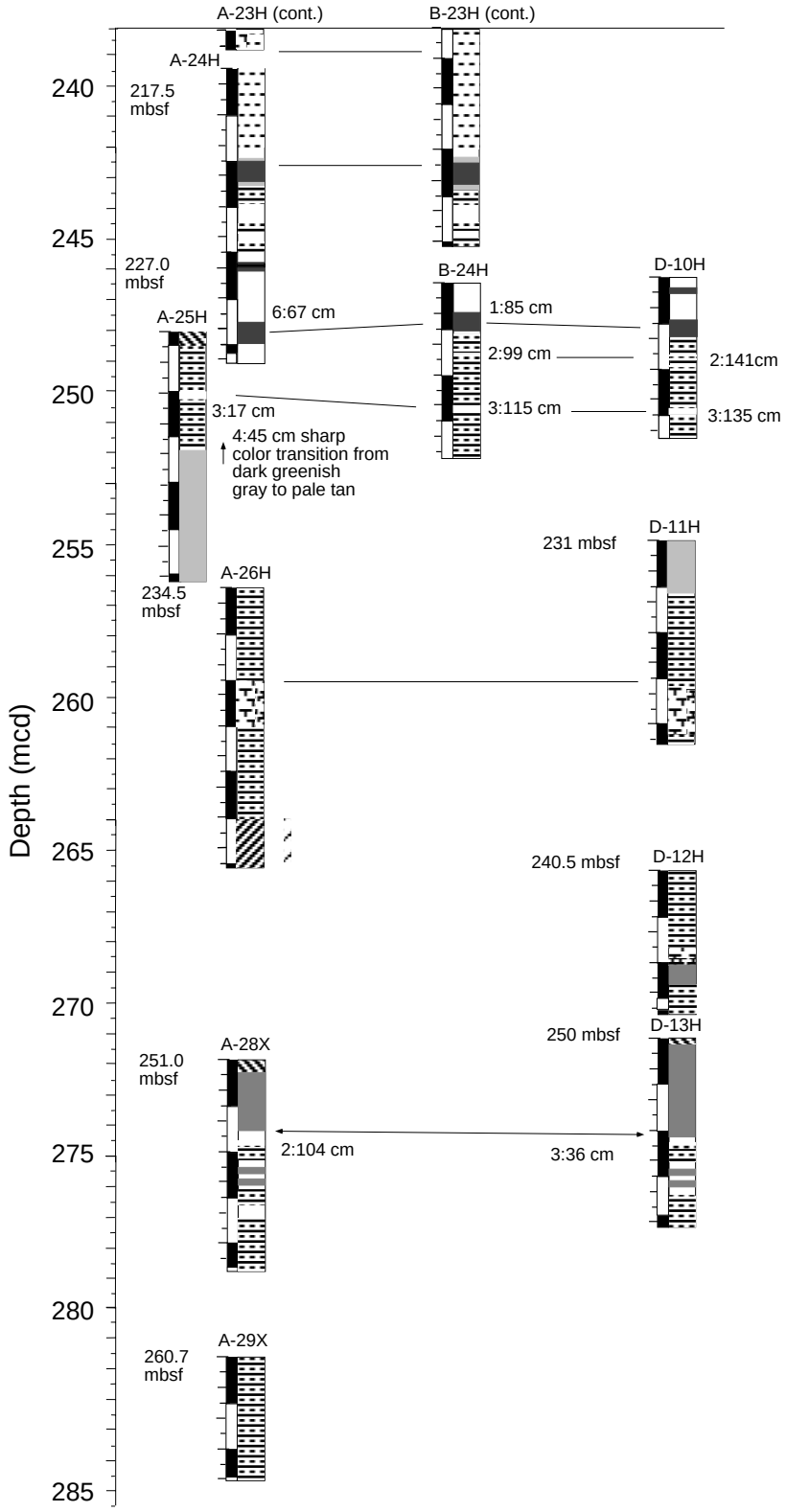

Figure F5 (continued).

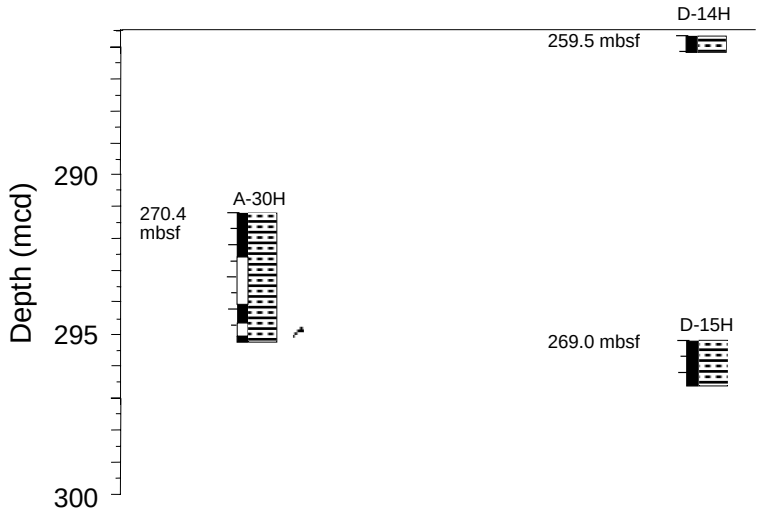

Figure F6. Ice-rafted debris layer, composed of volcaniclastic gravel and intercalated within mud-bearing diatom ooze of lithostratigraphic Subunit IA, probably representing a residual deposit (interval 177-1093C-11H-5, 65–110 cm).

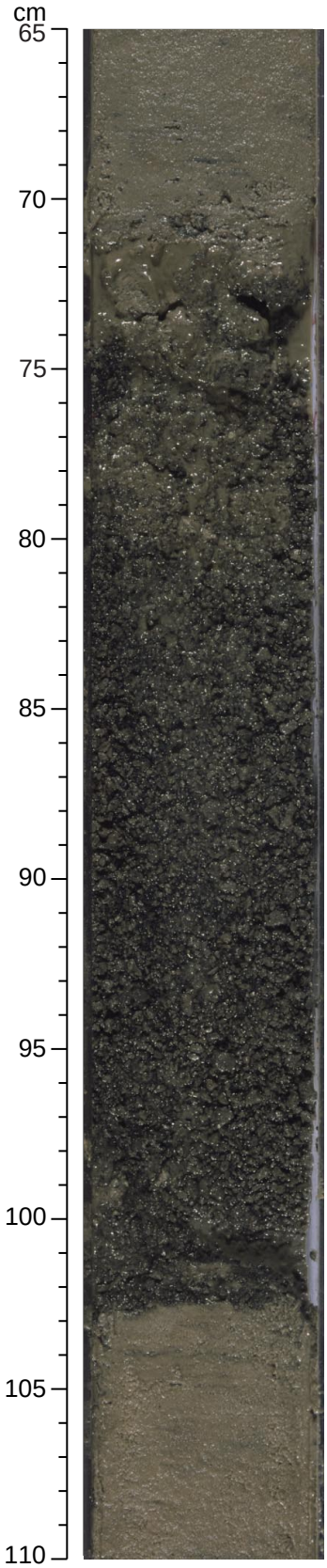

Figure F7. Diatom mat in lithostratigraphic Subunit IA, with characteristic rough spongy surface texture observed after scraping (interval 177-1093A-4H-2, 10–35 cm).

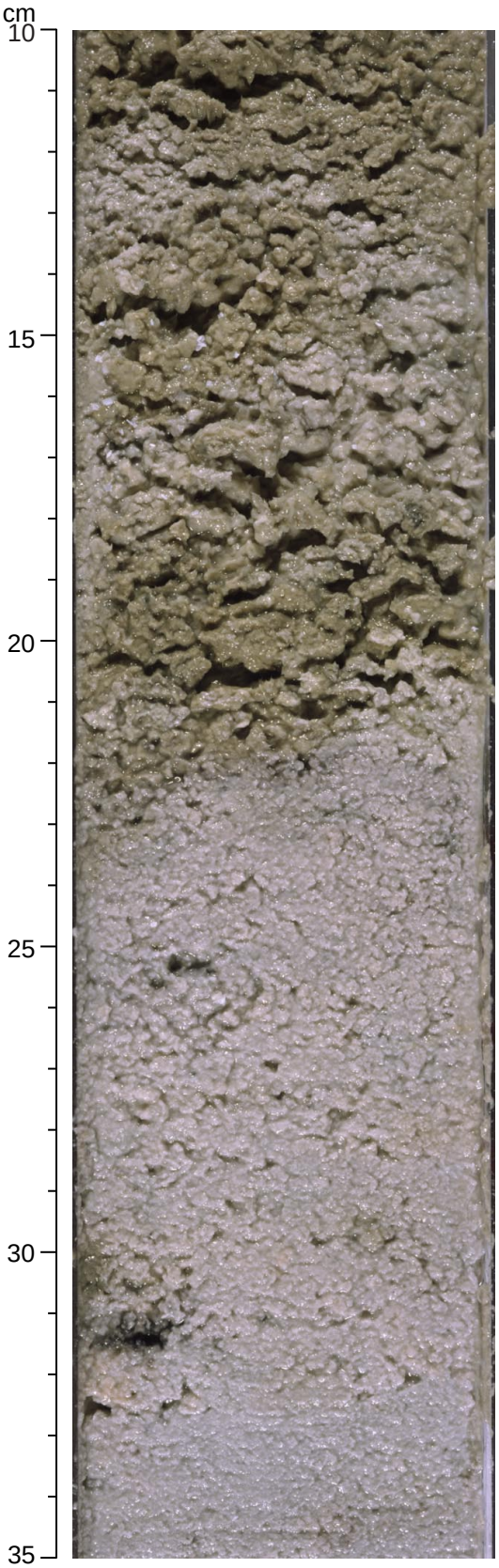

Figure F8. Color-laminated diatom mat in lithostratigraphic Subunit IA (interval 177-1093A-23H-4, 78–120 cm).

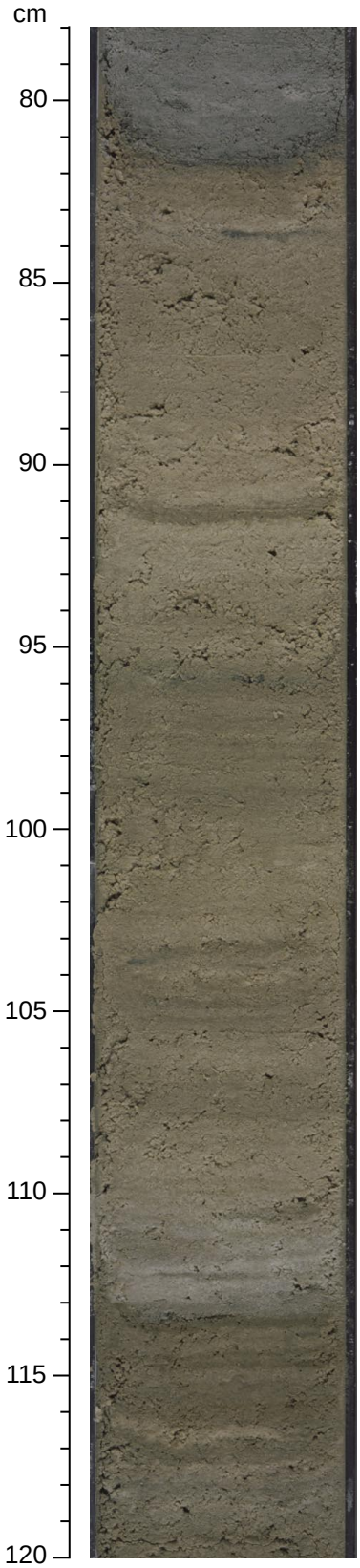

Figure F9. Compacted color-laminated diatom mat within muddy diatom ooze of lithostratigraphic Subunit IB (interval 177-1093D-38X-4, 110–136 cm).

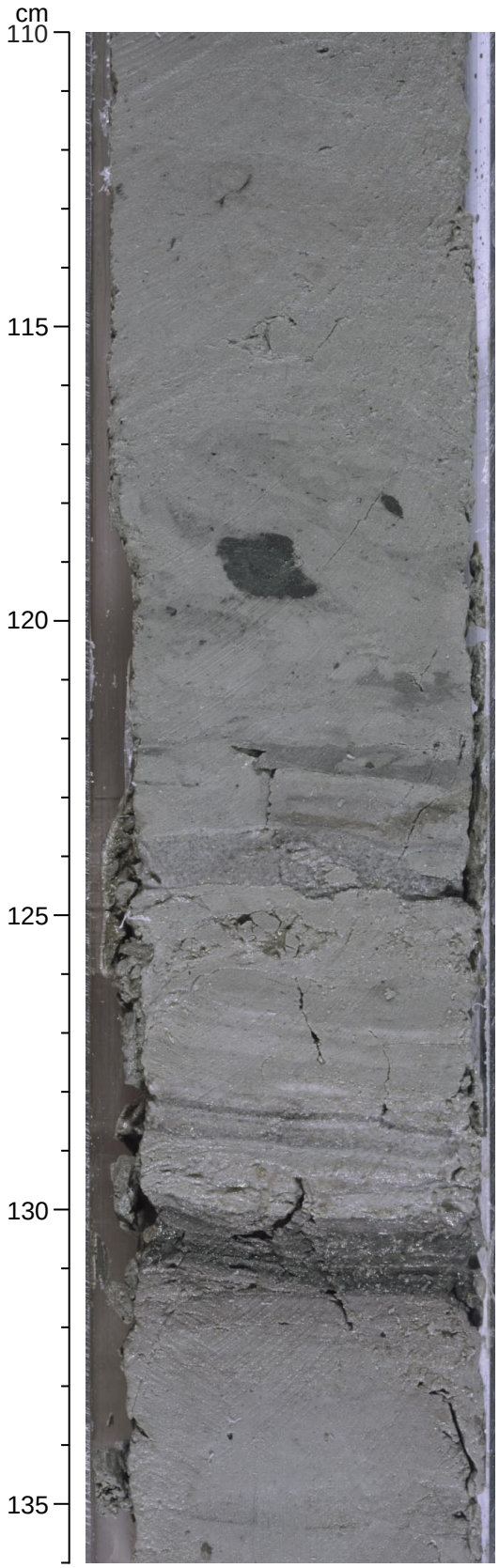

Figure F10. Smoothed (5-point average) color reflectance data (650–750 nm) for Site 1093. Holes 1093A through 1093F (curves arranged from left to right) are horizontally offset from each other by a constant (10%). Data from the top 20 cm of most cores have been removed. Note the difference in horizontal scale for the 0- to 50-mcd panel.

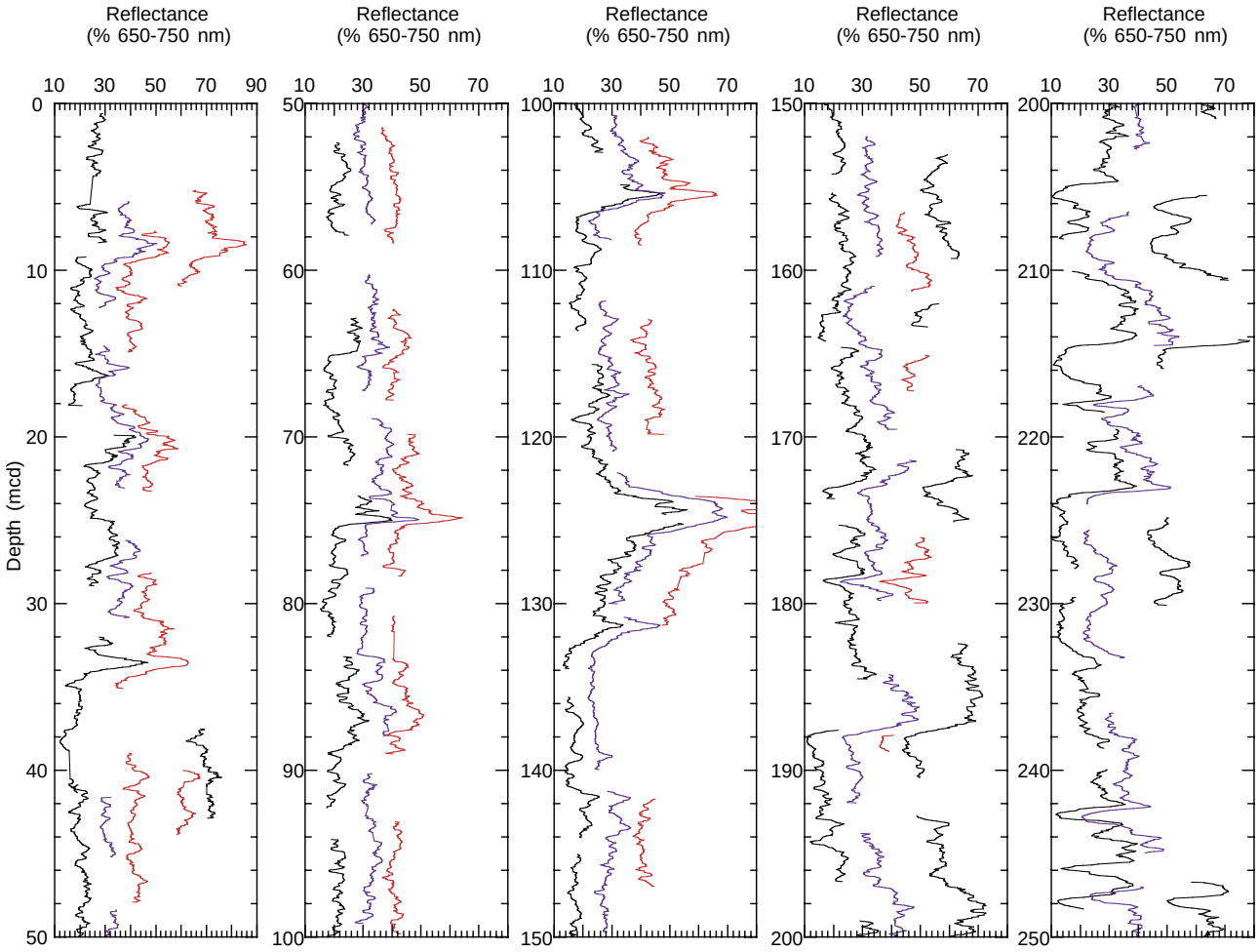

Figure F11. Smoothed (5-point average) magnetic susceptibility data (converted from instrument units to SI units) for Site 1093. Holes 1093A through 1093F (curves arranged from left to right) are horizontally offset from each other by a constant (5×10^{-5} SI units). Data from the top 20 cm of most cores have been removed. Note the change in horizontal scale for the 0- to 50-mcd and 200- to 250-mcd panels.

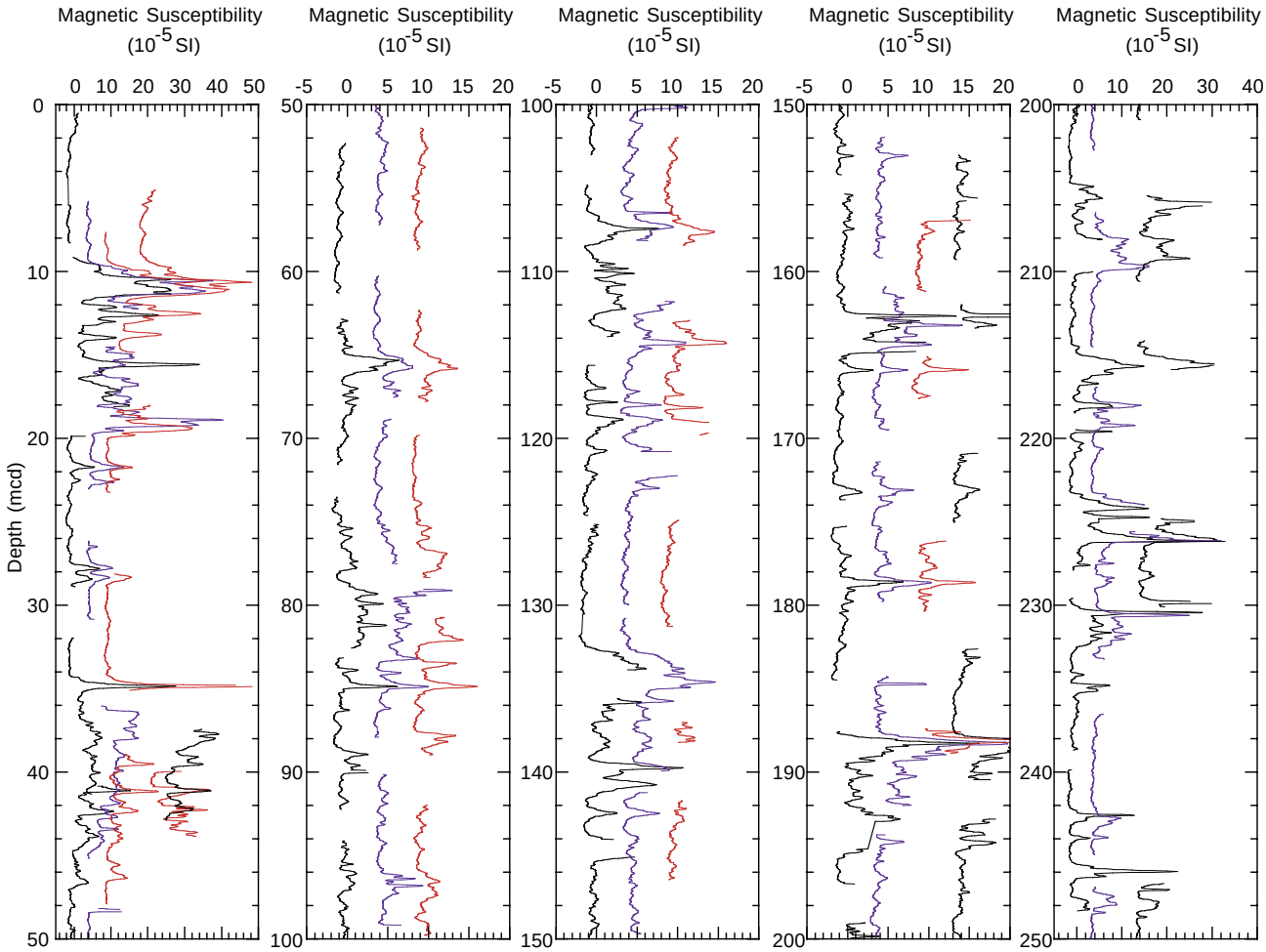

Figure F12. Smoothed (5-point average) GRA bulk density data for Site 1093. Holes 1093A through 1093F (curves arranged from left to right) are horizontally offset from each other by a constant (0.10 g/cm^3). Data from the top 20 cm of most cores have been removed. Note the differences in horizontal scale.

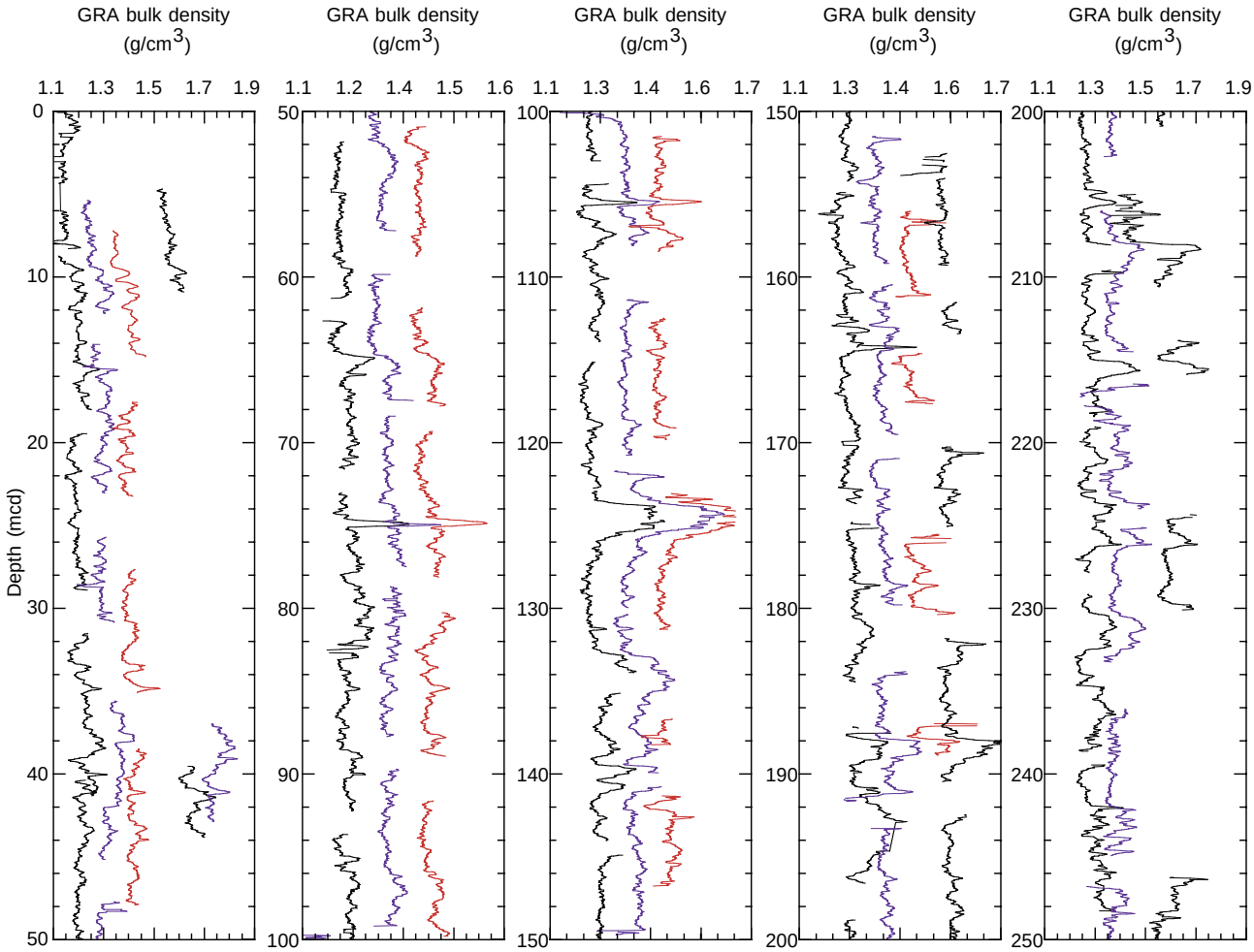

Figure F13. Spliced records of color reflectance, magnetic susceptibility, and GRA bulk density for Site 1093. All data sets were smoothed with a 5-point Gaussian filter. The horizontal lines in each plot identify the splice tie points (Table **T4,** p. 72).

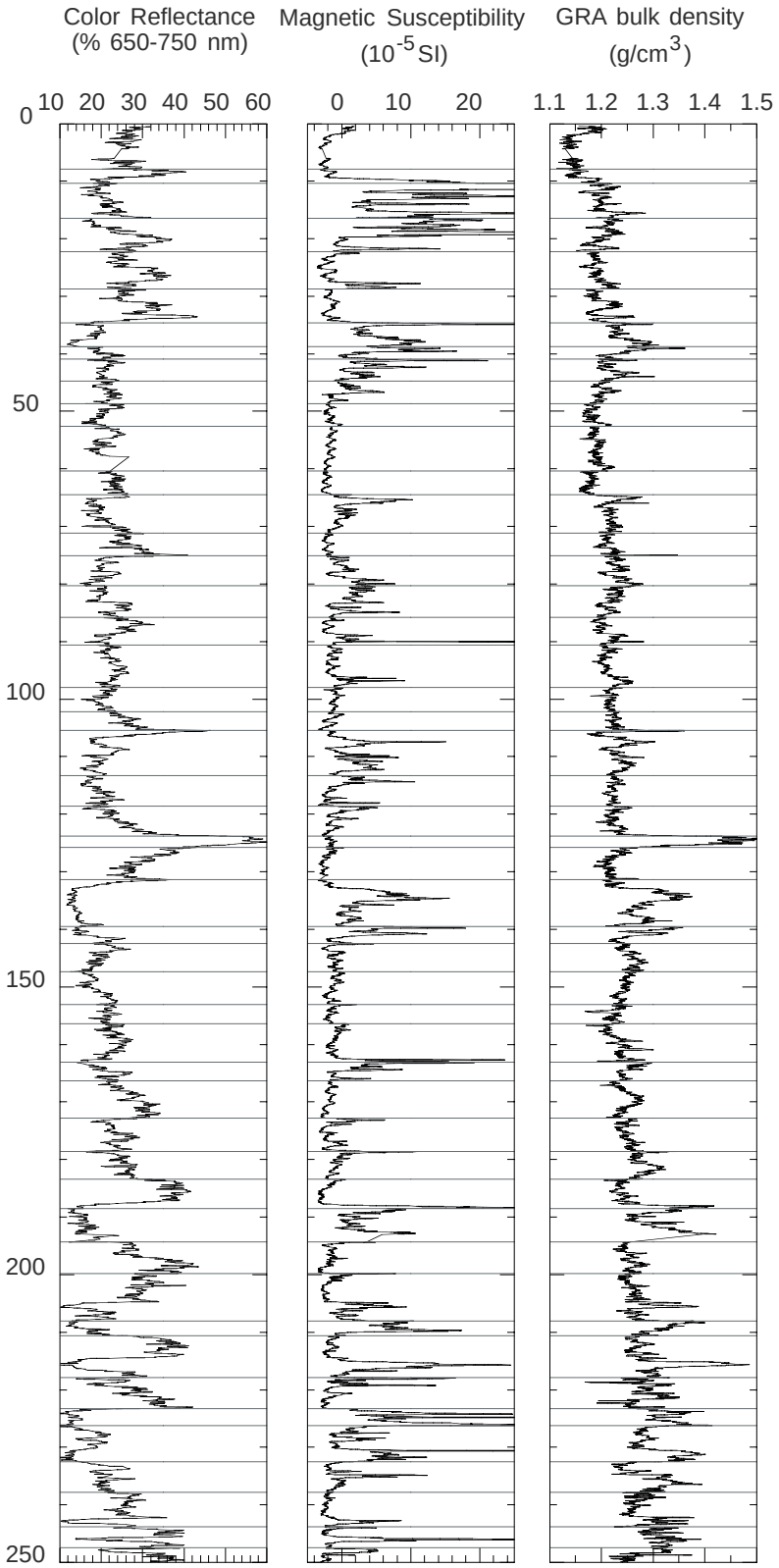

Figure F14. Biostratigraphic and magnetostratigraphic correlation chart for Site 1093, and selected absolute age designations. Dashed lines indicate possible hiatuses. Shaded intervals indicate sections with poor recovery. Magnetostratigraphy shading: black = normal polarity, white = reversed polarity. CN = calcareous nannofossils.

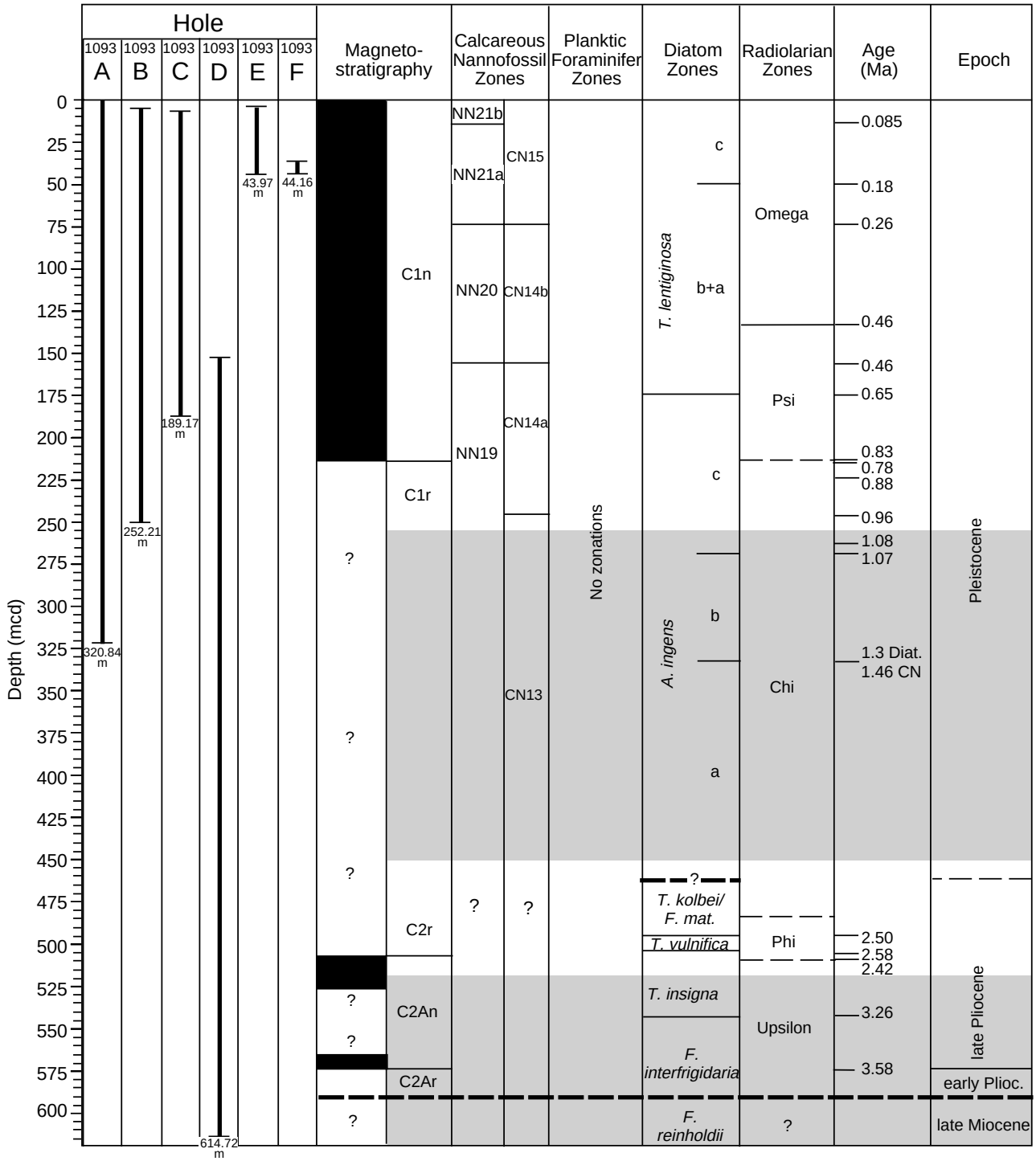

Figure F15. Age-depth plot of biostratigraphic and paleomagnetic events at Site 1093. Dashed lines indicate possible hiatuses. For age-depth assignments see Table T9, p. 87. The solid lines indicate a visual best fit through the age-depth control points. Corresponding sedimentation rate averages are given in parentheses.

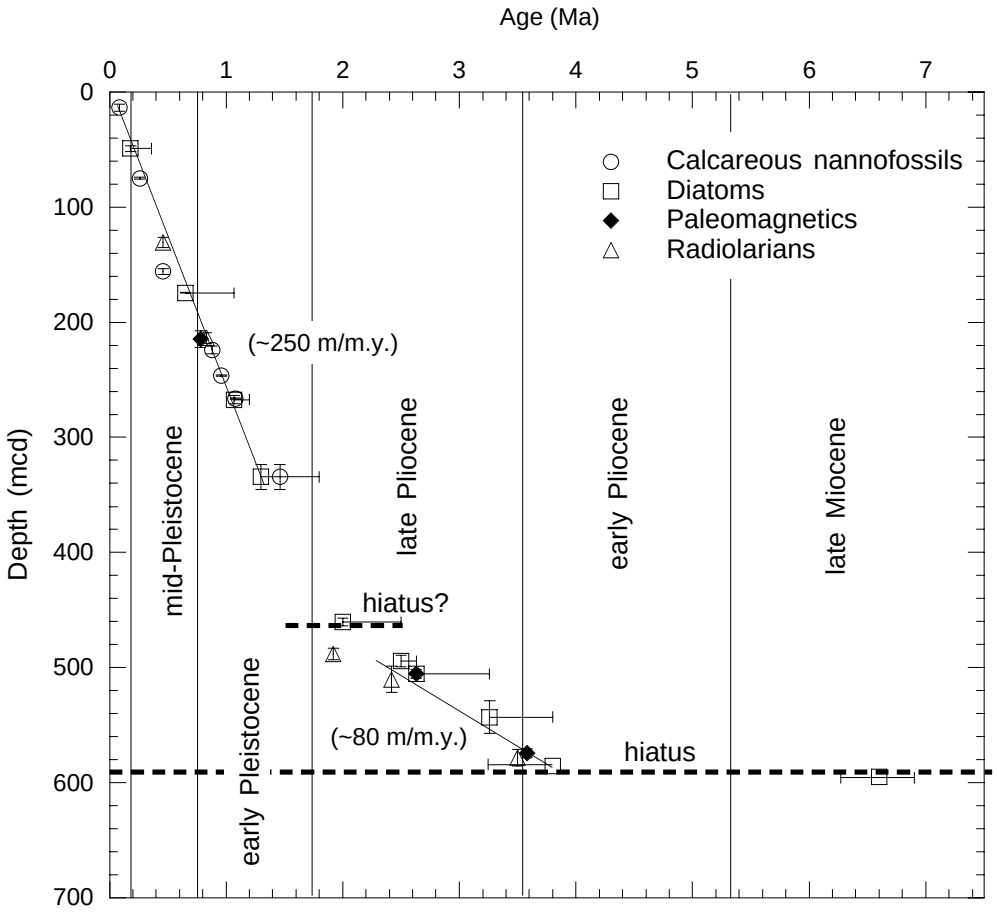

Figure F16. Inclination of the remanent magnetization after alternating-field demagnetization at peak fields of 25 mT for Holes 1093A and 1093B. The Brunhes and Matuyama Chrons are identified. Magnetic polarity shading: black = normal, white = reversed.

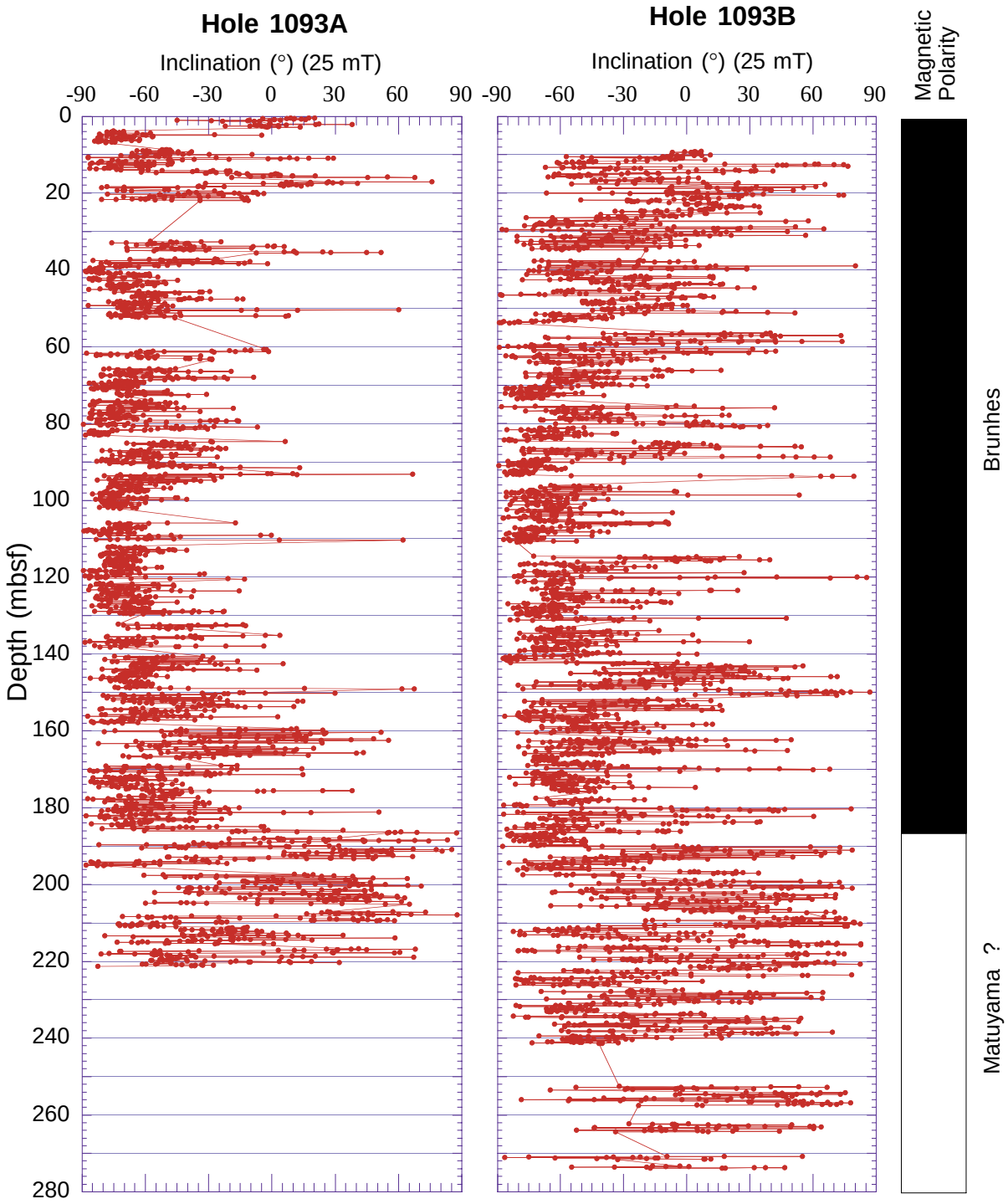

Figure F17. Inclination of the remanent magnetization after alternating-field demagnetization at peak fields of 25 mT for the XCB section at Hole 1093D. The Matuyama, Gauss, and Gilbert Chrons are identified. Magnetic polarity shading: black = normal, white = reversed.

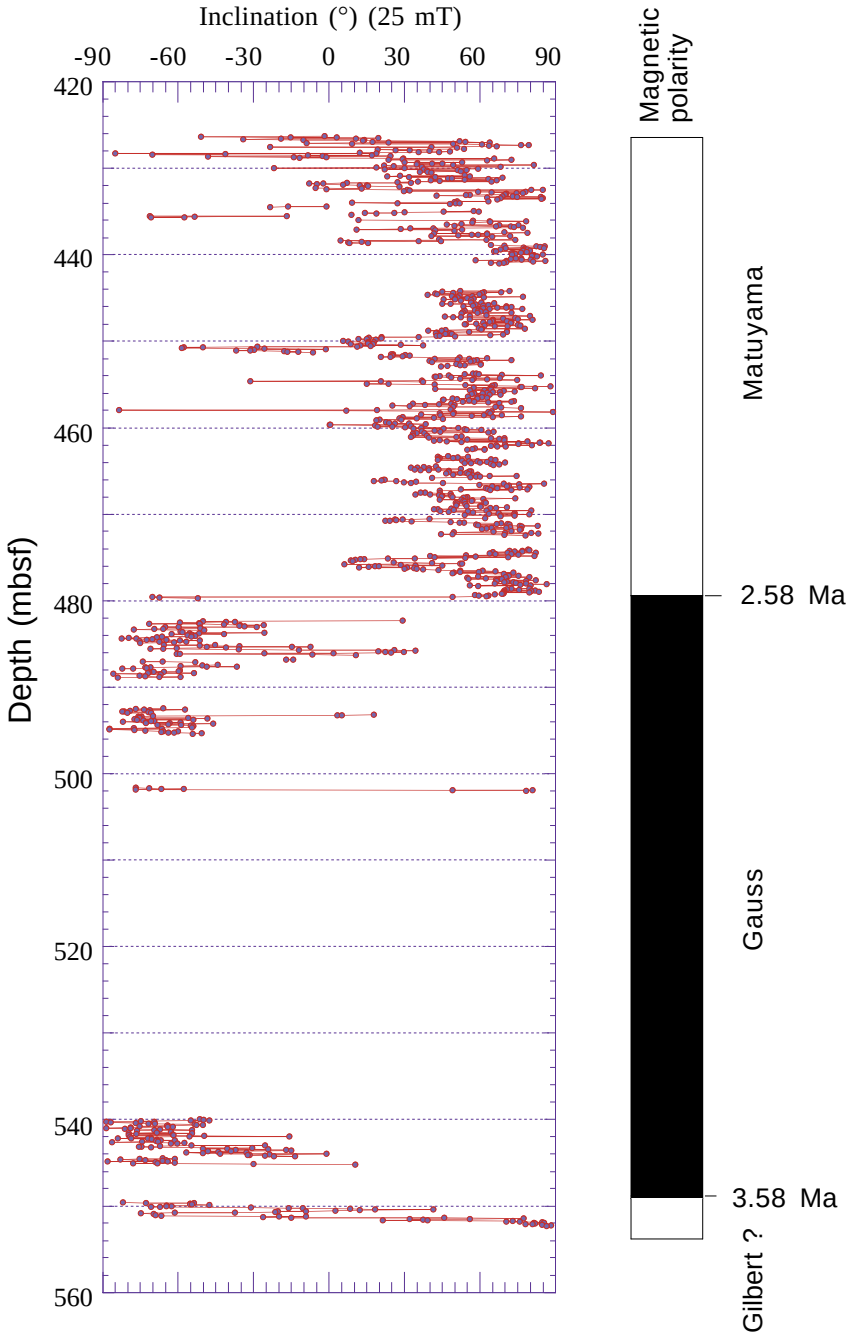

Figure F18. Concentration of methane vs. depth at Holes 1093A and 1093D; the data are reported in Table T12, p. 96.

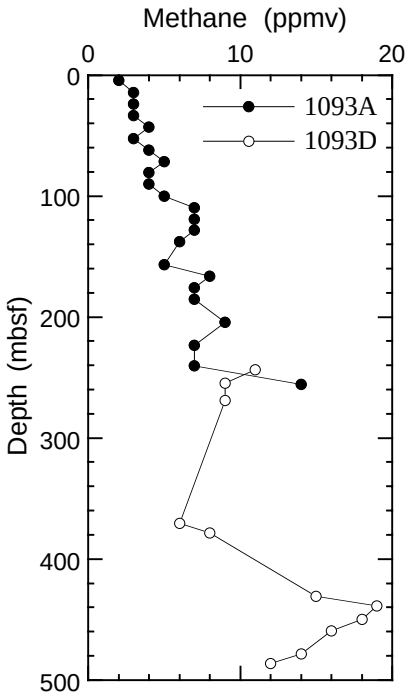

Figure F19. Interstitial water chemistry profiles vs. depth for chlorinity, alkalinity, pH, sodium, sulfate, calcium, magnesium, potassium, strontium, lithium, ammonium, phosphate, silica, manganese, and iron at Holes 1093A (open circles) and 1093D (solid circles); the data are reported in Table T13, p. 97.

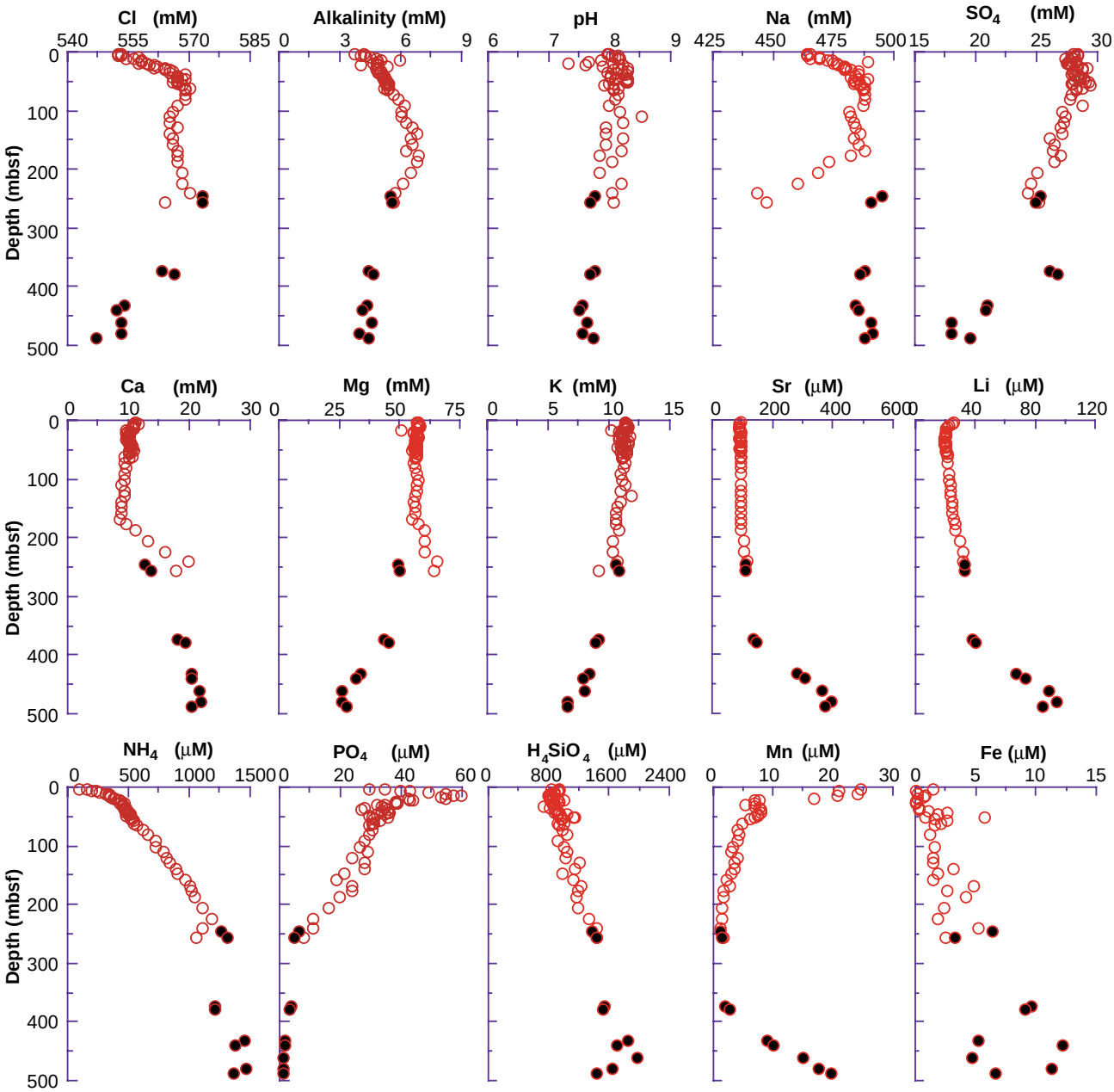

Figure F20. Concentration of calcium carbonate ($CaCO_3$), total organic carbon (TOC), total nitrogen (TN), total sulfur (TS), and TOC/TN vs. depth at Holes 1093A and 1093D; the data are reported in Table **T14,** p. 99.

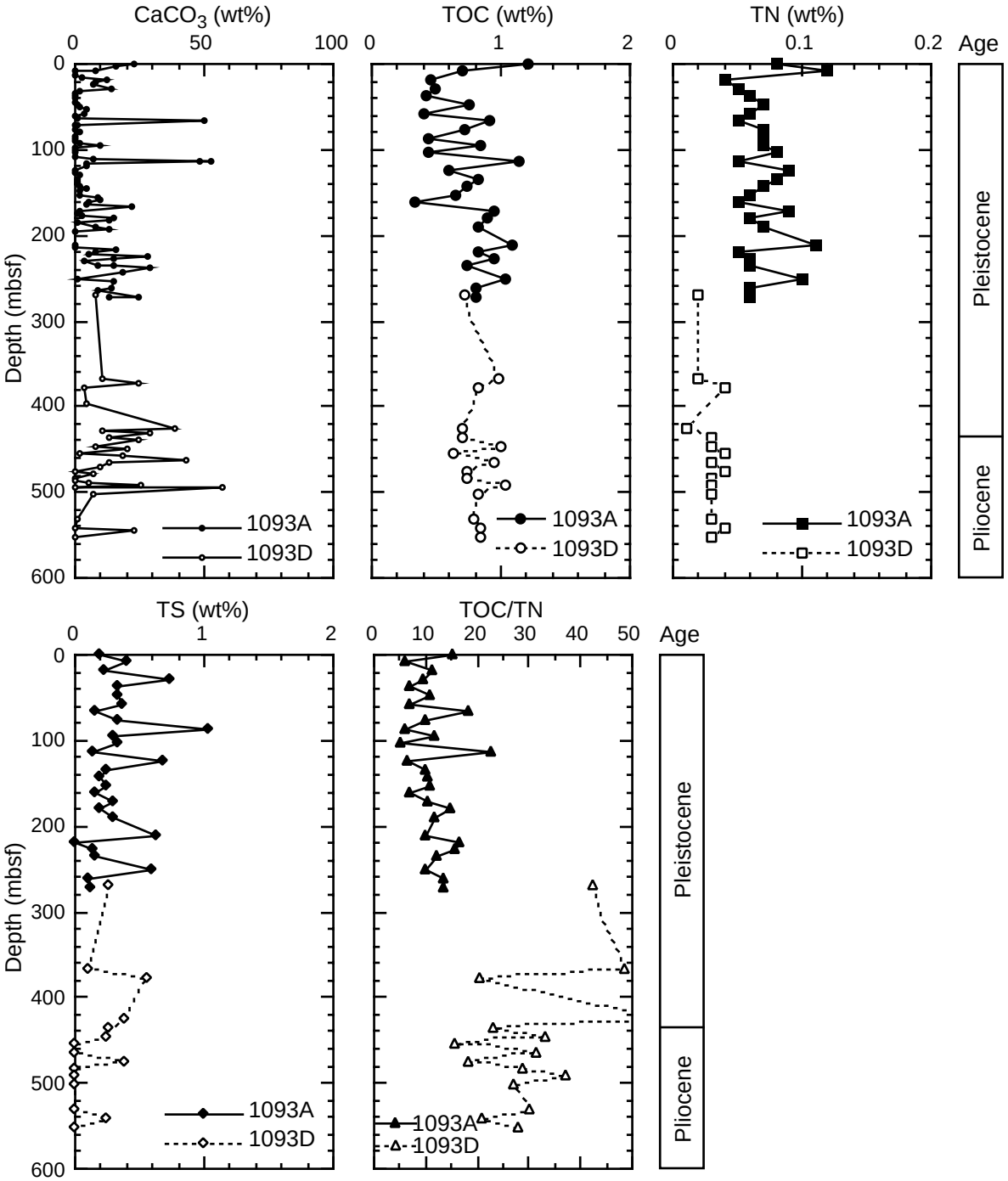

Figure F21. Total organic carbon (TOC) vs. total nitrogen (TN) at Hole 1093A. Lines show TOC/TN values of 5, 10, and 20.

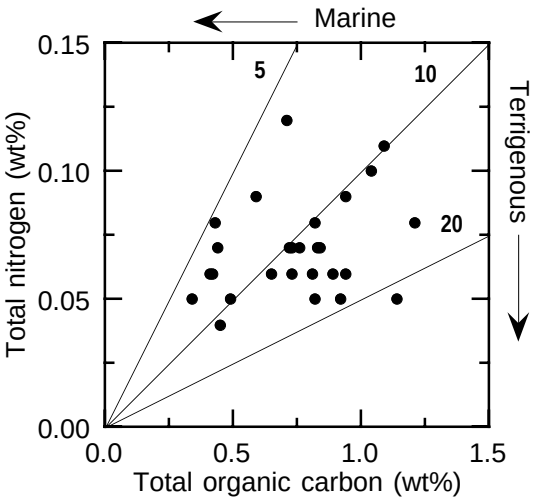

Figure F22. Site 1093 downhole variations of NGR (smoothed data), volume-specific magnetic susceptibility, porosity (open circles, MAD method) and OSU-SCAT resistivity (solid line), GRA bulk density (solid line = smoothed data) and MAD bulk density (open circles), and OSU-SCAT reflectance in the blue band. H = hiatus.

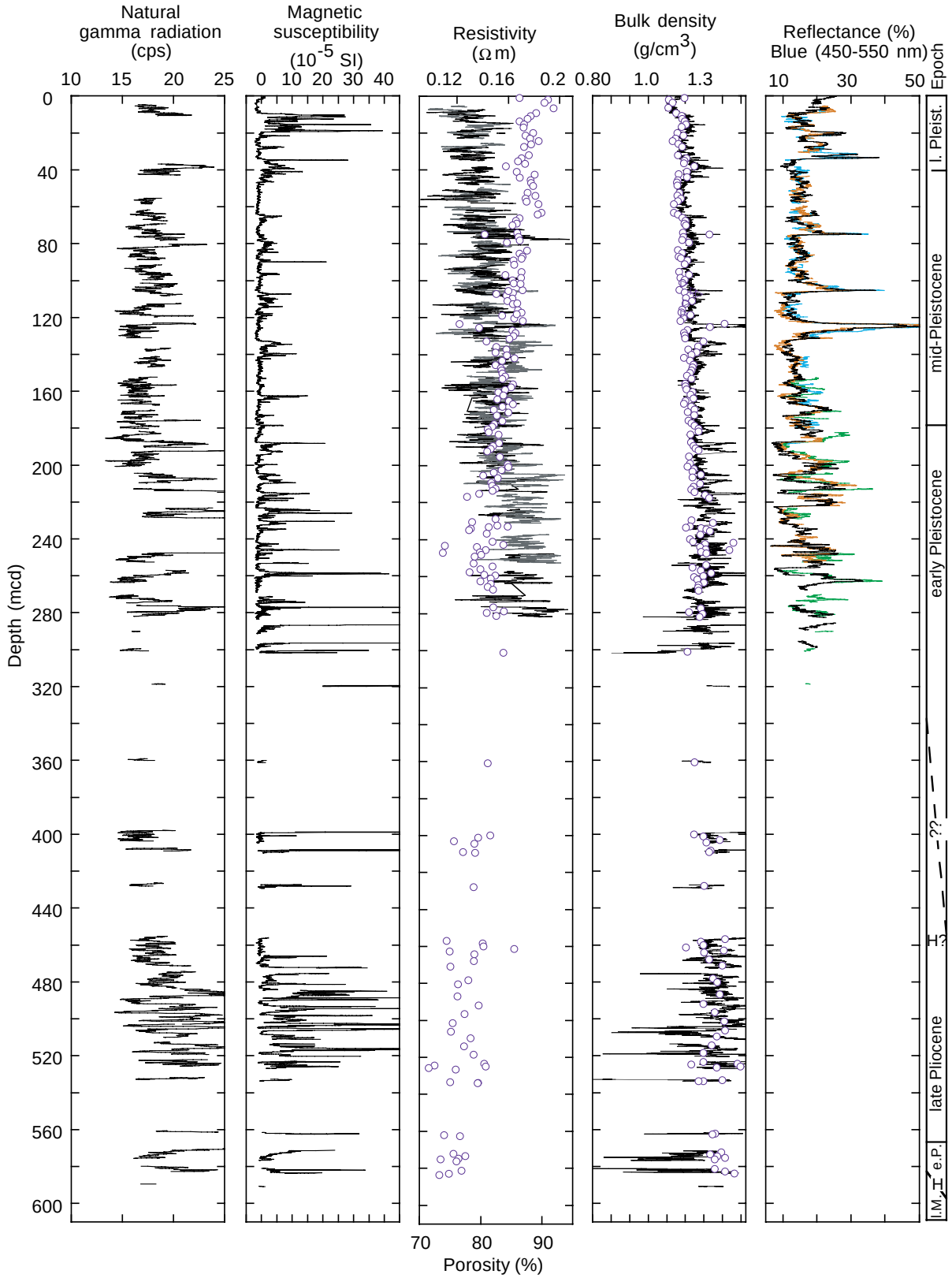

Figure F23. Relationship between GRA bulk density and gravimetric (MAD) bulk density at Site 1093.

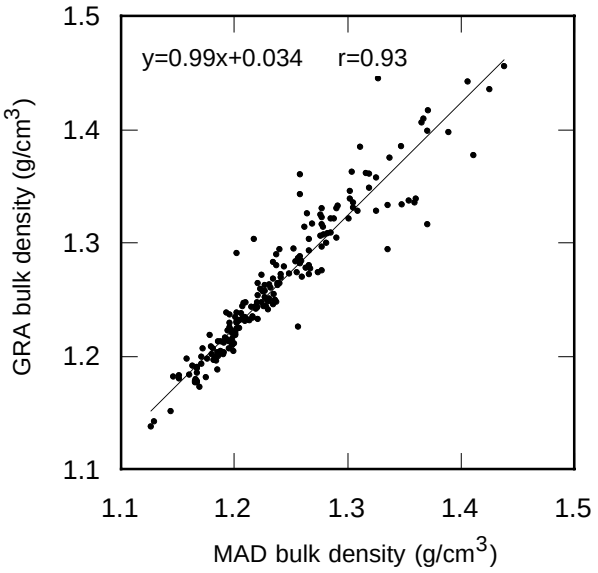

Figure F24. Preliminary correlation of reflectance (red/blue and blue band) between Sites 1093 (Holes 1093A and B) and 1091 (Holes 1091A and B). Thin subhorizontal lines = correlation points.

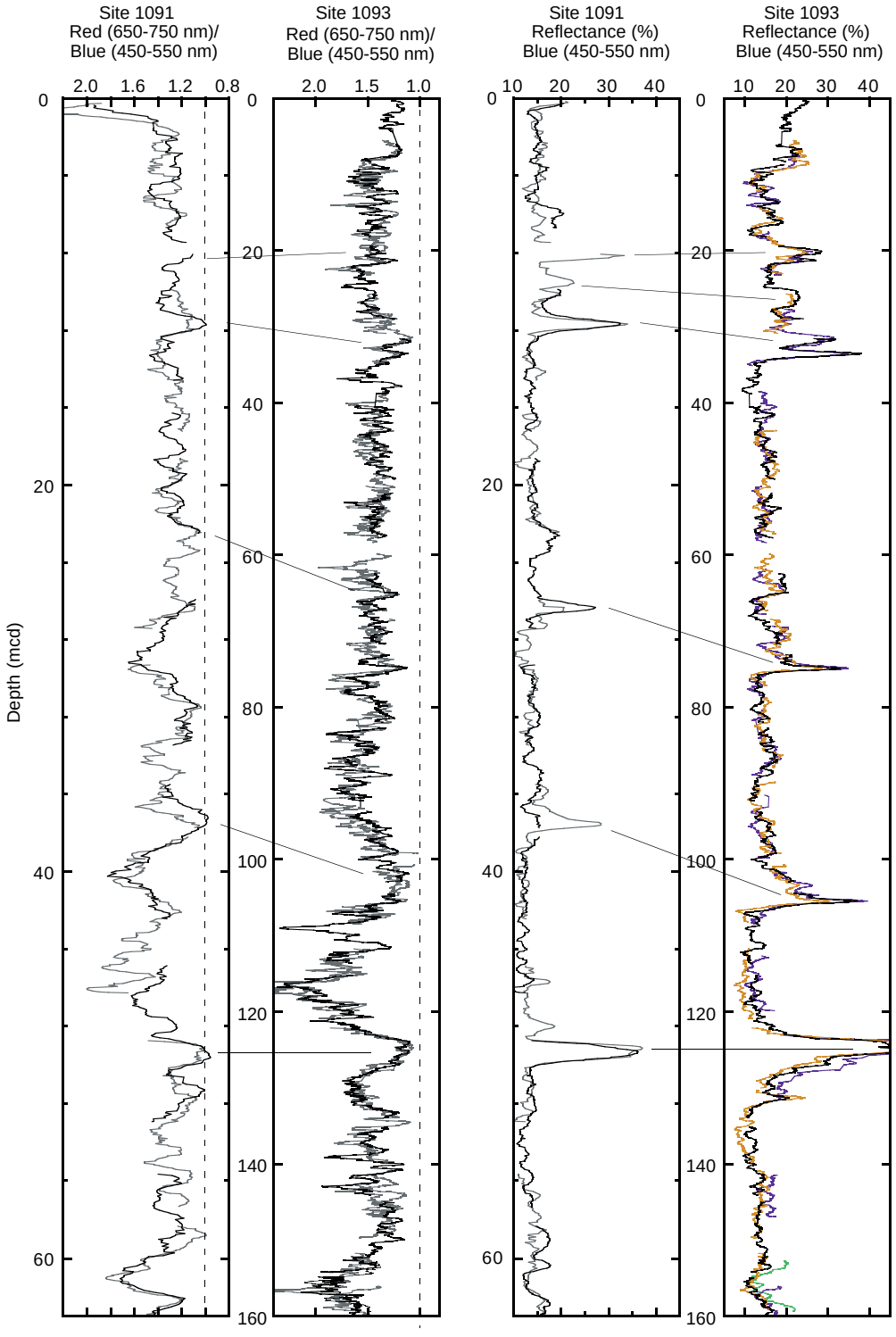

Figure F25. Volume-specific magnetic susceptibility, porosity (open circles) and OSU-SCAT resistivity (solid line), GRA bulk density (solid line) and MAD bulk density (open circles), and OSU-SCAT red/blue reflectance and ratio reflectance in the blue band for the upper 290 mcd at Site 1093. Multiple lines in the last two panels are for data from multiple holes.

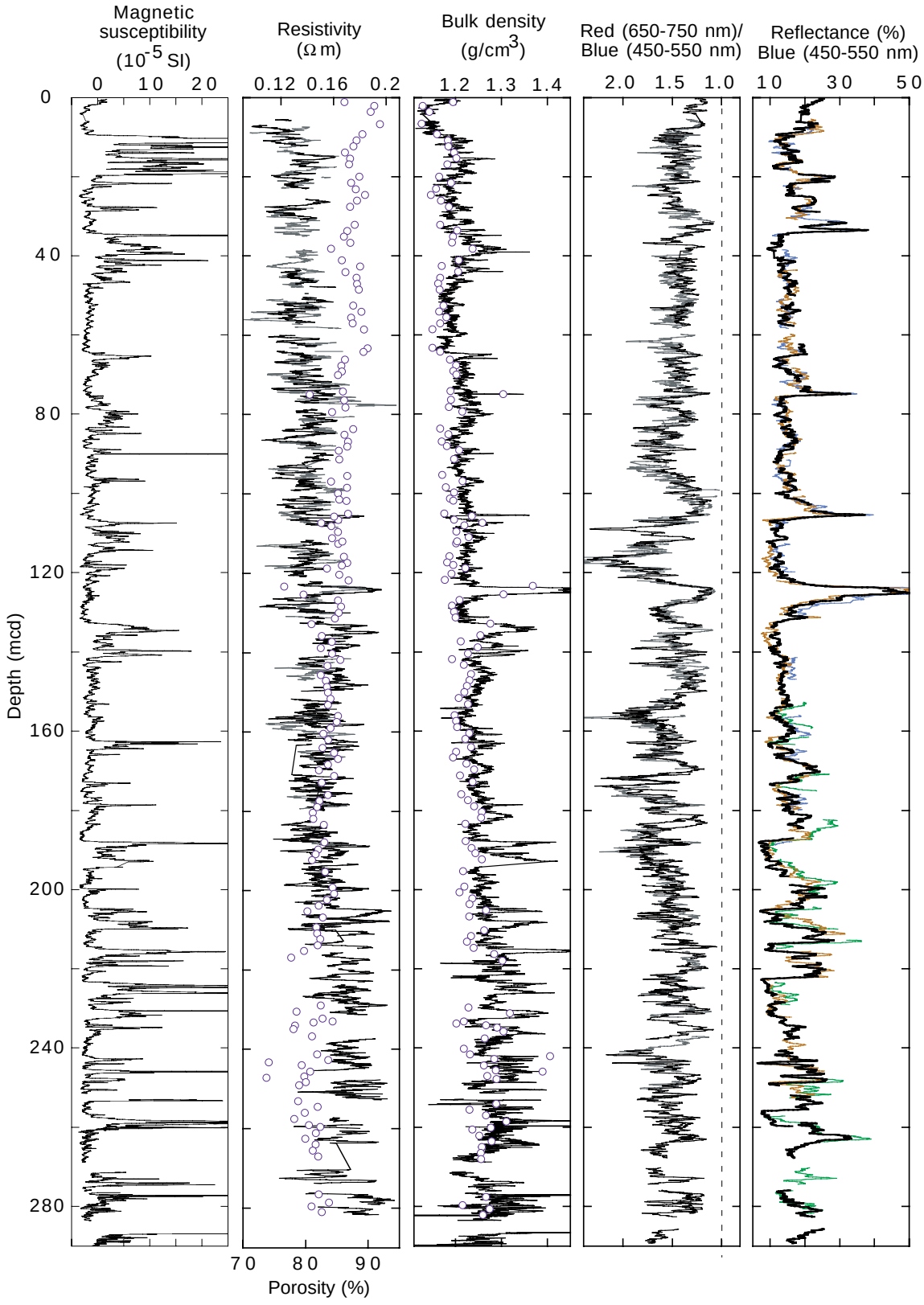

Figure F26. *P*-wave velocities at Site 1093 (small dots = PWL, solid circles = PWS3).

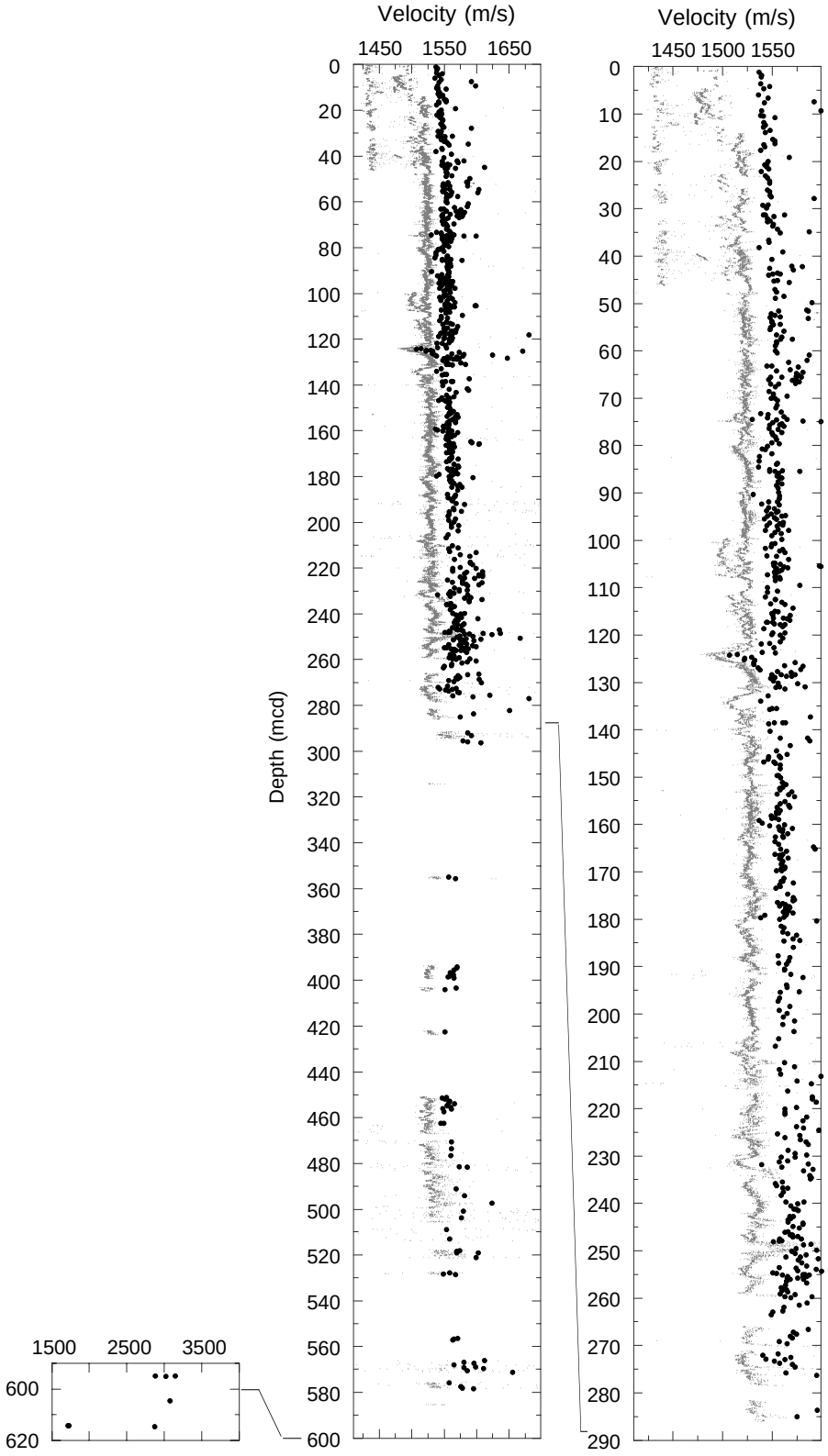

Figure F27. Thermal conductivity measurements of sediment cores at Site 1093. **A.** Frequency distribution of measured values. **B.** Correlation of measured values with interpolated GRA bulk density values. **C.** Thermal conductivity (solid circles) compared to interpolated GRA bulk density (open squares).

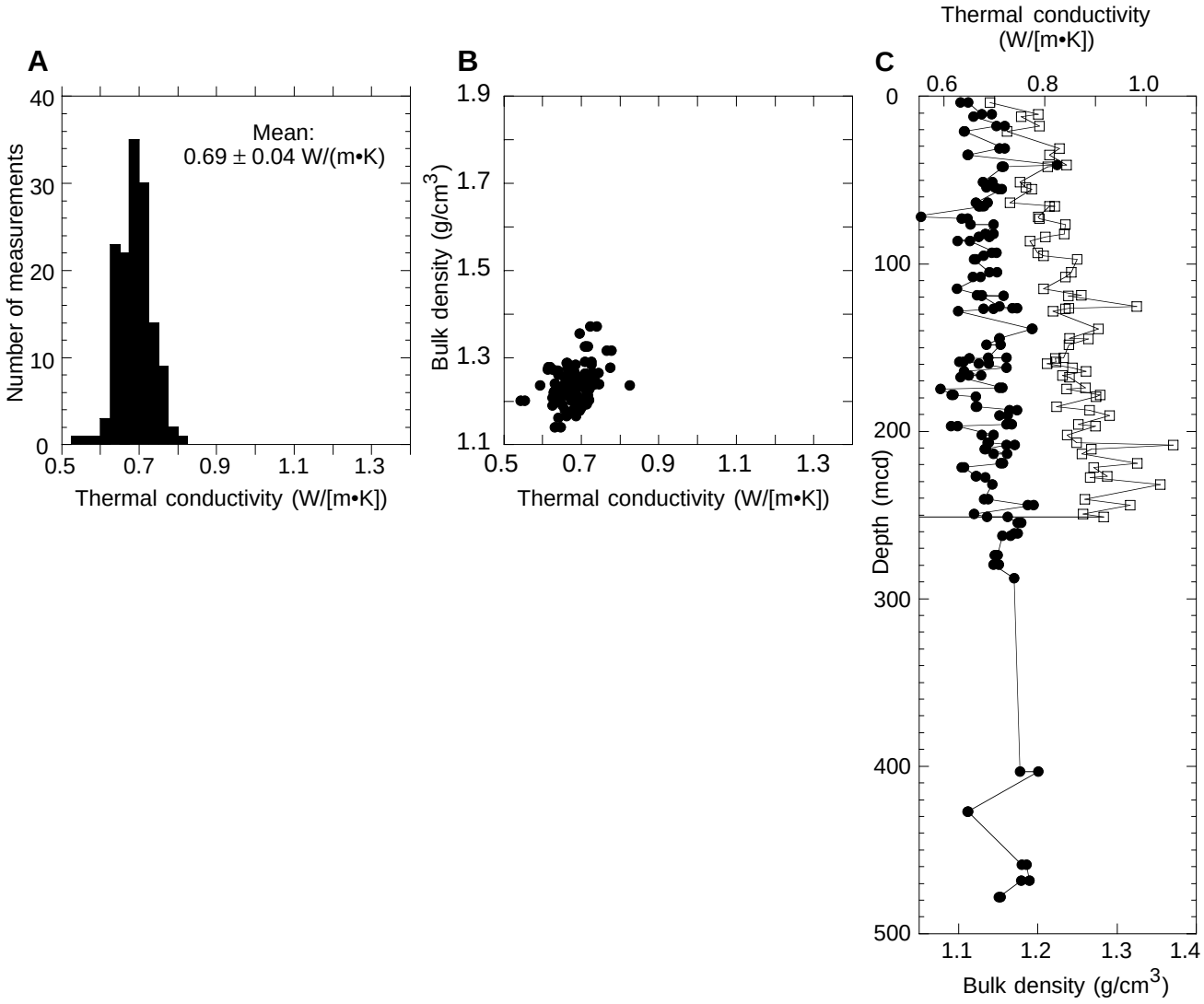

Figure F28. Downhole temperature measurements at Site 1093. Two plots are shown for each tool deployment: almost the entire time-temperature records (~1 hr) are shown on the left, and close-ups of the equilibration curves (~10 min) are shown on the right. The last two deployments (251 and 482 mbsf) were done with the DVTP, all other deployments were done with the APCT shoe. Circles represent the model curve (APCT) or data points (DVTP) used to calculate the equilibration temperature (horizontal solid line). Uncertainties (horizontal dashed lines) were estimated from the condition of the equilibration curves and from multiple curve-fit trials. A bottom-water measurement was taken with the barrel of Core 177-1093A-1H before the core was shot. Sediment measurements were taken after the corresponding cores were shot. (Continued on next two pages.)

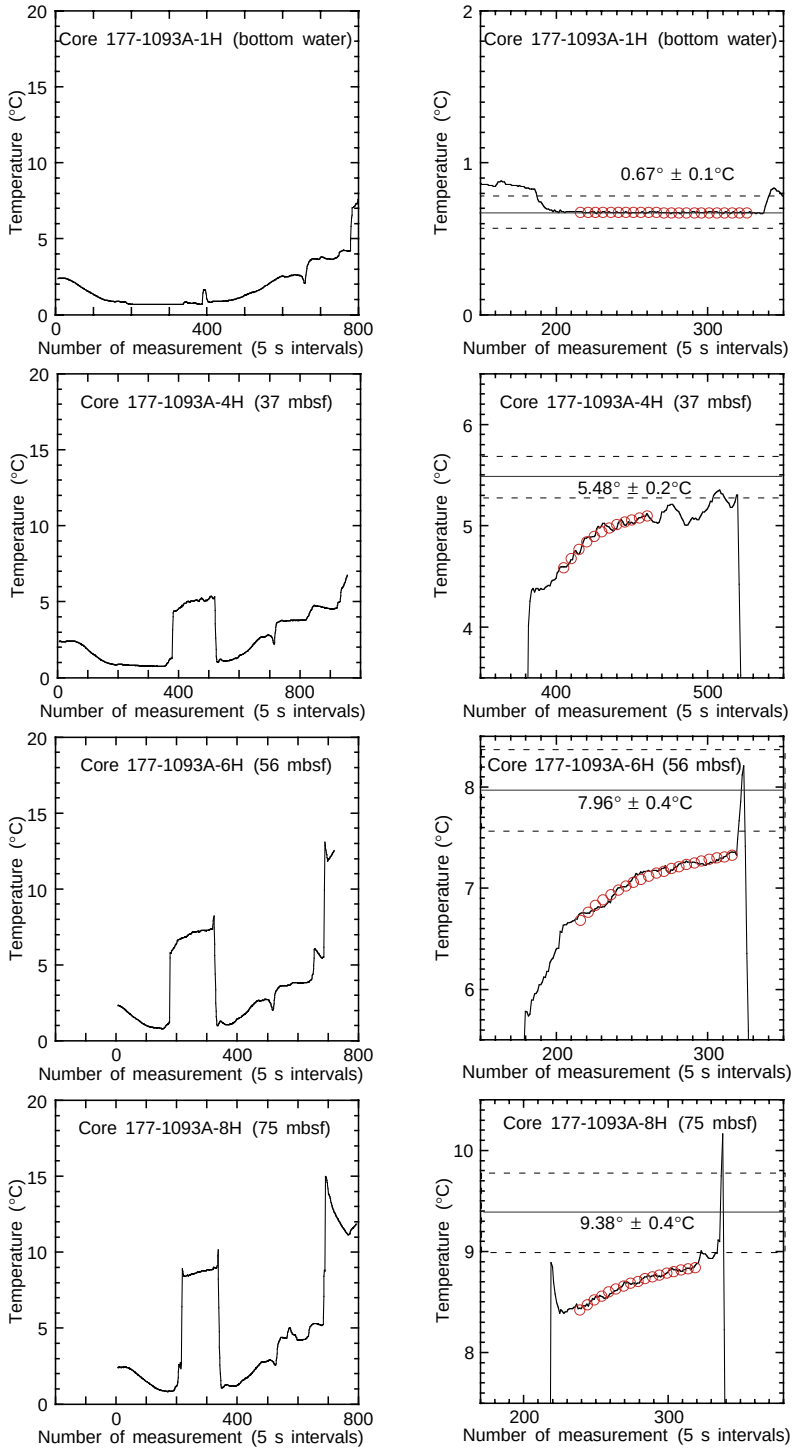

Figure F28 (continued).

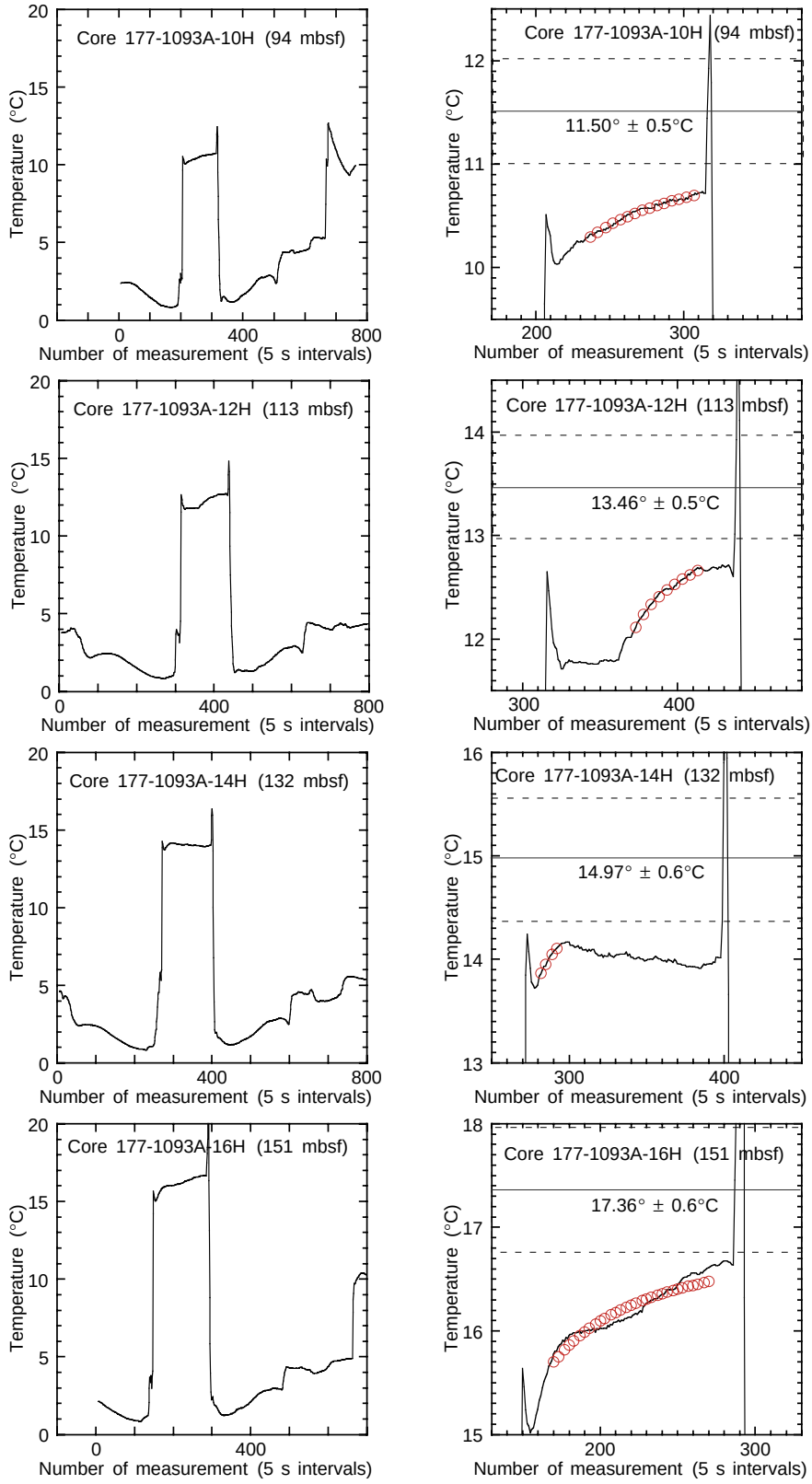

Figure F28 (continued).

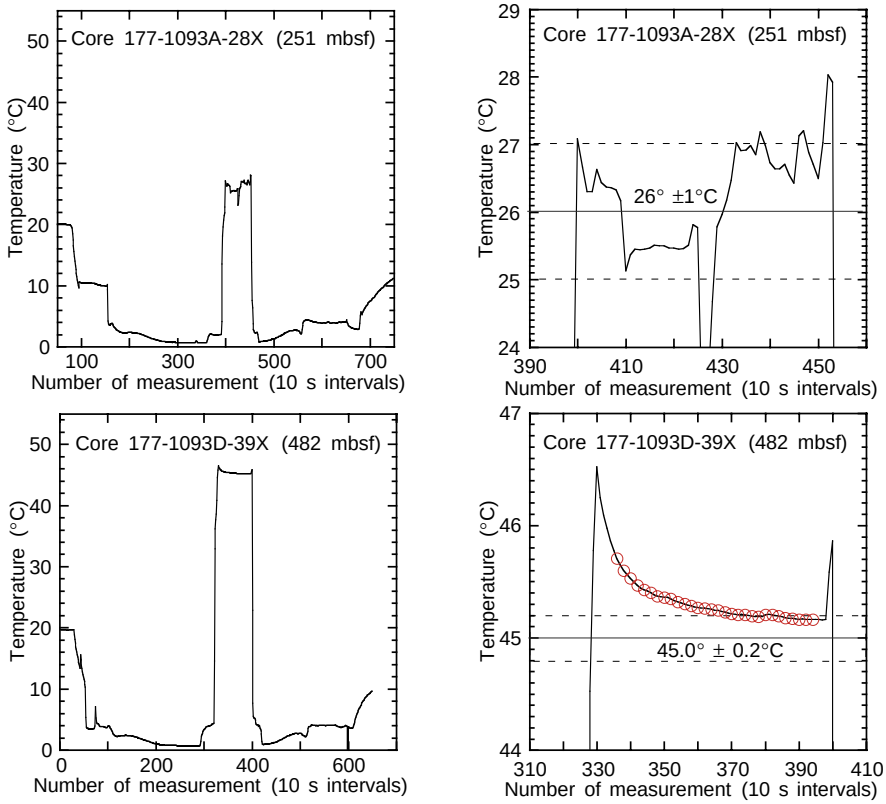

Figure F29. Depth-temperature curve for Site 1093.

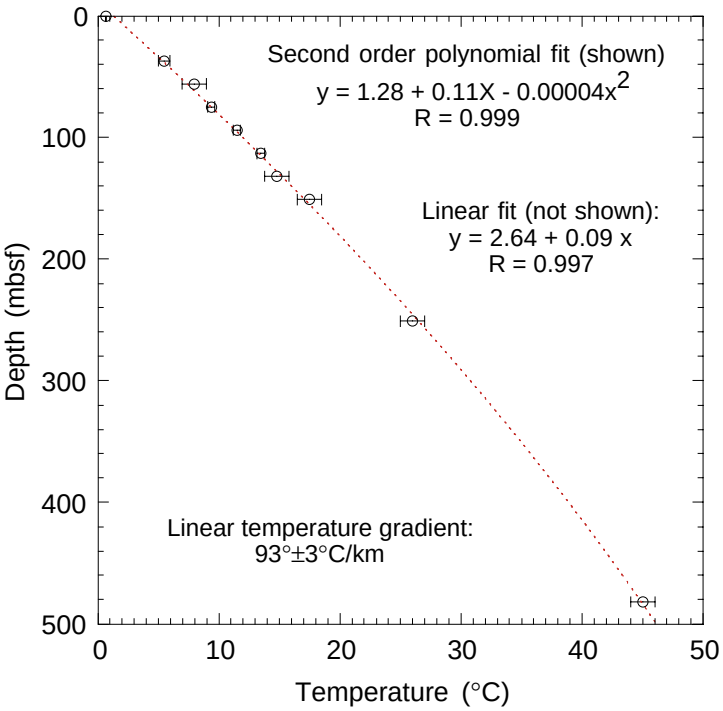

Figure F30. Site 1093 downhole wireline logs of caliper, total (hsgr) and uranium-free (hcgr) natural gamma, magnetic susceptibility, bulk density, porosity, and resistivity (imph = medium induction, sflu = shallow spherically focused resistivity). The measurements are plotted vs. mbsf which was adjusted from the wireline mbrf by subtracting the driller's depth to seafloor of 3635 mbrf (drill-string measurement).

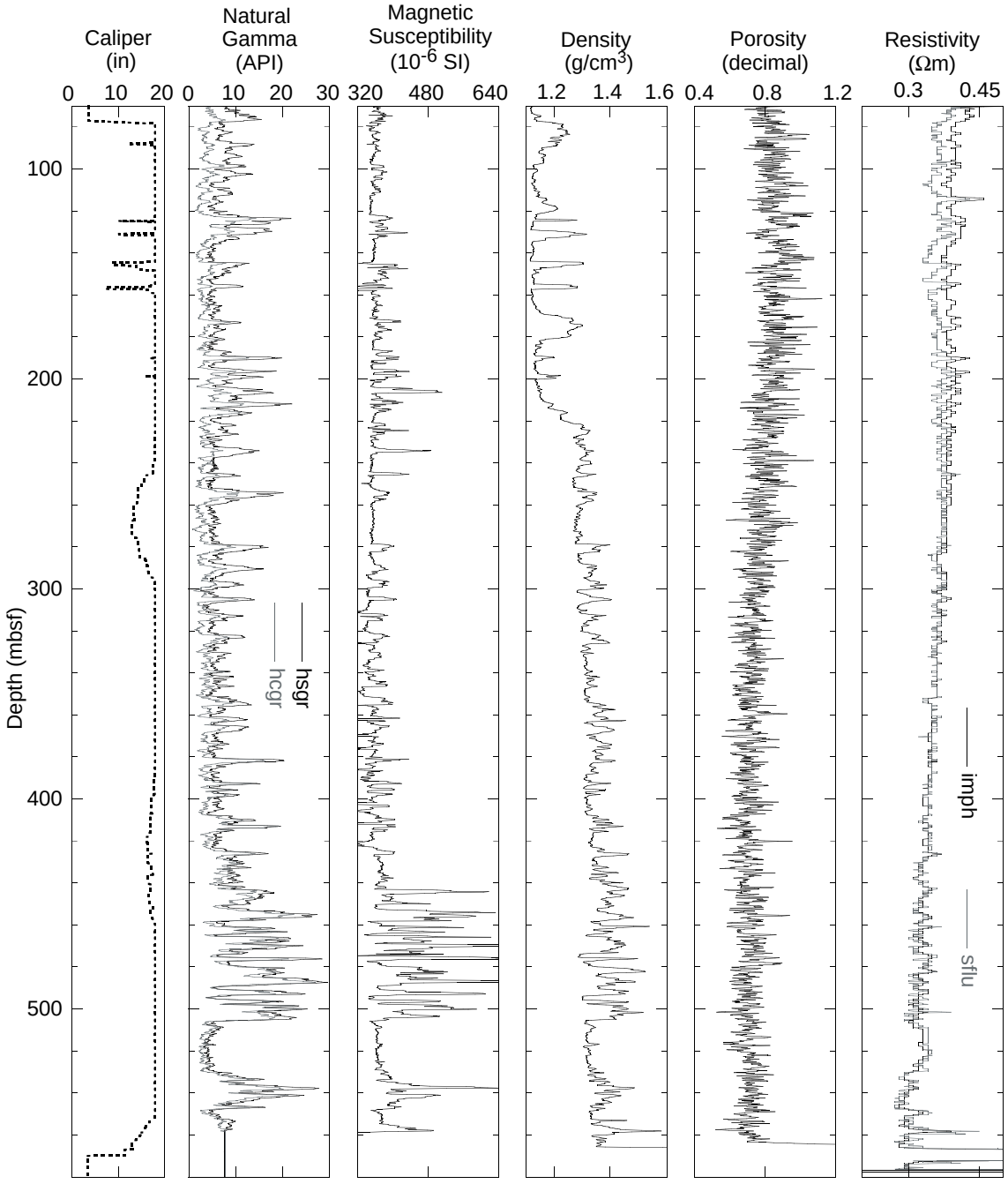

Figure F31. Site 1093 downhole total (hsgr) and uranium-free (hcgr) natural gamma-ray logs compared to calculated constituents thorium, potassium, and uranium. The logs are plotted vs. mbsf as in Fig. **F30,** p. 63.

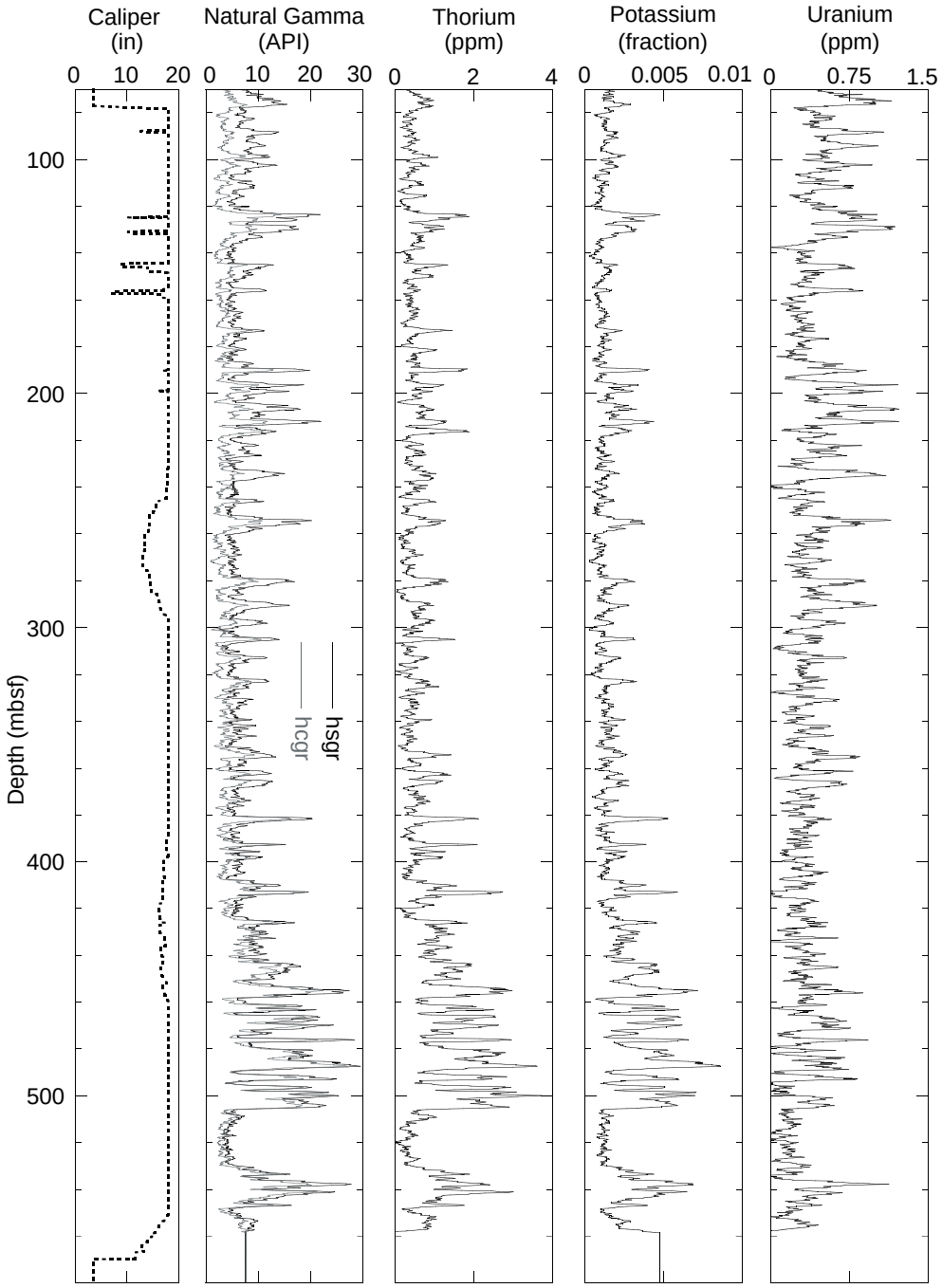

Figure F32. Site 1093 downhole magnetic susceptibility from the GHMT logging run compared to magnetic susceptibility from core logging (measured with the MST track). The downhole log data are plotted vs. mbsf and the core logging data are plotted vs. mcd (an expanded depth scale resulting from the construction of a complete stratigraphic section).

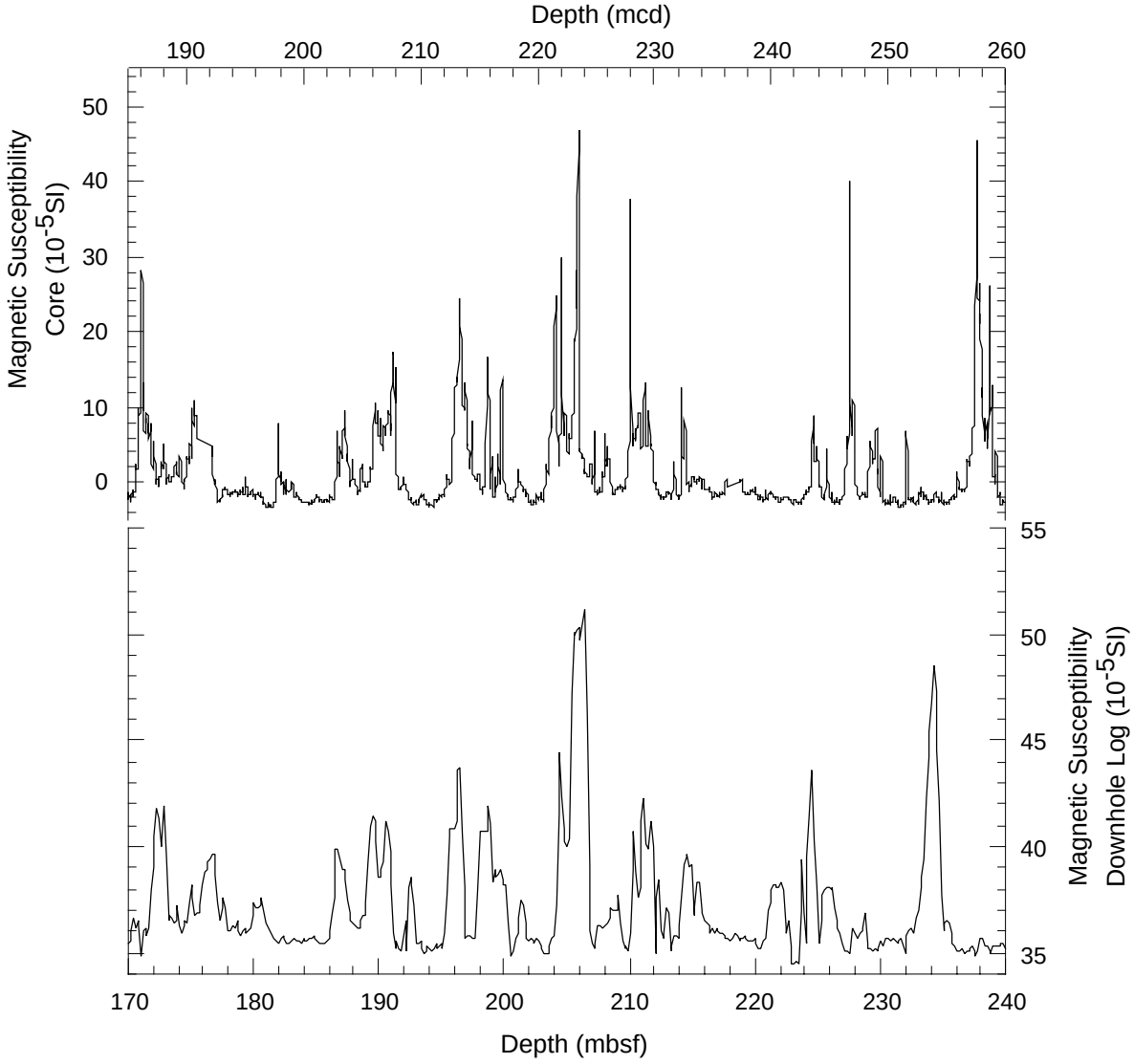

Table T1. Root-mean-square and interval velocities used for stacking of multichannel seismic data.

Time (s)	RMS velocity (m/s)	Interval velocity (m/s)	Depth from sea surface (m)
4896	1503.9	1503.9	3681.5
5272	1546.6	2021.9	4061.7
5576	1580.8	2086.6	4378.8
5936	1623.5	2180.6	4771.3
6130	1666.3	2661.7	5029.5

Notes: The data were collected at shotpoint 916 on Line AWI-94090 (Seismic streamer: 96 channels, 600 m active length, 770 m maximum offset). RMS = root mean square.

Table T2. X-ray diffraction data for Site 1093. (See table note. Continued on next page.)

Core, section, interval (cm)	Depth (mbsf)	Depth (mcd)	Bulk carbonate (wt%; coulometry)	Bulk opal (wt%; XRD peak intensity)	Bulk siliciclastics (wt%)
177-1093A-					
1H-1, 119-120	1.2	1.2	22.4	61.9	15.7
1H-3, 72-73	3.73	3.73	15.5	83.4	1.1
1H-5, 72-73	6.73	6.73	8.0	68.4	23.6
2H-1, 70-71	9.21	9.39	0.0	61.9	38.1
2H-3, 70-71	12.21	12.39	0.0	65.4	34.6
2H-5, 70-71	15.21	15.39	2.7	58.0	39.3
3H-1, 72-73	18.73	20.11	12.4	83.8	3.8
3H-3, 72-73	21.73	23.11	8.1	58.5	33.4
3H-5, 72-73	24.73	26.11	6.7	72.4	20.9
4H-1, 71-72	28.22	32.2	14.2	41.6	44.2
4H-3, 71-72	31.22	35.2	1.5	62.4	36.1
4H-5, 71-72	34.22	38.2	0.1	42.6	57.3
5H-1, 71-72	37.72	41.08	0.3	45.1	54.6
5H-3, 71-72	40.72	44.08	0.3	53.5	46.2
5H-5, 71-72	43.72	47.08	0.3	75.3	24.4
6H-1, 68-70	47.19	52.53	0.5	74.3	25.2
6H-5, 68-70	53.19	58.53	4.0	68.4	27.6
7H-3, 92-94	59.8	66.16	0.3	68.4	31.3
7H-5, 90-92	62.78	69.14	1.3	73.9	24.8
8H-2, 33-36	67.35	74.88	50.4	40.3	9.3
8H-5, 34-36	71.85	79.38	0.1	70.4	29.5
9H-4, 90-91	80.41	88.08	1.6	87.3	11.1
9H-6, 107-109	83.58	91.25	0.3	72.4	27.3
10H-2, 27-29	86.18	95.31	0.4	77.8	21.8
10H-6, 28-30	92.24	101.4	2.1	71.4	26.5
11H-1, 72-73	94.73	105.1	9.5	51.0	39.5
11H-3, 72-73	97.73	108.1	0.2	64.9	34.9
11H-5, 72-73	100.7	111.1	0.2	64.4	35.4
12H-1, 71-72	104.2	115.8	0.1	89.2	10.7
12H-3, 71-72	107.2	118.8	0.2	64.9	34.9
12H-5, 71-72	110.2	121.9	6.9	60.0	33.1
12H-7, 41-43	112.9	124.6	52.4	45.3	2.3
13H-1, 71-72	113.7	125.4	47.9	48.6	3.5
13H-3, 71-72	116.7	128.4	4.6	73.4	22.0
13H-5, 71-72	119.7	131.4	4.3	84.8	10.9
14H-1, 71-72	123.2	135.8	0.4	51.5	48.1
14H-3, 71-72	126.2	138.8	0.2	60.4	39.4
14H-5, 71-72	129.2	141.8	1.6	71.9	26.5
15H-2, 103-105	134.5	147.1	1.1	74.8	24.1
15H-6, 107-109	140.6	153.1	0.8	73.9	25.3
16H-1, 106-108	142.6	155.9	1.6	83.3	15.1
16H-3, 108-110	145.6	159	4.2	78.8	17.0
17H-1, 111-113	152.1	165.2	1.6	83.3	15.1
17H-3, 111-113	155.1	168.2	8.9	62.4	28.7
18H-1, 104-106	161.6	175.8	4.9	86.8	8.3
18H-3, 94-96	164.5	178.7	4.6	59.5	35.9
18H-5, 94-97	167.5	181.8	21.9	60.8	17.3
19H-1, 71-72	170.7	187.8	1.8	72.4	25.8
19H-3, 71-72	173.7	190.8	0.7	79.3	20.0
19H-6, 71-72	178.2	195.3	2.4	78.8	18.8
20H-1, 71-72	180.2	199.3	15.2	60.0	24.8
20H-3, 71-72	183.2	202.3	13.4	67.4	19.2
20H-5, 71-72	186.2	205.3	0.7	66.9	32.4
21H-1, 71-72	189.7	210.3	8.2	60.4	31.4
21H-3, 72-73	192.7	213.3	13.0	77.3	9.7
21H-5, 71-72	195.7	216.3	0.2	60.9	38.9
23H-2, 68-70	210.2	231.3	0.3	42.1	57.6
23H-6, 98-100	216.5	237.6	16.2	47.5	36.3
24H-3, 34-36	220.8	242.7	5.1	66.4	28.5
24H-6, 19-22	225.2	247.1	28.3	57.9	13.8
25H-2, 71-73	228.1	254.1	14.6	79.2	6.2
25H-6, 71-73	234.1	260.1	8.9	62.4	28.7
26H-3, 71-73	238.2	263.6	28.8	68.1	3.1
26H-6, 71-73	242.7	268.1	18.2	80.7	1.1
28X-1, 71-72	251.7	277.6	1.3	58.5	40.2

Table T2 (continued).

Core, section, interval (cm)	Depth (mbsf)	Depth (mcd)	Bulk carbonate (wt%; coulometry)	Bulk opal (wt%; XRD peak intensity)	Bulk siliciclastics (wt%)
28X-3, 71-72	254.7	280.6	14.8	49.0	36.2
29X-1, 61-62	261.3	287.2	14.0	60.4	25.6
29X-3, 61-62	264.3	290.2	9.2	71.9	18.9
30H-1, 82-83	271.2	297.1	24.7	75.0	0.3
30H-2, 82-83	272.5	298.4	13.1	61.4	25.5
177-1093D-					
15H-1, 66-68	269.7	301.2	7.6	91.2	1.2
27X-1, 100-102	368.4	399.9	10.2	89.1	0.7
27X-3, 107-109	371.5	403	24.7	66.8	8.5
28X-1, 99-101	378	409.5	3.2	48.0	48.8
30X-1, 90-92	396.8	428.3	4.0	82.8	13.2
33X-1, 66-67	425.4	456.9	38.6	56.6	4.8
33X-3, 92-93	428.6	460.1	10.2	76.1	13.7
33X-5, 72-73	431.4	462.9	28.8	53.3	17.9
34X-2, 62-63	436.4	467.9	12.8	57.0	30.2
34X-4, 72-73	439.5	471	24.5	43.0	32.5
35X-2, 129-130	446.7	478.2	7.5	41.6	50.9
35X-4, 36-39	448.8	480.3	20.2	62.5	17.3
36X-4, 71-72	458.5	490	18.7	57.2	24.1
36X-6, 51-52	461.3	492.8	43.4	49.9	6.7
37X-2, 58-61	465	496.5	13.1	66.8	20.1
37X-5, 97-98	469.9	501.4	10.0	33.6	56.4
38X-2, 68-69	474.7	506.2	0.0	47.5	52.5
38X-4, 98-99	478	509.5	6.6	36.1	57.3
39X-1, 72-73	482.7	514.2	0.0	59.0	41.0
39X-2, 61-62	484.1	515.6	0.0	40.6	59.4
39X-3, 72-73	485.7	517.2	0.0	56.5	43.5
39X-5, 72-73	488.7	520.2	4.9	51.0	44.1
40X-2, 133-135	494.4	525.9	25.7	23.5	50.8
40X-4, 9-12	495.6	527.1	56.9	14.9	28.2
41X-1, 48-50	501.8	533.3	7.3	42.7	50.0
44X-1, 89-91	531.1	562.6	1.1	64.2	34.7
45X-1, 72-74	540.6	572.1	0.0	35.6	64.4
46X-2, 36-38	551.4	582.9	0.0	49.0	51.0
50X-1, 5-7	588.1	619.6	0.0	15.8	84.2

Note: XRD = X-ray diffraction. This table is also available in ASCII format in the **TABLES** directory.

Table T3. Composite depths for Site 1093. (See table note. Continued on next two pages.)

Core	Depth (mbsf)	Offset (mbsf)	Depth (mcd)
177-1093A-			
1H	0.00	0	0.00
2H	8.50	0.18	8.68
3H	18.00	1.38	19.38
4H	27.50	3.98	31.48
5H	37.00	3.36	40.36
6H	46.50	5.34	51.84
7H	56.00	6.36	62.36
8H	65.50	7.53	73.03
9H	75.00	7.67	82.67
10H	84.50	9.13	93.63
11H	94.00	10.35	104.35
12H	103.50	11.63	115.13
13H	113.00	11.67	124.67
14H	122.50	12.43	134.93
15H	132.00	12.35	144.35
16H	141.50	13.19	154.69
17H	151.00	12.93	163.93
18H	160.50	14.11	174.61
19H	170.00	16.91	186.91
20H	179.50	18.87	198.37
21H	189.00	20.37	209.37
22H	198.50	20.31	218.81
23H	208.00	20.91	228.91
24H	217.50	21.71	239.21
25H	227.00	20.86	247.86
26H	234.50	20.09	254.59
28X	251.00	20.66	271.66
29X	260.70	20.66	281.36
30H	270.40	20.66	291.06
31X	275.40	20.66	296.06*
32X	280.50	20.66	301.16*
33X	290.10	20.66	310.76*
34X	299.80	20.66	320.46*
177-1093B-			
1H	0.00	5.28	5.28
2H	7.10	6.94	14.04
3H	16.60	9.08	25.68
4H	26.10	9.48	35.58
5H	35.60	12.1	47.70
6H	45.10	14.66	59.76
7H	54.60	13.77	68.37
8H	64.10	14.47	78.57
9H	73.60	16.09	89.69
10H	83.10	16.47	99.57
11H	92.60	18.71	111.31
12H	102.10	19.55	121.65
13H	111.60	18.53	130.13
14H	121.10	19.47	140.57
15H	130.60	20.71	151.31
16H	140.10	20.15	160.25
17H	149.60	21.15	170.75
18H	159.10	24.51	183.61
19H	168.60	24.49	193.09
20H	178.10	27.71	205.81
21H	187.60	28.67	216.27
22H	197.10	27.83	224.93
23H	206.60	29.27	235.87
24H	216.10	30.13	246.23
177-1093C-			
1H	0.00	7.06	7.06
2H	8.00	9.54	17.54
3H	17.50	10.14	27.64
4H	27.00	11.46	38.46
5H	36.50	14.42	50.92
6H	46.00	15.84	61.84
7H	55.50	13.81	69.31

Table T3 (continued).

Core	Depth (mbsf)	Offset (mbsf)	Depth (mcd)
8H	65.00	15.25	80.25
9H	74.50	17.01	91.51
10H	84.00	17.49	101.49
11H	93.50	18.96	112.46
12H	103.00	20.05	123.05
13H	112.50	23.87	136.37
14H	122.00	19.05	141.05
15H	131.50	24.33	155.83
16H	141.00	23.41	164.41
17H	150.50	24.83	175.33
18H	160.00	26.75	186.75
177-1093D-			
1H	136.00	16.31	152.31
2H	145.50	15.83	161.33
3H	155.00	15.05	170.05
4H	164.50	17.13	181.63
5H	174.00	18.05	192.05
6H	183.50	21.31	204.81
7H	193.00	20.51	213.51
8H	202.50	21.65	224.15
9H	212.00	21.65	233.65*
10H	221.50	24.53	246.03
11H	231.00	21.93	252.93
12H	240.50	25.21	265.71
13H	250.00	20.92	270.92
14H	259.50	25.92	285.42
15H	269.00	25.92	294.92
16H	278.50	25.92	304.42*
17H	288.00	25.92	313.92
18H	297.50	25.92	323.42*
19X	307.00	25.92	332.92*
20X	313.00	25.92	338.92*
21X	319.00	25.92	344.92*
22H	328.60	25.92	354.52
23X	329.60	25.92	355.52*
24X	338.30	25.92	364.22*
25X	348.00	25.92	373.92*
26X	357.70	25.92	383.62*
27X	367.40	25.92	393.32
28X	377.00	25.92	402.92
29X	386.20	25.92	412.12*
30X	395.90	25.92	421.82
31X	405.50	25.92	431.42*
32X	415.10	25.92	441.02*
33X	424.70	25.92	450.62
34X	434.30	25.92	460.22
35X	443.90	25.92	469.82
36X	453.30	25.92	479.22
37X	462.90	25.92	488.82
38X	472.50	25.92	498.42
39X	482.00	25.92	507.92
40X	491.60	25.92	517.52
41X	501.30	25.92	527.22
42X	510.90	25.92	536.82*
43X	520.60	25.92	546.52*
44X	530.20	25.92	556.12
45X	539.90	25.92	565.82
46X	549.50	25.92	575.42
47X	559.10	25.92	585.02
48X	568.80	25.92	594.72*

Table T3 (continued).

Core	Depth (mbsf)	Offset (mbsf)	Depth (mcd)
49X	578.40	25.92	604.32*
50X	588.00	25.92	613.92*
177-1093E-			
1H	4.00	0.59	4.59
2H	33.00	6.48	39.48
177-1093F-			
1H	34.00	2.92	36.92

Notes: * = cores that are part of the JANUS database but were not analyzed on the multisensor track because sufficient material was not available for analysis (e.g., core catchers). The mcd offset was arbitrarily chosen to be the same as the offset of the overlying core. This table is also available in ASCII format in the **TABLES** directory.

Table T4. Site 1093 splice tie points.

Core, section, interval (cm)	Depth (mbsf)	Depth (mcd)		Core, section, interval (cm)	Depth (mbsf)	Depth (mcd)
177-				177-		
1093A-1H-6, 41	7.92	7.92	tie to	1093B-1H-2, 113	2.64	7.92
1093B-1H-4, 58	5.08	10.36	tie to	1093A-2H-2, 18	10.18	10.36
1093A-2H-6, 24	16.24	16.42	tie to	1093B-2H-2, 88	9.48	16.42
1093B-2H-6, 70	15.30	22.24	tie to	1093A-3H-2, 136	20.86	22.24
1093A-3H-7, 40	27.40	28.78	tie to	1093C-3H-1, 114	18.64	28.78
1093C-3H-5, 100	24.50	34.64	tie to	1093A-4H-3, 16	30.66	34.64
1093A-4H-5, 130	34.80	38.78	tie to	1093F-1H-2, 36	35.86	38.78*
1093F-1H-3, 100	38.00	40.92	tie to	1093C-4H-2, 96	29.46	40.92
1093C-4H-5, 28	33.28	44.74	tie to	1093A-5H-3, 138	41.38	44.74
1093A-5H-6, 86	45.36	48.72	tie to	1093B-5H-1, 102	36.62	48.72
1093B-5H-4, 37	40.48	52.58	tie to	1093A-6H-1, 73	47.24	52.58*
1093A-6H-6, 102	55.02	60.36	tie to	1093B-6H-1, 60	45.70	60.36*
1093B-6H-5, 30	51.40	66.06	tie to	1093A-7H-3, 82	59.70	66.06
1093A-7H-6, 138	64.75	71.11	tie to	1093C-7H-2, 30	57.30	71.11
1093C-7H-6, 106	64.06	77.87	tie to	1093A-8H-4, 34	70.34	77.87
1093A-8H-5, 128	72.78	80.31	tie to	1093B-8H-2, 24	65.84	80.31
1093B-8H-5, 130	71.40	85.87	tie to	1093A-9H-3, 20	78.20	85.87*
1093A-9H-6, 50	83.00	90.67	tie to	1093B-9H-1, 98	74.58	90.67
1093B-9H-6, 76	81.86	97.95	tie to	1093A-10H-3, 142	88.82	97.95
1093A-10H-6 114	93.09	102.22	tie to	1093B-10H-2, 114	85.75	102.22*
1093B-10H-6, 36	90.96	107.43	tie to	1093A-11H-3, 8	97.08	107.43
1093A-11H-6, 146	102.96	113.31	tie to	1093B-11H-2, 50	94.60	113.31
1093B-11H-5, 128	99.88	118.59	tie to	1093A-12H-3, 46	106.96	118.59
1093A-12H-6, 122	112.22	123.85	tie to	1093B-12H-2, 70	104.30	123.85
1093B-12H-3, 108	106.18	125.73	tie to	1093A-13H-1, 106	114.06	125.73
1093A-13H-6, 120	121.70	133.37	tie to	1093B-13H-3, 24	114.84	133.37
1093B-13H-7, 20	120.80	139.33	tie to	1093A-14H-3, 140	126.90	139.33
1093A-14H-5, 144	129.94	142.37	tie to	1093B-14H-2, 30	122.90	142.37
1093B-14H-5, 62	127.72	147.19	tie to	1093A-15H-2, 134	134.84	147.19
1093A-15H-6, 80	140.30	152.65	tie to	1093B-15H-1, 133	131.94	152.65
1093B-15H-4, 38	135.48	156.19	tie to	1093A-16H-1, 150	143.00	156.19
1093A-16H-7, 18	149.70	162.89	tie to	1093B-16H-2, 114	142.74	162.89
1093B-16H-4, 144	146.04	166.19	tie to	1093A-17H-2, 76	153.26	166.19
1093A-17H-7, 14	160.14	173.07	tie to	1093B-17H-2, 82	151.92	173.07
1093B-17H-6, 14	157.24	178.39	tie to	1093A-18H-3, 78	164.28	178.39
1093A-18H-6, 110	169.10	183.21	tie to	1093D-4H-2, 8	166.08	183.21*
1093D-4H-5, 72	171.22	188.35	tie to	1093A-19H-1, 144	171.44	188.35
1093A-19H-5, 121	177.22	194.13	tie to	1093D-5H-2, 57	176.08	194.13*
1093D-5H-6, 5	181.56	199.61	tie to	1093A-20H-1, 123	180.74	199.61
1093A-20H-7, 50	189.00	207.87	tie to	1093B-20H-2, 56	180.16	207.87
1093B-20H-4, 9	182.70	210.41	tie to	1093A-21H-1, 102	190.04	210.41
1093A-21H-6, 88	197.38	217.75	tie to	1093B-21H-1, 148	189.08	217.75
1093B-21H-5, 85	194.46	223.13	tie to	1093A-22H-3, 130	202.82	223.13
1093A-22H-6, 42	205.76	226.07	tie to	1093B-22H-1, 114	198.24	226.07
1093B-22H-5, 140	204.50	232.33	tie to	1093A-23H-3, 42	211.42	232.33
1093A-23H-6, 125	216.76	237.67	tie to	1093B-23H-2, 27	208.40	237.67*
1093B-23H-6, 28	214.38	243.65	tie to	1093A-24H-3, 144	221.94	243.65
1093A-24H-6, 60	225.60	247.31	tie to	1093D-10H-1, 128	222.78	247.31
1093D-10H-4, 71	226.72	251.25				

Notes: * = problematic tie points (see text for discussion). This table is also available in ASCII format in the **TABLES** directory.

Table T5. Distribution of main calcareous nannofossil species in Holes 1093A, 1093B, and 1093D. (**See table note**. Continued on next four pages.)

Core, section, interval (cm)	Depth (mbsf)	Depth (mcd)	Abundance	Preservation	*Dictyococcites antarticus*	*Reticulofenestra pseudoumbilica*	*Discoaster brouweri*	*Dictyococcites productus*	*Reticulofenestra minuta*	*Reticulofenestra minutula*	*Coccolithus pelagicus*	*Pseudoemiliania lacunosa*	*Calcidiscus leptoporus*	*Calcidiscus macintyrei*	*Helicosphaera carteri*	*Gephyrocapsa* small	*Gephyrocapsa caribbeanica*	*Gephyrocapsa* medium (4-5.5 µm)	*Gephyrocapsa* large (>5.5 µm)	*Gephyrocapsa* sp. 3	*Reticulofenestra asanoi*	*Emiliania huxleyi*	Comments
177-1093A-																							
1H-1, 80-80	0.80	0.80	C	G									C		C	A						D	
1H-4, 60-60	5.10	5.10	F	G									A		F	A						A	
1H-6, 80-80	8.30	8.30	R	M									C		F			F				A	
1H-CC, 12-17	8.49	8.49	R	M									F		R	A		F				A	
2H-3, 30-30	11.80	11.98	R	P									R			C						A	
2H-5, 30-30	14.80	14.98	R	P							R					A				R		C	
2H-6, 30-30	16.30	16.48	R	M									R			C				C		C	
2H-CC, 12-17	18.09	18.27	B																				
3H-1, 30-30	18.30	19.68	A	M									C		R	D						A	
3H-2, 30-30	19.80	21.18	A	M									F			A						D	
3H-4, 30-30	22.80	24.18	C	P									C			A				C		D	
3H-CC, 11-16	27.69	29.07	R	P									C			R						A	
4H-1, 30-30	27.80	31.78	A	P									A		R					F		A	
4H-2, 40-40	29.40	33.38	A	M							F		A		F	A				C		A	
4H-2, 120-120	30.20	34.18	A	M					A		F		A			A				C		F	
4H-3, 30-30	30.80	34.78	R	P					A		F		C			A						?	
4H-4, 30-30	32.30	36.28	B																				
4H-CC, 10-15	37.49	41.47	B																				
5H-3, 30-30	40.30	43.66	B																				
5H-6, 30-30	44.80	48.16	R	P					C				C			C				C			
5H-7, 20-20	46.20	49.56	R	M							R		F			C		F				F	
5H-CC, 15-20	46.86	50.22	B																				
6H-2, 69-69	48.69	54.03	B																				
6H-6, 30-30	54.30	59.64	B																				
6H-CC, 0-10	56.01	61.35	R	M							F					C		C					
7H-1, 132-132	57.32	63.68	R	P									F		R	C		D				F	
7H-2, 35-35	57.85	64.21	R	M							F		C			C		F		F		R	
7H-CC, 24-29	65.52	71.83	R	M							F		C		R	A		C					
8H-1, 25-25	65.75	73.28	C	M							F		F		F		A					F	
8H-1, 140-140	66.90	74.43	C	M							F		C		R	A	A					C	
8H-2, 65-65	67.65	75.18	F	P							F				C	A	A					?	
8H-CC, 0-10	75.09	82.62	B																				
9H-CC, 15-20	84.77	92.44	B																				
10H-CC, 0-10	93.93	103.06	F	M							R	?	R		R	D							
11H-1, 30-30	94.30	104.65	F	M							F		F		R	D		F					
11H-2, 10-10	95.60	105.95	C	M							R				R	A	A	F					
11H-4, 40-40	98.90	109.25	B																				
11H-CC, 16-21	103.76	114.11	B																				
12H-2, 30-30	105.30	116.93	B																				
12H-5, 120-120	110.70	122.33	B																				
12H-7, 30-30	112.80	124.43	A	M							R					D	F	F					
12H-CC, 0-10	113.06	124.69	A	M							R				R	D		R					
13H-1, 80-80	113.80	125.47	A	P									F				D	F					
13H-3, 80-80	116.80	128.47	C	M									F		R	D		F		R			
13H-4, 30-30	117.80	129.47	C	M											R	D		A					
13H-5, 60-60	119.60	131.27	C	M									F		R	D		C					
13H-CC, 15-20	122.43	134.10	B																				
14H-5, 110-110	129.60	142.21	R	P							R					D		F					
14H-CC, 10-15	131.74	144.35	B																				
14H-5, 110-110	129.60	142.21	R	P							R					D		F					

Table T5 (continued).

Core, section, interval (cm)	Depth (mbsf)	Depth (mcd)	Abundance	Preservation	*Dictyococcites antarticus*	*Reticulofenestra pseudoumbilica*	*Discoaster brouweri*	*Dictyococcites productus*	*Reticulofenestra minuta*	*Reticulofenestra minutula*	*Coccolithus pelagicus*	*Pseudoemiliania lacunosa*	*Calcidiscus leptoporus*	*Calcidiscus macintyrei*	*Helicosphaera carteri*	*Gephyrocapsa* small	*Gephyrocapsa caribbeanica*	*Gephyrocapsa* medium (4-5.5 µm)	*Gephyrocapsa* large (>5.5 µm)	*Gephyrocapsa* sp. 3	*Reticulofenestra asanoi*	*Emiliania huxleyi*	Comments
15H-2, 40-40	133.90	146.43	R	P												D		F					
15H-5, 40-40	138.40	150.93	R	M							R	?				A		F					
15H-6, 40-40	139.90	152.43	R	M								R				A		F					
15H-7, 40-40	141.40	153.93	R	M							R	R	R			D		F					
15H-CC, 11-16	141.86	154.39	R	P												R		R					
16H-3, 129-129	145.79	159.16	A	P						R		F	R		R		D	R					
16H-4, 23-23	146.23	159.60	C	P							R	R					A	C					
16H-5, 94-94	148.44	161.81	C	P									R			C	A	F		R		?	
16H-CC, 0-10	150.92	164.29	B																				
17H-3, 119-119	155.19	168.30	C	P					C		R	C	F		R	C		R		R			
17H-4, 12-12	155.62	168.73	C	P					A		F	F	F		R	A				F			
17H-5, 12-12	157.12	170.23	A	M					C		C	A	C		R	A				A			
17H-5, 126-126	158.26	171.37	A	M					C		C	A	C		R					C	R		
17H-CC, 24-29	160.88	173.99	R	P								R				R							
18H-2, 10-10	162.10	176.39	C	P							C	A	C							F			
18H-3, 44-44	163.94	178.23	C	P						C		A	C	R						C			
18H-5, 30-30	166.80	181.09	C	P							F	C	C		F					A			
18H-6, 20-20	168.20	182.49	C	P							C	A	C		C					A			
18H-7, 70-70	170.20	184.49	C	P						C	C	C	C		F					F			
18H-CC, 10-15	170.37	184.66	F	M						C	R	C	C		F	F				R	R		
19H-1, 44-44	170.44	187.53	R	M						A	F	F	R		R	C					1		
19H-6, 44-44	177.94	195.03	B																				
19H-7, 60-60	179.60	196.69	R	M							R	C			F	D		F		R			
19H-CC, 17-22	179.85	196.94	B																				
20H-2, 30-30	181.30	200.35	C	P						C	F	F	R		R	D							
20H-4, 60-60	184.60	203.65	C	M						C	F	C	C			A					R		
20H-6, 50-50	187.50	206.55	R	M						D	F	C	F			R							
20H-CC, 17-22	189.28	208.33	B																				
21H-2, 110-110	191.60	212.15	C	M						F		F	C			D							
21H-4, 22-22	193.72	214.27	A	M					C	R		R	C		R	D				F			
21H-6, 40-40	196.90	217.45	A	M					A		F	F	C		F	D							
21H-CC, 48-53	198.48	219.03	B																				
22H-1, 30-30	198.80	219.29	C	P								F	C		R	A				R			
22H-1, 90-90	199.40	219.89	C	P								C	C		R		C			F			
22H-2, 30-30	200.30	220.79	A	M							R	C	C		R	C		R		F			
22H-CC, 0-10	207.46	227.95	R	P								R								R	R		
23H-3, 90-90	211.90	232.99	R	P							R		R							R	F		
23H-3, 122-122	212.22	233.31	R	P							C	C	C		R					R	F		
23H-5, 43-43	214.43	235.52	F	P							C										C		
23H-5, 128-128	215.28	236.37	C	P						F	F	C	C							F	A		
23H-6, 54-54	216.04	237.13	F	P						R	C		F								C		
23H-CC, 0-10	217.63	238.72	F	M						F	F	C	A							R	C		
24H-2, 130-130	220.30	242.19	A	P					A		A	C	A					R		F	C		
24H-5, 15-15	223.65	245.54	A	P					A		A		C		R	A				R	R		
24H-5, 140-140	224.90	246.79	A	M							A		C		R	A				cf.	F		
24H-6, 50-50	225.50	247.39	A	P						A	A	A	C		R	A					R		
24H-CC, 35-40	227.11	249.00	C	M						F	C	C	A								R		
25H-CC, 25-30	235.16	256.20	B																				
26H-6, 50-50	242.50	262.77	A	P						C	A	A	C			A					R		
26H-CC, 19-24	243.69	263.96	F	P							D	F	F		F	F		R					
28X-2, 100-100	253.50	274.34	C	M						A	A	C	F										
28X-3, 34-34	254.34	275.18	C	M					F	F	D	C						R					
28X-CC, 12-17	257.85	278.69	R	P					C			D											
29X-1, 30-30	261.00	281.84	F	R						A	A	F	F		R			R					
29X-CC, 13-18	264.63	285.47	B																				

Table T5 (continued).

Core, section, interval (cm)	Depth (mbsf)	Depth (mcd)	Abundance	Preservation	*Dictyococcites antarticus*	*Reticulofenestra pseudoumbilica*	*Discoaster brouweri*	*Dictyococcites productus*	*Reticulofenestra minuta*	*Reticulofenestra minutula*	*Coccolithus pelagicus*	*Pseudoemiliania lacunosa*	*Calcidiscus leptoporus*	*Calcidiscus macintyrei*	*Helicosphaera carteri*	*Gephyrocapsa* small	*Gephyrocapsa caribbeanica*	*Gephyrocapsa* medium (4-5.5 µm)	*Gephyrocapsa* large (>5.5 µm)	*Gephyrocapsa* sp. 3	*Reticulofenestra asanoi*	*Emiliania huxleyi*	Comments
30H-1, 50-50	270.90	291.74	F	M						C	R	A	F					C					
30H-2, 31-31	272.01	292.85	F	M					R	C	R	A	C										
177-1093B-																							
1H-2-,8-13	7.10	6.86	B																				
2H-3-0-10	16.16	17.04	R	P												C						A	
3H-4-8-13	21.89	30.26	A	M					A		F		C		C	A				C		F	
4H-1-9-14	35.84	35.67	B																				
5H-1-4-12	45.21	47.74	B																				
6H-5-15-20	53.08	65.91	B																				
7H-6-10-15	63.89	75.97	B																				
8H-6-7-12	73.39	86.14	R	M									R			A	D	R				?	
9H-CC, 10-15	83.24	99.33	B																				
10H-CC, 17-22	91.91	108.38	B																				
11H-CC, 12-17	102.29	121.00	B								F		F			D	A						
12H-2-40-40	104.00	123.55	A	M							R		R			D		F					
12H-3-40-40	105.50	125.05	A	M									F			D		F					
12H-4-100-100	107.60	127.15	C	M									C			D		C					
12H-CC, 18-23	110.00	130.23	C	M																			
13H-1-94-94	112.54	131.25	C	M							R		F		F	D		C					
13H-CC, 16-21	121.43	140.14	B																				
14H-1-110-110	122.20	141.85	R	P												D		R					
14H-CC, 11-16	130.23	149.88	R	M									F				C	R					
15H-5-40-40	136.42	157.31	R	M									R			D		F					
15H-6-40-40	137.92	158.81	R	M								R				D		F					
15H-6-70-70	138.22	159.11	R	M								C	R			D		F					
15H-CC, 6-40	138.50	159.32	F	R								R	R			D		R					
16H-CC, 7-12	149.33	169.66	F	M							C	C	F			D		F					
17H-CC, 7-12	158.62	179.95	R	P						F	R	A				F		F					
18H-CC, 0-7	167.39	192.08	B																				
19H-CC, 6-11	178.18	202.85	F	R							A	C	F			D		F		F			
20H-CC, 23-28	186.91	214.80	R	P									R			C				R			
21H-CC, 14-19	195.34	224.19	B																				
22H-CC, 15-20	205.44	233.45	R	P					R			F									R		Reworking
23H-CC, 24-29	215.80	245.25	A	M					A	F	D	C	F		R	C					R		
24H-CC, 0-10	221.80	252.11	C	P					A		D	C	A			C					F		
177-1093C-																							
1H-CC, 0-12	7.88	14.94	R	P										C			R			C		F	
2H-CC, 0-10	13.76	23.30	R	P					C				C		R					R		C	
3H-CC, 14-19	25.14	35.28	R	P					C		R		R		R	F						R	
4H-CC, 11-16	36.60	48.06	B																				
5H-CC, 11-16	44.50	58.92	R	P									R				C			A			
6H-CC, 17-22	52.17	68.01	B																				
7H-CC, 0-10	64.59	78.40	B																				
8H-CC, 24-29	74.05	89.30	B																				
9H-CC, 15-20	83.00	100.01	B																				
10H-CC, 8-15	91.06	108.55	B																				
11H-CC, 13-18	101.06	120.02	B																				
12H-CC, 6-11	111.34	131.39	F	P							F					D		F					
13H-CC, 13-18	114.37	138.42	B																				
14H-CC, 15-20	128.12	147.35	R	P								R				D		C					
15H-CC, 9-14	136.86	161.37	R	M							R	F				D							

Table T5 (continued).

Core, section, interval (cm)	Depth (mbsf)	Depth (mcd)	Abundance	Preservation	*Dictyococcites antarticus*	*Reticulofenestra pseudoumbilica*	*Discoaster brouweri*	*Dictyococcites productus*	*Reticulofenestra minuta*	*Reticulofenestra minutula*	*Coccolithus pelagicus*	*Pseudoemiliania lacunosa*	*Calcidiscus leptoporus*	*Calcidiscus macintyrei*	*Helicosphaera carteri*	*Gephyrocapsa* small	*Gephyrocapsa caribbeanica*	*Gephyrocapsa* medium (4-5.5 µm)	*Gephyrocapsa* large (>5.5 µm)	*Gephyrocapsa* sp. 3	*Reticulofenestra asanoi*	*Emiliania huxleyi*	Comments
16H-CC, 0-7	144.12	167.71	A	P					C	C		C	C			A				F			
17H-CC, 9-14	155.49	180.50	A	P							R	A	A		C					F			
18H-CC, 11-16	162.19	189.12	B																				
177-1093D-																							
1H-CC, 0-4	142.88	159.37	C	P					C			R				C	C						
2H-CC, 20-25	147.68	163.69	B																				
3H-CC, 0-10	159.90	175.13	F	P								F	F		R	C				R			
4H-CC, 14-19	173.37	190.68	B																				
5H-3, 0-0	177.00	195.23	C	P						F	C	C	C		R	C				F			
5H-6, 0-0	181.50	199.73	C	P							C	C	C		C	A				F			
5H-CC, 0-10	182.73	200.96	C	P						F		C	C		F	A							
6H-1, 0-0	183.50	204.99	C	P						F	C	C	C		R	C				F			
6H-CC, 0-10	189.17	210.66	C	P							R	F	C			A				F			
7H-1, 0-0	193.00	213.69	A	M					A			F	C		R	D				R			
8H-3, 0-0	205.50	227.33	R	P								D									R		
8H-4, 0-0	207.00	228.83	F	P					C	C	F	C	F								F		
8H-CC, 10-15	208.42	230.25	B																				
10H-3, 0-0	224.50	249.21	A	M						F	D	C	C			A					F		
10H-4, 0-0	226.00	250.71	A	G					C		D	C	C			C					C		
10H-CC, 0-10	226.74	251.45	A	M					C	F	D	C	A		R	A					C		
11H-2, 0-0	232.50	254.61	R	P							C	C	C								R		
11H-3, 0-0	234.00	256.11	A	P						C	D	C	F								?		
11H-4, 0-0	235.50	257.61	A	M						F	D	C	C			C					C		
11H-5, 0-0	237.00	259.11	A	M					A	F	D	A	C		F						R		
11H-CC, 0-10	237.67	259.78	A	M					C	F	D	A	C		F	A					F		
12H-1, 0-0	240.50	265.89	C	P							D	R	C		R								
12H-4, 0-0	245.00	270.09	C	P						A		A	C		R	C							Reworking
12H-CC, 15-20	245.52	270.61	R	P					C	C		C	C										
13H-4, 0-0	254.50	275.60	C	P						A		A	C		R	C			R				
14H-CC, 0-10	259.98	286.08	R	P					F	C	R	A	F			C			R				Reworking R
15H-CC, 0-5	270.39	296.49	F	M					C	A	R	A	F		R	R							
15H-1, 0-0	269.00	295.10	R	M					F	M		C	R		R			R					Reworking R
16H-CC, 0-5	278.50	304.60	R	P																			Dissolution (no identifiable forms)
17H-CC, 0-10	288.43	314.53	R	P							A	C	F			F			C				
18H-CC, 0-2	297.50	323.60	R	P						R		R	F					C	A				
21X-CC, 0-1	319.00	345.10	C	P							D	R	R					F					
27X-CC, 9-14	373.37	399.47	A	P						F	A	C	C			A		?					
28X-CC, 5-15	378.78	404.88	C	P						C		C	F			C		?					
32X-CC, 20-24	415.30	441.40	B																				
33X-CC, 13-18	434.38	460.48	B																				
34X-CC, 24-29	441.35	467.45	B																				
35X-2, 30-30	445.70	471.80	C	M						C	D	F	F	R									
35X-4-40-40	448.80	474.90	C	M							D	C				F							
35X-5-80-80	450.70	476.80	C	M							D	F	F		R	R							
35X-CC, 0-1	452.99	479.09	B																				
36X-3-90-90	457.20	483.30	C	M					F	C	D	F											
36X-4-90-90	458.70	484.80	C	M					F	C	D	F											
36X-5-90-90	460.20	486.30	F	M					F	R	A	F	A					R					
36X-6-70-70	461.50	487.60	C	M			R			F	D	F											
36X-CC, 24-29	462.96	489.06	B																				
37X-CC, 20-25	472.74	498.84	B																				
38X-CC, 48-53	480.16	506.36	B																				
39X-CC, 13-18	489.12	515.22	B																				
40X-CC, 4-6	495.54	521.64	R	P					A	A	R	R				F							

Table T5 (continued).

Core, section, interval (cm)	Depth (mbsf)	Depth (mcd)	Abundance	Preservation	*Dictyococcites antarticus*	*Reticulofenestra pseudoumbilica*	*Discoaster brouweri*	*Dictyococcites productus*	*Reticulofenestra minuta*	*Reticulofenestra minutula*	*Coccolithus pelagicus*	*Pseudoemiliania lacunosa*	*Calcidiscus leptoporus*	*Calcidiscus macintyrei*	*Helicosphaera carteri*	*Gephyrocapsa* small	*Gephyrocapsa caribbeanica*	*Gephyrocapsa* medium (4-5.5 µm)	*Gephyrocapsa* large (>5.5 µm)	*Gephyrocapsa* sp. 3	*Reticulofenestra asanoi*	*Emiliania huxleyi*	Comments
41X-1, 0-0	501.30	527.40	F	P				A	F		C		F										
41X-CC, 26-31	502.69	528.79	B																				
44X-1, 0-0	530.20	556.30	R	P				R				R				R							
45X-3, 0-0	542.90	569.00	C	P				A		F	A		F										
46X-1, 0-0	549.50	575.60	C	P				A			C	R											
47X-1, 0-0	559.10	585.20	C	P				F		C	C	R	F										
48X-CC, 17-19	568.97	595.07	B																				
50X-CC, 0-2	588.60	614.70	C	P	C	cf.																	late Miocene assemblage
177-1093E-																							
1H-CC, 10-15	10.50	11.09	B																				
2H-CC, 13-18	37.94	44.42	B																				

Notes: Abundance abbreviations: D = dominant, A = abundant, C = common, F = few, R = rare, B = barren. Preservation abbreviations: G = good, M = moderate, P = poor. For more specific definitions, refer to the "**Explanatory Notes**" chapter. The distributions of the species are mainly described in stratigraphic intervals where events are identified. This table is also available in ASCII format in the **TABLES** directory.

Table T6. Summary of biostratigraphic age assignments for Site 1093. (See table note. Continued on next three pages.)

Core, section, interval (cm)	Depth (mbsf)	Depth (mcd)	Calcareous nannofossil zone	Calcareous nannofossil age (Ma)	Diatom zone	Diatom age (Ma)	Diatom comment	Radiolaria zone	Radiolaria age (Ma)	Comment
177-1093A-										
1H-CC, 12-17	8.49	8.49	NN21b	0-0.085	*T. lentiginosa* Subzone c	0-0.18		Omega	0-0.46	
2H-3, 30-30	11.80	11.98	NN21b	0-0.085						
2H-5, 30-30	14.80	14.98	NN21a	0.085-0.26						
2H-CC, 12-17	18.09	18.27			*T. lentiginosa* Subzone c	0-0.18		Omega	0-0.46	
3H-4, 30-30	22.80	24.18	NN21a	<0.26						
3H-CC, 11-16	27.69	29.07			*T. lentiginosa* Subzone c	0-0.18		Omega	0-0.46	
4H-1, 1-1	27.51	31.49			*T. lentiginosa* Subzone c	0-0.18				
4H-2-120-120	30.20	34.18	NN21a	0.085-0.26						
4H-3, 30-30	30.80	34.78	NN21a	0.085-0.26						
4H-CC, 10-15	37.49	41.47			*T. lentiginosa* Subzone c	0-0.18	Cold-water assemblage	Omega	0-0.46	Barren CN
5H-3, 1-1	40.01	43.37			*T. lentiginosa* Subzone c	0-0.18	Cold-water assemblage			
5H-5, 1-1	43.01	46.37			*T. lentiginosa* Subzone c	0-0.18	Cold-water assemblage			
5H-6, 1-1	44.51	47.87			*T. lentiginosa* Subzone c	0-0.18	*H. karstenii* present			
5H-CC, 15-20	46.86	50.22			*T. lentiginosa* Subzone b,a	0.18-0.65	*H. karstenii* present	Omega	0-0.46	
6H-1, 1-1	46.51	51.85			*T. lentiginosa* Subzone b,a	0.18-0.65	*H. karstenii* present			
6H-2, 1-1	48.01	53.35			*T. lentiginosa* Subzone b,a	0.18-0.65	*H. karstenii* present			
6H-3, 1-1	49.51	54.85			*T. lentiginosa* Subzone b,a	0.18-0.65	*H. karstenii* present			Barren CN
6H-CC, 0-10	56.01	61.35	NN21a		*T. lentiginosa* Subzone b,a	0.18-0.65	*H. karstenii* present	Omega	0-0.46	Barren CN
7H-CC, 24-29	65.47	71.83	NN21a		*T. lentiginosa* Subzone b,a	0.18-0.65	*H. karstenii* present	Omega	0-0.46	
8H-1, 1-1	65.51	73.04			*T. lentiginosa* Subzone b,a	0.18-0.65	*H. karstenii* present			
8H-2, 1-1	67.01	74.54			*T. lentiginosa* Subzone b,a	0.18-0.65	*H. karstenii* present			
8H-3, 1-1	68.51	76.04			*T. lentiginosa* Subzone b,a	0.18-0.65	Cold-water assemblage			Barren CN
8H-5, 1-1	71.51	79.04			*T. lentiginosa* Subzone b,a	0.18-0.65	Cold-water assemblage			
8H-CC, 0-10	75.09	82.62			*T. lentiginosa* Subzone b,a	0.18-0.65	Cold-water assemblage	Omega	0-0.46	
9H-3, 1-1	78.01	85.68			*T. lentiginosa* Subzone b,a	0.18-0.65				
9H-CC, 15-20	84.77	92.44			*T. lentiginosa* Subzone b,a	0.18-0.65		Omega	0-0.46	
10H-6, 1-1	91.96	101.09			*T. lentiginosa* Subzone b,a	0.18-0.65				
10H-7, 1-1	93.46	102.59			*T. lentiginosa* Subzone b,a	0.18-0.65				
10H-CC, 0-10	93.93	103.06	NN20	0.26-0.46	*T. lentiginosa* Subzone b,a	0.18-0.65		Omega	0-0.46	
11H-1, 1-1	94.01	104.36			*T. lentiginosa* Subzone b,a	0.18-0.65				Barren CN
11H-CC, 16-21	103.76	114.11			*T. lentiginosa* Subzone b,a	0.18-0.65		Omega	0-0.46	
12H-CC, 0-10	113.06	124.69	NN20	0.26-0.46	*T. lentiginosa* Subzone b,a	0.18-0.65		Omega	0-0.46	Almost barren CN
13H-1, 1-1	113.01	124.68			*T. lentiginosa* Subzone b,a	0.18-0.65				Barren CN
13H-1, 10-10	113.10	124.77			*T. lentiginosa* Subzone b,a	0.18-0.65	*A. ingens* reworked			
13H-1, 75-75	113.75	125.42			*T. lentiginosa* Subzone b,a	0.18-0.65	*A. ingens* reworked			
13H-2, 1-1	114.51	126.18			*T. lentiginosa* Subzone b,a	0.18-0.65	*A. ingens* reworked			
13H-2, 40-40	114.90	126.57			*T. lentiginosa* Subzone b,a	0.18-0.65	*A. ingens* reworked			
13H-2, 120-120	115.70	127.37			*T. lentiginosa* Subzone b,a	0.18-0.65	*A. ingens* reworked			
13H-3, 1-1	116.01	127.68			*T. lentiginosa* Subzone b,a	0.18-0.65	*A. ingens* reworked			
13H-3, 80-81	116.80	128.47						Omega	0-0.46	Barren CN
13H-4, 80-81	118.30	129.97						Psi	0.46-0.83	Barren CN
13H-CC, 15-20	122.43	134.10			*T. lentiginosa* Subzone b,a	0.18-0.65	Cold-water assemblage	Psi	0.46-0.83	
14H-CC, 10-15	131.74	144.35			*T. lentiginosa* Subzone b,a	0.18-0.65	*A. ingens* reworked	Psi	0.46-0.83	
15H-5, 40-40	138.40	150.93	NN20	0.26-0.46						Barren CN

Table T6 (continued).

Core, section, interval (cm)	Depth (mbsf)	Depth (mcd)	Calcareous nannofossil zone	Calcareous nannofossil age (Ma)	Diatom zone	Diatom age (Ma)	Diatom comment	Radiolaria zone	Radiolaria age (Ma)	Comment
15H-6, 40-40	139.90	152.43	NN20	0.26-0.46						
15H-CC, 11-16	141.86	154.39	NN20	0.26-0.46	*T. lentiginosa* Subzone b,a	0.18-0.65	*A. ingens* reworked	Psi	0.46-0.83	
16H-3, 129-129	145.79	159.16	NN19	>0.46						Barren CN
16H-CC, 0-10	150.92	164.29			*T. lentiginosa* Subzone b,a	0.18-0.65	*A. ingens* reworked	Psi	0.46-0.83	
17H-CC, 24-29	160.88	173.99			*T. lentiginosa* Subzone b,a	0.18-0.65	*A. ingens* reworked			
18H-2, 1-1	162.01	176.30			*A. ingens* Subzone c	0.65-1.3				
18H-4, 1-1	165.01	179.30			*A. ingens* Subzone c	0.65-1.3				
18H-CC, 10-15	170.37	184.66	NN19	>0.46	*A. ingens* Subzone c	0.65-1.07				
19H-3, 1-1	173.01	190.10			*A. ingens* Subzone c	0.65-1.07				
19H-6, 1-1	177.51	194.60			*A. ingens* Subzone c	0.65-1.07				
19H-CC, 17-22	179.85	196.94			*A. ingens* Subzone c	0.65-1.07				
20H-2, 1-1	181.01	200.06			*A. ingens* Subzone c	0.65-1.07				
20H-7, 1-1	188.51	207.56			*A. ingens* Subzone c	0.65-1.07				
20H-CC, 17-22	189.28	208.33			*A. ingens* Subzone c	0.65-1.07		Psi	0.46-0.83	
21H-CC, 48-53	198.48	219.03			*A. ingens* Subzone c	0.65-1.07		Chi	0.83-1.92	
22H-2, 30-30	200.30	220.79	NN19	0.46-0.88						
22H-CC, 0-10	207.46	227.95	NN19	0.88-1.08	*A. ingens* Subzone c	0.65-1.07				
23H-CC, 0-10	217.63	238.72	NN19	0.88-0.96	*A. ingens* Subzone c	0.65-1.07		Chi	0.83-1.92	
24H-5, 15-15	223.65	245.54	NN19	0.88-0.96						
24H-5, 140-140	224.90	246.79	NN19	0.96-1.08						
24H-CC, 35-40	227.11	249.00	NN19	0.96-1.08	*A. ingens* Subzone c	0.65-1.07	*T. longissima* ooze			
25H-CC, 25-30	235.16	256.20			*A. ingens* Subzone c	0.65-1.07		Chi	0.83-1.92	
26H-6, 50-50	242.50	262.77	NN19	0.96-1.08						Barren CN
26H-CC, 19-24	243.69	263.96	NN19	>1.08	*A. ingens* Subzone c	0.65-1.07		Chi	0.83-1.92	Barren CN
28X-1, 1-1	251.01	271.85			*A. ingens* Subzone b	1.07-1.3				Barren CN
28X-CC, 12-17	257.85	278.69			*A. ingens* Subzone b	1.07-1.3		Chi	0.83-1.92	
29X-CC, 13-18	264.63	285.47			*A. ingens* Subzone b	1.07-1.3	*T. longissima* ooze	Chi	0.83-1.92	Barren CN
30H-CC, 15-20	274.26	295.10	NN19	1.08-1.24	*A. ingens* Subzone b	1.07-1.3		Chi	0.83-1.92	
31X-CC, 0-2	275.40	296.24			*A. ingens* Subzone b	1.07-1.3		Chi	0.83-1.92	
177-1093B-										
1H-CC, 8-13	7.10	12.38			*T. lentiginosa* Subzone c	0-0.18				Barren CN
2H-CC, 0-10	16.16	23.10			*T. lentiginosa* Subzone c	0-0.18		Omega	0-0.46	
3H-CC, 8-13	21.89	30.97			*T. lentiginosa* Subzone c	0-0.18				Barren CN
4H-CC, 9-14	35.84	45.32			*T. lentiginosa* Subzone c	0-0.18				
5H-CC, 4-12	45.21	57.31			*T. lentiginosa* Subzone b,a	0.18-0.65	*H. karstenii* present			
6H-CC, 15-20	53.08	67.74			*T. lentiginosa* Subzone b,a	0.18-0.65	*H. karstenii* present	Omega	0-0.46	
7H-CC, 10-15	63.89	77.66			*T. lentiginosa* Subzone b,a	0.18-0.65				
8H-CC, 7-12	73.39	87.86			*T. lentiginosa* Subzone b,a	0.18-0.65	*H. karstenii* present			
9H-CC, 10-15	83.24	99.33			*T. lentiginosa* Subzone b,a	0.18-0.65	*H. karstenii* present			
10H-CC, 17-22	91.91	108.38			*T. lentiginosa* Subzone b,a	0.18-0.65	Warm-water assemblage	Omega	0-0.46	Barren CN
11H-CC, 12-17	102.29	121.00			*T. lentiginosa* Subzone b,a	0.18-0.65				
12H-1, 130-130	103.40	122.95			*T. lentiginosa* Subzone b,a	0.18-0.65				
12H-2, 110-110	104.70	124.25			*T. lentiginosa* Subzone b,a	0.18-0.65	*A. ingens* reworked			
12H-3, 40-40	105.50	125.05			*T. lentiginosa* Subzone b,a	0.18-0.65	*A. ingens* reworked			
12H-4, 60-60	107.20	126.75			*T. lentiginosa* Subzone b,a	0.18-0.65	*A. ingens* reworked			Barren CN

Table T6 (continued).

Core, section, interval (cm)	Depth (mbsf)	Depth (mcd)	Calcareous nannofossil zone	Calcareous nannofossil age (Ma)	Diatom zone	Diatom age (Ma)	Diatom comment	Radiolaria zone	Radiolaria age (Ma)	Comment
12H-CC, 18-23	110.68	130.23			*T. lentiginosa* Subzone b,a	0.18-0.65	*A. ingens* reworked			
13H-1, 50-50	112.10	130.81			*T. lentiginosa* Subzone b,a	0.18-0.65				
13H-CC, 16-21	121.43	140.14			*T. lentiginosa* Subzone b,a	0.18-0.65	*A. ingens* reworked			
14H-CC, 11-16	130.23	149.88			*T. lentiginosa* Subzone b,a	0.18-0.65	*A. ingens* reworked	Psi	0.46-0.83	
15H-5, 40-40	136.42	157.31	NN20	0.26-0.46	*T. lentiginosa* Subzone b,a	0.18-0.65	*A. ingens* reworked			
15H-6, 40-40	137.92	158.81	NN19	0.46-0.88	*T. lentiginosa* Subzone b,a	0.18-0.65	*A. ingens* reworked			Almost barren CN
15H-CC, 13-18	138.50	159.39			*T. lentiginosa* Subzone b,a	0.18-0.65	*A. ingens* reworked			
16H-CC, 7-12	149.33	169.66			*T. lentiginosa* Subzone b,a	0.18-0.65	*A. ingens* reworked			
17H-CC, 7-12	158.62	179.95			*A. ingens* Subzone c	0.65-1.3				
18H-CC, 0-7	167.39	192.08			*A. ingens* Subzone c	0.65-1.07	*A. ingens* acme	Psi	0.46-0.83	
19H-CC, 6-11	178.18	202.85			*A. ingens* Subzone c	0.65-1.07				
20H-CC, 23-28	186.91	214.80			*A. ingens* Subzone c	0.65-1.07				
21H-CC, 14-19	195.34	224.19	NN19	0.46-.88?	*A. ingens* Subzone c	0.65-1.07				
22H-CC, 15-20	205.44	233.45	NN19	0.88-1.08?	*A. ingens* Subzone c	0.65-1.07	*T. longissima* ooze	Chi	0.83-1.92	
23H-CC, 24-29	215.80	245.25		0.88-1.08	*A. ingens* Subzone c	0.65-1.07				
24H-CC, 0-10	221.80	252.11		0.88-1.08	*A. ingens* Subzone c	0.65-1.07				Barren CN
177-1093C-										
1H-CC, 0-12	7.88	14.94	NN21a	<0.26				Omega	0-0.46	
2H-CC, 0-10	13.76	23.30	NN21a	<0.26						
3H-CC, 14-19	25.14	35.28	NN21a	<0.26				Omega	0-0.46	
5H-CC, 11-16	44.50	58.92		?				Omega	0-0.46	
6H-CC, 17-22	52.17	68.01			*T. lentiginosa* Subzone b,a	0.18-0.65	*H. karstenii* present			
7H-CC, 0-10	64.59	78.40			*T. lentiginosa* Subzone b,a	0.18-0.65		Omega	0-0.46	
12H-CC, 6-11	111.34	131.39	NN20?	<0.46?						
13H-CC, 13-18	114.37	138.42						Psi	0.46-0.83	
14H-CC, 15-20	128.12	147.35	NN19?	>0.46?						
15H-CC, 9-14	136.86	161.37	NN19	>0.46						
16H-CC, 0-7	144.12	167.71	NN19	>0.46						
17H-CC, 9-14	155.49	180.50	NN19	>0.46				Psi	0.46-0.83	
177-1093D-										
1H-CC, 0-4	142.88	159.37	NN19?	>0.46?	*T. lentiginosa* Subzone b,a	0.18-0.65	*A. ingens* reworked	?	?	
2H-CC, 20-25	147.68	163.69			*T. lentiginosa* Subzone b,a	0.18-0.65	*A. ingens* reworked			
3H-CC, 0-10	159.90	175.13	NN19	>0.46	*A. ingens* Subzone c	0.65-1.3				
4H-CC, 14-19	173.37	190.68			*A. ingens* Subzone c	0.65-1.07				
5H-CC, 0-10	182.73	200.96	NN19	>0.46	*A. ingens* Subzone c	0.65-1.07	Warm-water assemblage	?	?	
6H-CC, 0-10	189.17	210.66	NN19	>0.46	*A. ingens* Subzone c	0.65-1.07	Warm-water assemblage			
7H-1, 0-1	193.00	213.69	NN19	0.46-0.88						
7H-CC, 0-10	195.26	215.95			*A. ingens* Subzone c	0.65-1.07				
8H-3, 0-1	205.50	227.33	NN19	0.88-1.08						
8H-CC, 10-15	208.42	230.25			*A. ingens* Subzone c	0.65-1.07	Cold-water assemblage			
10H-CC, 0-10	226.74	251.45			*A. ingens* Subzone c	0.65-1.07		Chi	0.83-1.92	
11H-CC, 0-10	237.67	259.78	NN19	0.88-1.08	*A. ingens* Subzone c	0.65-1.07	*T. longissima* ooze			Barren CN
12H-1, 0-1	240.50	265.89	NN19	>1.08						Barren CN
12H-CC, 15-20	245.22	270.61	NN19	>1.08	*A. ingens* Subzone b	1.07-1.3				Barren CN
14H-CC, 0-10	259.98	286.08			*A. ingens* Subzone b	1.07-1.3		Chi	0.83-1.92	

Table T6 (continued).

Core, section, interval (cm)	Depth (mbsf)	Depth (mcd)	Calcareous nannofossil zone	Calcareous nannofossil age (Ma)	Diatom zone	Diatom age (Ma)	Diatom comment	Radiolaria zone	Radiolaria age (Ma)	Comment
15H-CC, 0-5	270.39	296.49			*A. ingens* Subzone b	1.07-1.3				
16H-CC, 0-5	278.50	304.60			*A. ingens* Subzone b	1.07-1.3				Barren CN
17H-CC, 0-10	288.43	314.53			*A. ingens* Subzone b	1.07-1.3		Chi	0.83-1.92	
18H-CC, 0-2	297.50	323.60			*A. ingens* Subzone b	1.07-1.3				reworked assemblage?
21X-CC, 0-1	319.00	345.10			*A. ingens* Subzone a	1.3-1.8	Warm-water assemblage			Barren CN
22H-CC, 0-5	329.75	355.85			*A. ingens* Subzone a	1.3-1.8	*A. ingens* ooze			
27X-CC, 9-14	373.37	399.47			*A. ingens* Subzone a	1.3-1.8		Chi	0.83-1.92	Barren CN
28X-CC, 5-15	378.78	404.88			*A. ingens* Subzone a	1.3-1.8				
29X-CC, 13-18	395.70	421.80			*A. ingens* Subzone a	1.3-1.8	Warm-water assemblage			
32X-CC, 20-24	415.30	441.40			*A. ingens* Subzone a	1.3-1.8	*A. ingens* acme			
33X-CC, 13-18	434.38	460.48			*A. ingens* Subzone a	1.3-1.8	*A. ingens* acme	Chi	0.83-1.92	
34X-1, 0-1	434.43	460.53			T. kolbei/F. matuyamae	2.0-2.5				
34X-3, 0-1	437.30	463.40			T. kolbei/F. matuyamae	2.0-2.5				
34X-5, 0-1	440.30	466.40			T. kolbei/F. matuyamae	2.0-2.5				
34X-CC, 24-29	441.35	467.45			T. kolbei/F. matuyamae	2.0-2.5				
35X-3, 0-1	446.90	473.00			T. kolbei/F. matuyamae	2.0-2.5				
35X-7, 0-1	452.50	478.60			T. kolbei/F. matuyamae	2.0-2.5				
35X-CC, 0-1	452.99	479.09			T. kolbei/F. matuyamae	2.0-2.5		Chi	0.83-1.92	
36X-CC, 24-29	462.96	489.06		<1.69?	T. kolbei/F. matuyamae	2.0-2.5		Phi	1.92-2.42	
37X-3, 0-1	465.90	492.00			T. kolbei/F. matuyamae	2.0-2.5				
37X-6, 0-1	470.40	496.50			T. vulnifica	2.5-2.6				
37X-CC, 20-25	472.74	498.84			T. vulnifica	2.5-2.6		Phi	1.92-2.42	
38X-5, 0-1	478.50	504.60			T. vulnifica	2.5-2.6				
38X-CC, 48-53	480.26	506.36			T. insigna	2.6-3.3				
39X-CC, 13-18	489.12	515.22			T. insigna	2.6-3.3				
40X-1, 38-38	491.98	518.08			T. insigna	2.6-3.3	*T. longissima* ooze			
40X-CC, 17-22	495.67	521.77			T. insigna	2.6-3.3		Upsilon	2.61-3.5	
41X-CC, 26-31	502.69	528.79			T. insigna	2.6-3.3	*T. longissima* ooze	Upsilon	2.61-3.5	
44X-CC, 20-25	531.31	557.41			F. interfrigidaria	3.3-3.8				
45X-CC, 0-10	545.28	571.38			F. interfrigidaria	3.3-3.8		Upsilon	2.61-3.5	
46X-CC, 11-16	552.51	578.61			F. interfrigidaria	3.3-3.8				
47X-CC, 0-10	559.40	585.50			F. interfrigidaria	3.3-3.8		Upsilon	3.5-4.57	
48X-CC, 8-9	568.88	594.98			F. reinholdii	5.6-6.4	*N. mirabilis* ooze			
50X-CC, 0-2	588.60	614.70			Unzoned		No diatoms	?	?	
177-1093E-										
1H-CC, 10-15	10.50	11.09			*T. lentiginosa* Subzone c	0-0.18	Cold-water assemblage			
2H-CC, 13-18	37.94	44.42			*T. lentiginosa* Subzone c	0-0.18				
177-1093F-										
1H-CC, 13-18	40.06	43.11			*T. lentiginosa* Subzone c	0-0.18	Cold-water assemblage			

Notes: CN = calcareous nannofossil. This table is also available in ASCII format in the **TABLES** directory.

Table T7. Distribution of major planktic foraminifer species at Site 1093. (**See table note.** Continued on next two pages.)

Core, section, interval (cm)	Depth (mbsf)	Depth (mcd)	Abundance	Preservation	*Globigerina bulloides*	*Globigerina quinqueloba*	*Globigerinita uvula*	*Globorotalia inflata*	*Globorotalia puncticulata*	*Globorotalia puncticuloides*	*Neogloboquadrina pachyderma* (sinistral)
177-1093A-											
1H-CC, 12-17	8.49	8.49	C	G							D
2H-CC, 12-17	18.09	18.27	R	G							D
3H-CC, 11-16	27.69	29.07	R	M							D
4H-CC, 10-15	37.49	41.47	R	G							D
5H-CC, 15-20	46.86	50.22	F	G	F						D
6H-CC, 0-10	56.01	61.35	C	G	R	R					D
7H-CC, 24-29	65.47	71.83	C	G							D
8H-CC, 0-10	75.09	82.62	B								
9H-CC, 15-20	84.77	92.44	B								
10H-CC, 0-10	93.93	103.06	F	G	A	F				P	D
11H-CC, 16-21	103.76	114.11	R	G	P						
12H-CC, 0-10	113.06	124.69	A	M	D					F	D
13H-CC, 15-20	122.43	134.10	R	G							D
14H-CC, 10-15	131.74	144.35	R	G	D						D
15H-CC, 11-16	141.86	154.39	R	G							D
16H-CC, 0-10	150.92	164.29	B								
17H-CC, 24-29	160.88	173.99	C	G							D
18H-CC, 10-15	170.37	184.66	A	G							D
19H-CC, 17-22	179.85	196.94	A	G		F					D
20H-CC, 17-22	189.28	208.33	R	G							D
21H-CC, 48-53	198.48	219.03	R	M							D
22H-CC, 0-10	207.46	227.95	A	G							D
23H-CC, 0-10	217.63	238.72	C	D						R	D
24H-CC, 35-40	227.11	249.00	A	G							D
25H-CC, 25-30	235.16	256.20	C	G							D
26H-CC, 19-24	243.69	263.96	A	G					F	R	D
28X-CC, 12-17	257.85	278.69	A	G					R	R	D
29X-CC, 13-18	264.63	285.47	A	G					R	R	D
30H-CC, 15-20	274.26	295.10	A	G					R		D
31X-CC, 0-2	275.40	296.24	A	G		A	R				D
177-1093B-											
1H-CC, 8-13	7.10	12.38	R	G							D
2H-CC, 0-10	16.16	23.10	R	G							D
3H-CC, 8-13	21.89	30.97	A	G	F			R			D
4H-CC, 9-14	35.84	45.32	B								
5H-CC, 4-12	45.21	57.31	R	G							D
6H-CC, 15-20	53.08	67.74	R	G							D
7H-CC, 10-15	63.89	77.66	R	G							D
8H-CC, 7-12	73.39	87.86	C	G							D
9H-CC, 10-15	83.24	99.33	R	G							D
10H-CC, 17-22	91.91	108.38	R	G							D
11H-CC, 12-17	102.29	121.00	B								
12H-CC, 18-23	110.68	130.23	C	G	F						D
13H-CC, 16-21	121.43	140.14	R	M							D
14H-CC, 11-16	130.23	149.88	R	G							D
15H-CC, 13-18	138.50	159.39	C	G							D
16H-CC, 7-12	149.33	169.66	A	G	R	R					D
17H-CC, 7-12	158.62	179.95	A	M		R					D
18H-CC, 0-7	167.39	192.08	B								
19H-CC, 6-11	178.18	202.85	A	G							D
20H-CC, 23-28	186.91	214.80	R	G							D

Table T7 (continued).

Core, section, interval (cm)	Depth (mbsf)	Depth (mcd)	Abundance	Preservation	*Globigerina bulloides*	*Globigerina quinqueloba*	*Globigerinita uvula*	*Globorotalia inflata*	*Globorotalia puncticulata*	*Globorotalia puncticuloides*	*Neogloboquadrina pachyderma* (sinistral)
21H-CC, 14-19	195.34	224.19	R	G							D
22H-CC, 15-20	205.44	233.45	F	G							D
23H-CC, 24-29	215.80	245.25	A	G						R	D
24H-CC, 0-10	221.80	252.11	A	G					R	R	D
177-1093C-											
1H-CC, 0-12	7.88	14.94	R	G							D
2H-CC, 0-10	13.76	23.30	C	G							D
3H-CC, 14-19	25.14	35.28	R	G	R						D
4H-CC, 11-16	36.60	48.06	C	G							D
5H-CC, 11-16	44.50	58.92	A	G							D
6H-CC, 17-22	52.17	68.01	R	G	R						D
7H-CC, 0-10	64.59	78.40	R	G							D
8H-CC, 24-29	74.05	89.30	R	M	R						D
9H-CC, 15-20	83.00	100.01	B								
10H-CC, 8-15	91.06	108.55	R	G	D					R	R
11H-CC, 13-18	101.06	120.02	R	G	D						D
12H-CC, 6-11	111.34	131.39	C	G	F						D
13H-CC, 13-18	114.37	138.42	R	M							D
14H-CC, 15-20	128.12	147.35	A	G							D
15H-CC, 9-14	136.86	161.37	A	G							D
16H-CC, 0-7	144.12	167.71	F	G							D
17H-CC, 9-14	155.49	180.50	A	G	R	F				R	D
18H-CC, 11-16	162.19	189.12	R	G							D
177-1093D-											
1H-CC, 0-4	142.88	159.37	A	G							D
2H-CC, 20-25	147.68	163.69	B								
3H-CC, 0-10	159.90	175.13	A	G							D
4H-CC, 14-19	173.37	190.68	R	G							D
5H-CC, 0-10	182.73	200.96	A	G							D
6H-CC, 0-10	189.17	210.66	F	G							D
7H-CC, 0-10	195.26	215.95	R	G							D
8H-CC, 10-15	208.42	230.25	B								
10H-CC, 0-10	226.74	251.45	A	G		R					D
11H-CC, 0-10	237.67	259.78	A	G	R				R		D
12H-CC, 15-20	245.22	270.61	A	G	R						D
13H-CC			A	G						P	D
14H-CC, 0-10	259.98	286.08	A	G		R			R	F	D
15H-CC, 0-5	270.39	296.49	A	G					R		D
16H-CC, 0-5	278.50	304.60	A	G						R	D
17H-CC, 0-10	288.43	314.53	A	G							D
18H-CC, 0-2	297.50	323.60	A	M							D
21X-CC, 0-1	319.00	345.10									
27X-CC, 9-14	373.37	399.47	A	M							D
28X-CC, 5-15	378.78	404.88	F	M							D
30X-CC, 13-18	398.00	424.10									
32X-CC, 20-24	415.30	441.40	F	M					P		D
33X-CC, 13-18	434.38	460.48	R	M							D
34X-CC, 24-29	441.35	467.45	B								
35X-CC, 0-1	452.99	479.09	B								
36X-CC, 24-29	462.96	489.06	R	M							D
37X-CC, 20-25	472.74	498.84	B								
38X-CC, 48-53	480.26	506.36	T	P							D
39X-CC, 13-18	489.12	515.22	B								
40X-CC, 17-22	495.67	521.77	B								

Table T7 (continued).

Core, section, interval (cm)	Depth (mbsf)	Depth (mcd)	Abundance	Preservation	*Globigerina bulloides*	*Globigerina quinqueloba*	*Globigerinita uvula*	*Globorotalia inflata*	*Globorotalia puncticulata*	*Globorotalia puncticuloides*	*Neogloboquadrina pachyderma* (sinistral)
41X-CC, 26-31	502.69	528.79	B								
44X-CC, 20-25	531.31	557.41	B								
45X-CC, 0-10	545.28	571.38	B								
46X-CC, 11-16	552.51	578.61	B								
47X-CC, 0-10	559.40	585.50	B								
48X-CC, 17-19	568.97	595.07	B								
177-1093E-											
1H-CC, 10-15	10.50	11.09	R	M		R					D
2H-CC, 13-18	37.94	44.42	B								

Notes: Abundance abbreviations: D = dominant, A = abundant, C = common, F = few, R = rare, P = present, B = barren. Preservation abbreviations: G = good, M = moderate, P = poor. For more specific definitions, refer to the "**Explanatory Notes**" chapter. This table is also available in ASCII format in the **TABLES** directory.

Table T8. Distribution of benthic foraminifers at Site 1093. (See table note. Continued on next page.)

Core, section, interval (cm)	Depth (mbsf)	Depth (mcd)	Abundance	Preservation	*Anomalinoides* sp.	*Astrononion* sp.	*Cassidulina reniforme*	*Chilostomella oolina*	*Cibicidoides* spp.	*Cibicidoides wuellerstorfi*	*Cribrostomoides* sp.	*Dentalina* sp.	*Eggerella bradyi*	*Ehrenbergina* sp.	*Epistominella exigua*	*Fissurina* spp.	*Francesita* sp.	*Globobulimina* sp.	*Globocassidulina subglobosa*	*Gyroidinoides soldanii*	*Gyroidinoides* spp.	Indeterminates (agg.)	Indeterminates (calc.)	*Lagena* spp.	*Lenticulina* sp.	*Martinotiella* sp.	*Melonis barleeanum*	*Melonis pompilioides*	*Miliolinella* sp.	*Nuttallides umbonifera*	*Oolina* spp.	*Ophthalmidium* spp.	*Oridorsalis umbonatus*	*Paralissoina* sp.	*Polymorphinia* spp.	*Pullenia bulloides*	*Pullenia quinqueloba*	*Pullenia subcarinata*	*Pullenia* sp.	*Pyrgo murrhina*	*Quinqueloculina* sp.	*Reophax* sp.	*Siphotextularia* sp.	*Sphaeroidina bulloides*	*Trifarina angulosa*	*Trilocculina trihedra*	*Uvigerina hispidicostata*	Sample sum	Number of species	Abundance (specimens/cm³)
177-1093A-																																																		
1H-CC, 12-17	8.49	8.49																																																		
2H-CC, 12-17	18.09	18.27	R	M					1													1		1			6								1													10	5	0.5
3H-CC, 11-16	27.69	29.07	R	M						3						2			2								33						2		9	7						4				62	9	3.1
4H-CC, 10-15	37.49	41.47	R	M											1				3						8		4								1											17	5	0.9
5H-CC, 15-20	46.86	50.22	R	M						1										1				1		4									3	1										11	6	0.6
6H-CC, 0-10	56.01	61.35	R	M					1						4											6									5	6			2	2		1				27	8	1.4
7H-CC, 24-29	65.47	71.83	R	P									1	1									1				5								3					2						13	6	0.7
8H-CC, 0-10	75.09	82.62	R	P																					2										1						2					5	3	0.3
9H-CC, 15-20	84.77	92.44	B																																													0		0.0
10H-CC, 0-10	93.93	103.06	F	M	1	1				1	1		4			1			1	3				1		11						2		1	6		1									35	14	1.8
11H-CC, 16-21	103.76	114.11	R	P																						2																					2	1	0.1
12H-CC, 0-10	113.06	124.69	C	M	1			1	1	8		1	9	3	7	7			2	4				2	1		11	24	1	1		1	7		2	21	2	4		14	3		3	1		3	145	32	9.1
13H-CC, 15-20	122.43	134.10	R	M																						3									1												4	2	0.2
14H-CC, 10-15	131.74	144.35	R	P																		1																									1	1	0.1
15H-CC, 11-16	141.86	154.39	R	M																				1		1																					2	2	0.1
16H-CC, 0-10	150.92	164.29	R	M																						1																					2	2	0.1
17H-CC, 24-29	160.88	173.99	F	M		1		2	2			1		2		2			4	1	2				1	9					1		5		10	10	6					1	1		5	66	21	3.3
18H-CC, 10-15	170.37	184.66	F	M					2					2		1			6								3						6		2								1		1	24	9	3.6
19H-CC, 17-22	179.85	196.94	F	G					1	7			2		1	1			3			3	1		1	1	13						4		17	10	1		7	2		1				76	19	3.8
20H-CC, 17-22	189.28	208.33	F	M						1								1								7									1					1	1					12	6	0.6
21H-CC, 48-53	198.48	219.03	F	M				2		3			4			2			1			1	2		1		9						15		4	4	3		4					1	2	58	17	2.9
22H-CC, 0-10	207.46	227.95	F	G										1		2	1				1				1		51									13	1	2		4			1		1	79	12	7.9
23H-CC, 0-10	217.63	238.72	F	M									3			1											4						1		3	1										13	6	0.7
24H-CC, 35-40	227.11	249.00	R	M						4																	3								9											16	3	0.8
25H-CC, 25-30	235.16	256.20	F	M			2			6					1	4					2						33						1	1	19	5	3					1		1		79	14	4.0
26H-CC, 19-24	243.69	263.96	R	M						1						1			3								7						1		4	2		1					1				21	9	1.1
28X-CC, 12-17	257.85	278.69	R	M					1				1			1			1		1				1		7								2												15	8	0.8
29X-CC, 13-18	264.63	285.47	R	M						2									1																													3	2	0.2
30H-CC, 15-20	274.26	295.10	R	G																															1												1	1	0.1
31X-CC, 0-2	275.4	296.24	R	M															1								2																					3	2	0.2
177-1093D-																																																		
27X-CC, 9-14	373.37	399.47	R	P								1		1		1										5									4												12	5	0.6
28X-CC, 5-15	378.78	404.88	R	M						3						1											6								1	4		1		1	1		2				20	9	1.0
32X-CC, 20-24	415.30	441.40	R	P						2		1				2											9								1												15	6	0.8
33X-CC, 13-18	434.38	460.48	B																																													0		0.0
34X-CC, 24-29	441.35	467.45	B																																													0		0.0

Table T8 (continued).

Core, section, interval (cm)	Depth (mbsf)	Depth (mcd)	Abundance	Preservation	*Anomalinoides* sp.	*Astrononion* sp.	*Cassidulina reniforme*	*Chilostomella oolina*	*Cibicidoides* spp.	*Cibicidoides wuellerstorfi*	*Cribrostomoides* sp.	*Dentalina* sp.	*Eggerella bradyi*	*Ehrenbergina* sp.	*Epistominella exigua*	*Fissurina* spp.	*Francesita* sp.	*Globobulimina* sp.	*Globocassidulina subglobosa*	*Gyroidinoides soldanii*	*Gyroidinoides* spp.	Indeterminates (agg.)	Indeterminates (calc.)	*Lagena* spp.	*Lenticulina* sp.	*Martinotiella* sp.	*Melonis barleeanum*	*Melonis pompilioides*	*Miliolinella* sp.	*Nuttallides umbonifera*	*Oolina* spp.	*Ophthalmidium* spp.	*Oridorsalis umbonatus*	*Parafissurina* sp.	*Polymorphinid* spp.	*Pullenia bulloides*	*Pullenia quinqueloba*	*Pullenia subcarinata*	*Pullenia* sp.	*Pyrgo murrhina*	*Quinqueloculina* sp.	*Reophax* sp.	*Siphotextularia* sp.	*Sphaeroidina bulloides*	*Trifarina angulosa*	*Triloculina trihedra*	*Uvigerina hispidicostata*	Sample sum	Number of species	Abundance (specimens/cm^3)
35X-CC, 0-1	452.99	479.09	B																																													0		0.0
36X-CC, 24-29	462.96	489.06	R	P										1					1																2	2												6	4	0.3
37X-CC, 20-25	472.74	498.84	B																																													0		0.0
38X-CC, 48-53	480.26	506.36	R	P									1							1											1																	3	3	0.2
39X-CC, 13-18	489.12	515.22	B																																													0		0.0
40X-CC, 17-22	495.67	521.77	R	M																															1												1	1	0.1
41X-CC, 26-31	502.69	528.79	B																																													0		0.0
44X-CC, 20-25	531.31	557.41	B																																													0		0.0
45X-CC, 0-10	545.28	571.38	R	M						1						1																			3		1										6	4	0.3
46X-CC, 11-16	552.51	578.61	R	P																												2																2	1	0.1
47X-CC, 0-10	559.40	585.50	R	P									1																																				1	1	0.1

Notes: Abundance abbreviations: C = common, F = few, R = rare, B = barren. Preservation abbreviations: G = good, M = moderate, P = poor. For more specific definitions, refer to the **"Explanatory Notes"** chapter). This table is also available in ASCII format in the **TABLES** directory.

Table T9. Control points used to calculate sedimentation rates at Site 1093.

Code	Event/Zone/Chron	Depth range of stratigraphic datums: Top Core, section, interval (cm)	Top Depth (mbsf)	Top Depth (mcd)	Base Core, section, interval (cm)	Base Depth (mbsf)	Base Depth (mcd)	Mean Depth (mbsf)	Mean Depth (mcd)	Age (Ma)	Sedimentation rate (m/m.y.)
		177-			177-						
CN	acme *E. huxleyi*	1093A-2H-3, 30-30	11.8	11.98	1093A-2H-5, 30-30	14.8	14.98	13.30	13.48	0.085	
DIAT	TOP *T. lentiginosa* Subzone b	1093A-5H-6, 1-1	44.51	47.87	1093A-5H-CC, 15-20	46.86	50.22	45.68	49.04	0.18	
CN	FO *E. huxleyi*	1093A-8H-1, 140-140	66.90	74.43	1093A-8H-2, 65-65	67.65	75.18	67.28	74.81	0.26	
RAD	BOT Omega Zone	1093A-13H-4, 80-81	118.30	130	1093A-13H-5, 80-81	119.80	131.5	119.05	130.72	0.46	
CN	LO *P. lacunosa*	1093A-15H-6, 40-40	139.90	152.43	1093A-16H-3, 129-129	145.79	159.2	142.84	155.80	0.46	
DIAT	TOP *A. ingens* Subzone c	1093A-17H-CC, 24-29	160.88	174	1093D-3H-CC, 0-10	159.90	175.1	160.39	174.56	0.65	
PMAG	BOT C1n (Brunhes)	1093A-20H-7, 30-30	188.80	208	1093A-22H-2, 80-80	200.80	222	194.80	214.63	0.78	
RAD	BOT Psi Zone	1093A-20H-CC, 17-22	189.28	208.3	1093A-21H-CC, 48-53	198.48	219	193.88	213.68	0.83	~250
CN	LO *R. asanoi*	1093A-22H-2, 30-30	200.30	220.8	1093D-8H-3, 0-0	205.50	227.3	202.90	224.06	0.88	
CN	RE *Gephyrocapsa* medium (4-5.5 µm)	1093A-24H-5, 15-15	223.65	245.5	1093A-24H-5, 140-140	224.90	246.8	224.28	246.16	0.96	
DIAT	TOP *A. ingens* Subzone b	1093A-26H-CC, 19-24	243.69	264	1093D-12H-CC, 15-20	245.22	270.6	244.46	267.28	1.07	
CN	FO *R. asanoi*	1093A-26H-6, 50-50	242.50	262.8	1093A-26H-CC, 19-24	243.69	264	243.10	263.36	1.08	
DIAT	TOP *A. ingens* Subzone a	1093D-18H-CC, 0-2	297.50	323.6	1093D-21X-CC, 0-1	319.00	345.1	308.25	334.35	1.30	
CN	FO *Gephyrocapsa* large (>5.5 µm)	1093D-18H-CC, 0-2	297.50	323.6	1093D-21X-CC, 0-1	319.00	345.1	308.25	334.35	1.46	
RAD	BOT Chi Zone	1093D-35X-CC, 0-1	452.99	479.1	1093D-36X-CC, 24-29	462.96	489.1	457.98	484.08	1.92	
DIAT	TOP *T. kolbei-F. matuyamae* Zone	1093D-33X-CC, 13-18	434.38	460.5	1093D-34X-1, 0-1	434.43	460.5	434.40	460.50	2.00	
RAD	BOT Phi Zone	1093D-37X-CC, 20-25	472.74	498.8	1093D-40X-CC, 17-22	495.67	521.8	484.21	510.30	2.42	
DIAT	TOP *T. vulnifica* Zone	1093D-37X-3, 0-1	465.90	492	1093D-37X-6, 0-1	470.40	496.5	468.15	494.25	2.50	
PMAG	BOT C2r (Matuyama)	1093D-38X-5, 50-50	479.00	505.1	1093D-38X-5, 50-50	482.50	508.6	480.75	506.85	2.58	~80
DIAT	TOP *T. insigna* Zone	1093D-38X-5, 0-1	478.50	504.6	1093D-38X-CC, 48-53	480.26	506.4	479.38	505.48	2.63	
DIAT	TOP *F. interfrigidara* Zone	1093D-41X-CC, 26-31	502.69	528.8	1093D-44X-CC, 20-25	531.31	557.4	517.00	543.10	3.26	
PMAG	BOT C2An (Gauss)	1093D-45X-3, 130-130	544.20	570.3	1093D-46X-2, 100-100	552.00	578.1	548.10	574.20	3.58	
DIAT	BOT *F. interfrigidara* Zone	1093D-47X-CC, 0-10	559.40	585.5	1093D-47X-CC, 0-10	559.40	585.5	559.40	585.50	3.80	
DIAT	*Neobrunia mirabilis* ooze	1093D-48X-CC, 8-9	568.88	595	1093D-48X-CC, 8-9	568.88	595	568.88	594.98	6.3-6.9	

Notes: Code abbreviations: CN = calcareous nannofossil, DIAT = diatom, RAD = radiolaria, PMAG = magnetic polarity. Event abbreviations: FO = first occurrence, LO = last occurrence, RE = reentrance, TOP = top of zone, BOT = bottom of zone. This table is also available in ASCII format in the **TABLES** directory.

Table T10. Diatom, silicoflagellate, ebridian, *Actiniscus*, sponge spicule, and opaline phytolith occurrence in smear slides investigated from Site 1093. (**See table note.** Continued on next four pages.)

Core, section, interval (cm)	Depth (mbsf)	Depth (mcd)	Diatom abundance	Diatom preservation	Silicoflagellate occurrence	Ebridian occurrence	Actiniscus occurrence	Sponge spicule occurrence	Opaline phytolith occurrence	*Actinocyclus actinochilus*	*Actinocyclus dimorphus*	*Actinocyclus fasciculatus*	*Actinocyclus ingens*	*Actinocyclus karstenii*	*Actinocyclus praeactinochilus*	*Asteromphalus hookeri*	*Asteromphalus parvulus*	*Azpeitia nodulifer*	*Azpeitia tabularis*	*Chaetoceros* spp.	*Coscinodiscus marginatus*	*Ethmodiscus rex*	*Eucampia antarctica*	*Fragilariopsis angulata*	*Fragilariopsis barronii*	*Fragilariopsis curta*	*Fragilariopsis interfrigidaria*	*Fragilariopsis kerguelensis*	*Fragilariopsis matuyamae*	*Fragilariopsis reinholdii*	*Fragilariopsis ritscheri*	*Fragilariopsis separanda*	*Fragilariopsis weaveri*	*Fragilariopsis* sp. A (Gersonde, 1991)	*Hemidiscus cuneiformis*	*Hemidiscus karstenii*	*Hemidiscus triangularus*	*Neobrunia mirabilis*	*Proboscia alata*	*Proboscia barboi*	*Rhizosolenia antennata* fo. *semispina*	*Rouxia antarctica*	*Rouxia heteropolara*	*Rouxia isopolica*	*Rouxia naviculoides*	*Stephanopyxis turris*	*Thalassionema nitzschioides*	*Thalassionema nitzschioides* var. *parva*	*Thalassiosira complicata*	*Thalassiosira convexa*	*Thalassiosira convexa* var. *aspinosa*	*Thalassiosira elliptipora*	*Thalassiosira fasciculata*	*Thalassiosira gracilis*	*Thalassiosira insigna*	Transition *T. insigna* / *T. oliverana*	*Thalassiosira inura*	*Thalassiosira kolbei*	*Thalassiosira lentiginosa*	*Thalassiosira lentiginosa* var. *obovatus*	*Thalassiosira oestrupii*	*Thalassiosira oliverana*	*Thalassiosira tetraoestrupii* var. *reimeri*	*Thalassiosira torokina*	*Thalassiosira vulnifica*	*Thallassiothrix antarctica-longissima* gr.	Diatom zone	Diatom age (Ma)
177-1093A-																																																																				
1H-CC, 12-17	8.49	8.49	A	G	T	B	B	B	B														R					D																										R					C							R	*T. lentiginosa* Subzone c	0-0.18
2H-CC, 12-17	18.09	18.27	A	G	T	B	B	B	B										R			X						A																															C							R	*T. lentiginosa* Subzone c	0-0.18
3H-CC, 11-16	27.69	29.07	A	G	T	B	B	B	B										R				R					A																										R					C			R				F	*T. lentiginosa* Subzone c	0-0.18
4H-1, 1-1	27.51	31.49	A	G	B	B	B	B	B																			A																										R					C		R	R				F	*T. lentiginosa* Subzone c	0-0.18
4H-CC, 10-15	37.49	41.47	C	M	T	B	B	B	B														F					C																															C							R	*T. lentiginosa* Subzone c	0-0.18
5H-3, 1-1	40.01	43.37	A	G-M	R	B	B	B	B				T*										C			R		A																R											T				C							F	*T. lentiginosa* Subzone c	0-0.18
5H-5, 1-1	43.01	46.37	A	G	R	B	B	B	B										R				F			R		D				R																											C		R	F				F	*T. lentiginosa* Subzone c	0-0.18
5H-6, 1-1	44.51	47.87	A	G	R	B	B	B	B							R			F				R			R		A				R				R																		R					C		R	F				F	*T. lentiginosa* Subzone c	0-0.18
5H-CC, 15-20	46.86	50.22	C	M	T	B	B	B	B									T	R									A								F																		R					C							F	*T. lentiginosa* Subzone a + b	0.18-0.65
6H-1, 1-1	46.51	51.85	A	G	B	B	B	B	B									T	R									A								R																							C			R				F	*T. lentiginosa* Subzone a + b	0.18-0.65
6H-2, 1-1	48.01	53.35	A	G	T	B	B	B	B										F									A								R																		F					C		F					F	*T. lentiginosa* Subzone a + b	0.18-0.65
6H-3, 1-1	49.51	54.85	A	G	T	B	B	B	B										F									A								R											R												F		F					F	*T. lentiginosa* Subzone a + b	0.18-0.65
6H-CC, 0-10	56.01	61.35	A	G	T	B	B	B	B														T					D								F																		R					C								*T. lentiginosa* Subzone a + b	0.18-0.65
7H-CC, 24-29	65.47	71.83	A	G	B	B	B	B	B										F									D								F																		R					C							F	*T. lentiginosa* Subzone a + b	0.18-0.65
8H-1, 1-1	65.51	73.04	A	G	B	B	B	B	B										F									A								R																							F			R				F	*T. lentiginosa* Subzone a + b	0.18-0.65
8H-2, 1-1	67.01	74.54	A	G	T	B	B	B	B										F									A								R																							F							C	*T. lentiginosa* Subzone a + b	0.18-0.65
8H-3, 1-1	68.51	76.04	A	G	B	B	B	B	B	R													F					A																															C			F				F	*T. lentiginosa* Subzone a + b	0.18-0.65
8H-5, 1-1	71.51	79.04	A	G	B	B	B	B	B	R													F					A																															A			F				F	*T. lentiginosa* Subzone a + b	0.18-0.65
8H-CC, 0-10	75.09	82.62	A	G	T	B	B	B	B														C					D																															F							F	*T. lentiginosa* Subzone a + b	0.18-0.65
9H-3, 1-1	78.01	85.68	A	G	T	B	B	B	B										R									D																										R					F							R	*T. lentiginosa* Subzone a + b	0.18-0.65
9H-CC, 15-20	84.77	92.44	A	G	T	B	B	B	B										R									D																										R					F							R	*T. lentiginosa* Subzone a + b	0.18-0.65
10H-6, 1-1	91.96	101.09	A	G	B	B	B	B	B										F									D								R																							F							F	*T. lentiginosa* Subzone a + b	0.18-0.65
10H-7, 1-1	93.46	102.59	A	G	T	B	B	B	B										F									D								R																		R					C		R					F	*T. lentiginosa* Subzone a + b	0.18-0.65
10H-CC, 0-10	93.93	103.06	A	G	T	B	B	B	B														R					D								T																		R					C			R				F	*T. lentiginosa* Subzone a + b	0.18-0.65
11H-1, 1-1	94.01	104.36	A	G	B	B	B	B	B	R																		A								R-F																							C		R					F	*T. lentiginosa* Subzone a + b	0.18-0.65
11H-CC, 16-21	103.76	114.11	A	G	T	B	B	B	B										R									D																															F							F	*T. lentiginosa* Subzone a + b	0.18-0.65
12H-CC, 0-10	113.06	124.69	C	M	T	B	B	B	B										F									D																															C							F	*T. lentiginosa* Subzone a + b	0.18-0.65
13H-1, 1-1	113.01	124.68	C-F	M	B	B	B	B	B										F					R				C				R															F												F							R	*T. lentiginosa* Subzone a + b	0.18-0.65
13H-1, 10-10	113.10	124.77	C	M	T	B	B	B	B				R*					R	F-C				F					A																			F												C							R	*T. lentiginosa* Subzone a + b	0.18-0.65
13H-1, 75-75	113.75	125.42	A	G	T	B	B	B	B				R*						F									D																			F												C							F	*T. lentiginosa* Subzone a + b	0.18-0.65
13H-2, 1-1	114.51	126.18	A	M	R	B	B	B	B				R*						F				R					A																				R											F							C	*T. lentiginosa* Subzone a + b	0.18-0.65
13H-2, 40-40	114.90	126.57	A	G	T	B	B	B	B				R*						F				R					A																			F												F		R					F	*T. lentiginosa* Subzone a + b	0.18-0.65

Table T10 (continued).

Core, section, interval (cm)	Depth (mbsf)	Depth (mcd)	Diatom abundance	Diatom preservation	Silicoflagellate occurrence	Ebridian occurrence	*Actiniscus* occurrence	Sponge spicule occurrence	Opaline phytolith occurrence	*Actinocyclus actinochilus*	*Actinocyclus dimorphus*	*Actinocyclus fasciculatus*	*Actinocyclus ingens*	*Actinocyclus karstenii*	*Actinocyclus praeactinochilus*	*Asteromphalus hookeri*	*Asteromphalus parvulus*	*Azpeitia nodulifer*	*Azpeitia tabularis*	*Chaetoceros* spp.	*Coscinodiscus marginatus*	*Ethmodiscus rex*	*Eucampia antarctica*	*Fragilariopsis angulata*	*Fragilariopsis barronii*	*Fragilariopsis curta*	*Fragilariopsis interfrigidaria*	*Fragilariopsis kerguelensis*	*Fragilariopsis matuyamae*	*Fragilariopsis reinholdii*	*Fragilariopsis ritscheri*	*Fragilariopsis separanda*	*Fragilariopsis weaveri*	*Fragilariopsis* sp. A (Gersonde, 1991)	*Hemidiscus cuneiformis*	*Hemidiscus karstenii*	*Hemidiscus triangularus*	*Neobrunia mirabilis*	*Proboscia alata*	*Proboscia barboi*	*Rhizosolenia antennata* fo. *semispina*	*Rouxia antarctica*	*Rouxia heteropolara*	*Rouxia isopolica*	*Rouxia naviculoides*	*Stephanopyxis turris*	*Thalassionema nitzschioides*	*Thalassionema nitzschioides* var. *parva*	*Thalassiosira complicata*	*Thalassiosira convexa*	*Thalassiosira convexa* var. *aspinosa*	*Thalassiosira elliptipora*	*Thalassiosira fasciculata*	*Thalassiosira gracilis*	*Thalassiosira insigna*	Transition *T. insigna* / *T. oliverana*	*Thalassiosira inura*	*Thalassiosira kolbei*	*Thalassiosira lentiginosa*	*Thalassiosira lentiginosa* var. *obovatus*	*Thalassiosira oestrupii*	*Thalassiosira oliverana*	*Thalassiosira tetraoestrupii* var. *reimeri*	*Thalassiosira torokina*	*Thalassiosira vulnifica*	*Thallassiothrix antarctica-longissima* gr.	Diatom zone	Diatom age (Ma)
13H-2, 120-120	115.70	127.37	A	G	T	B	B	B	B				T-R*						F-C									A																			F												C			R				C	*T. lentiginosa* Subzone a + b	0.18-0.65
13H-3, 1-1	116.01	127.68	A	G	R	B	B	B	B				R*						F				R					D																															F							F	*T. lentiginosa* Subzone a + b	0.18-0.65
13H-CC, 15-20	122.43	134.10	F	M	B	B	B	B	B	R													C			F		A																															F							R	*T. lentiginosa* Subzone a + b	0.18-0.65
14H-CC, 10-15	131.74	144.35	A	G	T	B	B	B	B				R*						R				R					A																F															C			R				F	*T. lentiginosa* Subzone a + b	0.18-0.65
15H-CC, 11-16	141.86	154.39	A	G	R	B	B	B	B				R*										F					D				R												R										R					F							R	*T. lentiginosa* Subzone a + b	0.18-0.65
16H-CC, 0-10	150.92	164.29	A	G	R	B	B	B	B				R*						R	R			F					C																R										R					F							C	*T. lentiginosa* Subzone a + b	0.18-0.65
17H-CC, 24-29	160.88	173.99	A	G	R	B	B	B	B				R*			R							R					D			R																					R							C							F	*T. lentiginosa* Subzone a + b	0.18-0.65
18H-2, 1-1	162.01	176.30	A	G	R	B	B	B	B				R*						F				R					A				R																											C							F	*A. ingens* Subzone c	0.65-1.3
18H-4, 1-1	165.01	179.30	A	G	R	B	B	B	B				F			R							R					A				R																						R					C			F				F	*A. ingens* Subzone c	0.65-1.3
18H-CC, 10-15	170.37	184.66	A	G	R	B	B	B	B				F				R		F				R					D																										R					C			R				R	*A. ingens* Subzone c	0.65-1.07
19H-3, 1-1	173.01	190.10	A	G-M	R	B	B	B	B				F										R					A				R												R															F			R				F	*A. ingens* Subzone c	0.65-1.07
19H-6, 1-1	177.51	194.60	A	M	R	B	B	B	B				F			R							R					C				R																											F			R				F	*A. ingens* Subzone c	0.65-1.07
19H-CC, 17-22	179.85	196.94	A	G	R	B	B	B	B				F						F									D				R												R			T							R					F			F				F	*A. ingens* Subzone c	0.65-1.07
20H-2, 1-1	181.01	200.06	A	G	R	B	B	B	B				F						F				R					A				R												R															F			R				C	*A. ingens* Subzone c	0.65-1.07
20H-7, 1-1	188.51	207.56	A	G	B	B	B	B	B				F						F				R					C				R												R								R							C			F				F	*A. ingens* Subzone c	0.65-1.07
20H-CC, 17-22	189.28	208.33	A	M	R	B	B	B	B				F									X						A																R								R	R						F							F	*A. ingens* Subzone c	0.65-1.07
21H-CC, 48-53	198.48	219.03	A	G-M	R	B	B	B	B				A				T		R									C				R												R								R							F			C				F	*A. ingens* Subzone c	0.65-1.07
22H-CC, 0-10	207.46	227.95	A	G	B	B	B	B	B				C															C																								F							C			C				F	*A. ingens* Subzone c	0.65-1.07
23H-CC, 0-10	217.63	238.72	A	G	R	B	B	B	B				F						R				R					A			R	R												F								R							C			F				F	*A. ingens* Subzone c	0.65-1.07
24H-CC, 35-40	227.11	249.00	A	G	B	B	B	B	B				F										R					C																								R							C			F				A	*A. ingens* Subzone c	0.65-1.07
25H-CC, 25-30	235.16	256.20	A	G-M	B	B	B	B	B				F															C																								R							C			R				C	*A. ingens* Subzone c	0.65-1.07
26H-CC, 19-24	243.69	263.96	A	G	R	B	B	B	B				C															C																								R							F			F				A	*A. ingens* Subzone c	0.65-1.07
28X-1, 1-1	251.01	271.85	A	G-M	R	B	B	B	B				A				R		R				R					C			R																						F						C							F	*A. ingens* Subzone b	1.07-1.3
28X-CC, 12-17	257.85	278.69	A	G	T	B	B	B	B				A															C																															F							F	*A. ingens* Subzone b	1.07-1.3
29X-CC, 13-18	264.63	285.47	A	P	B	B	B	B	B				R																																																					D	*A. ingens* Subzone b	1.07-1.3
30H-CC, 15-20	274.26	295.10	A	G	B	B	B	B	B				C															C																																						A	*A. ingens* Subzone b	1.07-1.3
31X-CC, 0-2	275.40	296.24	A	G	B	B	B	B	B			R	A															C																															F							F	*A. ingens* Subzone b	1.07-1.3
177-1093B-																																																																				
1H-CC, 8-13	7.10	12.38	A	G	B	B	B	B	B	T										R			R					A																															F							R	*T. lentiginosa* Subzone c	0-0.18
2H-CC, 0-10	16.16	23.10	A	G-M	R	B	B	B	B	T									F				R					A																															F			R				R	*T. lentiginosa* Subzone c	0-0.18
3H-CC, 8-13	21.89	30.97	A	G	R	B	B	B	B							R			R				R					C				R																											F			R				C	*T. lentiginosa* Subzone c	0-0.18
4H-CC, 9-14	35.84	45.32	A	G	F	B	B	B	B							T			R				R					A				R																											F		R	R				F	*T. lentiginosa* Subzone c	0-0.18
5H-CC, 4-12	45.21	57.31	A	G	R	B	B	B	B											R			R			T		A			R	R				R																		R					C		R					F	*T. lentiginosa* Subzone a + b	0.18-0.65
6H-CC, 15-20	53.08	67.74	A	G-M	R	B	B	B	B										F				R					A				R				R																							C		R	R				F	*T. lentiginosa* Subzone a + b	0.18-0.65
7H-CC, 10-15	63.89	77.66	A	G	R	B	B	B	B	R										R			F					A																															C			R				R	*T. lentiginosa* Subzone a + b	0.18-0.65

Table T10 (continued).

Core, section, interval (cm)	Depth (mbsf)	Depth (mcd)	Diatom abundance	Diatom preservation	Silicoflagellate occurrence	Ebridian occurrence	*Actiniscus* occurrence	Sponge spicule occurrence	Opaline phytolith occurrence	*Actinocyclus actinochilus*	*Actinocyclus dimorphus*	*Actinocyclus fasciculatus*	*Actinocyclus ingens*	*Actinocyclus karstenii*	*Actinocyclus praeactinochilus*	*Asteromphalus hookeri*	*Asteromphalus parvulus*	*Azpeitia nodulifer*	*Azpeitia tabularis*	*Chaetoceros* spp.	*Coscinodiscus marginatus*	*Ethmodiscus rex*	*Eucampia antarctica*	*Fragilariopsis angulata*	*Fragilariopsis barronii*	*Fragilariopsis curta*	*Fragilariopsis interfrigidaria*	*Fragilariopsis kerguelensis*	*Fragilariopsis matuyamae*	*Fragilariopsis reinholdii*	*Fragilariopsis ritscheri*	*Fragilariopsis separanda*	*Fragilariopsis weaveri*	*Fragilariopsis* sp. A (Gersonde, 1991)	*Hemidiscus cuneiformis*	*Hemidiscus karstenii*	*Hemidiscus triangularus*	*Neobrunia mirabilis*	*Proboscia alata*	*Proboscia barboi*	*Rhizosolenia antennata* fo. *semispina*	*Rouxia antarctica*	*Rouxia heteropolara*	*Rouxia isopolica*	*Rouxia naviculoides*	*Stephanopyxis turris*	*Thalassionema nitzschioides*	*Thalassionema nitzschioides* var. *parva*	*Thalassiosira complicata*	*Thalassiosira convexa*	*Thalassiosira convexa* var. *aspinosa*	*Thalassiosira elliptipora*	*Thalassiosira fasciculata*	*Thalassiosira gracilis*	*Thalassiosira insigna*	Transition *T. insigna* / *T. oliverana*	*Thalassiosira inura*	*Thalassiosira kolbei*	*Thalassiosira lentiginosa*	*Thalassiosira lentiginosa* var. *obovatus*	*Thalassiosira oestrupii*	*Thalassiosira oliverana*	*Thalassiosira tetraoestrupii* var. *reimeri*	*Thalassiosira torokina*	*Thalassiosira vulnifica*	*Thallassiothrix antarctica-longissima* gr.	Diatom zone	Diatom age (Ma)
8H-CC, 7-12	73.39	87.86	A	G	R	B	B	B	B										F				R					D				F				R																		R					F							R	*T. lentiginosa* Subzone a + b	0.18-0.65
9H-CC, 10-15	83.24	99.33	A	M	B	B	B	B	B										F				R					A				R				R																							C							F	*T. lentiginosa* Subzone a + b	0.18-0.65
10H-CC, 17-22	91.91	108.38	A	G	B	B	B	B	B							T			F				R					D																															F			R				R	*T. lentiginosa* Subzone a + b	0.18-0.65
11H-CC, 12-17	102.29	121.00	A	G	R	B	B	B	B	T									F				R					A				R																											F							R	*T. lentiginosa* Subzone a + b	0.18-0.65
12H-1, 130-130	103.40	122.95	A	G	B	B	B	B	B										R				R					A																															F							F	*T. lentiginosa* Subzone a + b	0.18-0.65
12H-2, 110-110	104.70	124.25	C	G	T	B	B	B	B				T						R									A																										R					C							F	*T. lentiginosa* Subzone a + b	0.18-0.65
12H-3, 40-40	105.50	125.05	A	G	B	B	B	B	B				T					F										A											R								R							F					C			R				F	*T. lentiginosa* Subzone a + b	0.18-0.65
12H-4, 60-60	107.20	126.75	A	G	T	B	B	B	B				R						R									D																										R					C			R				F	*T. lentiginosa* Subzone a + b	0.18-0.65
12H-CC, 18-23	110.68	130.23	A	G	F	B	B	B	B				T						C				R					C																															C							F	*T. lentiginosa* Subzone a + b	0.18-0.65
13H-1, 50-50	112.10	130.81	A	G	B	B	B	B	B										F				F					A																															C							F	*T. lentiginosa* Subzone a + b	0.18-0.65
13H-CC, 16-21	121.43	140.14	A	M	B	B	B	B	B	R			T							R			R			R		A			R													T															F							F	*T. lentiginosa* Subzone a + b	0.18-0.65
14H-CC, 11-16	130.23	149.88	A	G-M	R	B	B	B	B				T						R	R			R					C			R	R												R															C		R	R				R	*T. lentiginosa* Subzone a + b	0.18-0.65
15H-CC, 13-18	138.50	159.39	A	G	B	B	B	B	B				T-R						R	R			R					D				R												F															F		R	R				R	*T. lentiginosa* Subzone a + b	0.18-0.65
16H-CC, 7-12	149.33	169.66	A	M	R	B	B	B	B				R						R									C				R																						R					F			R				R	*T. lentiginosa* Subzone a + b	0.18-0.65
17H-CC, 7-12	158.62	179.95	A	G	R	B	B	B	B				R			T	T		F				R					D																															F			R				R	*A. ingens* Subzone c	0.65-1.3
18H-CC, 0-7	167.39	192.08	A	G	R	B	B	B	B				A			T			T	R			R					C				R												R															F			R				R	*A. ingens* Subzone c	0.65-1.07
19H-CC, 6-11	178.18	202.85	A	G	B	B	B	B	B				C						F									A			R																												F							R	*A. ingens* Subzone c	0.65-1.07
20H-CC, 23-28	186.91	214.80	A	G-M	B	B	B	B	B				C			T							R					F				R																				R							F			R				R	*A. ingens* Subzone c	0.65-1.07
21H-CC, 14-19	195.34	224.19	A	M	B	B	B	B	B				F							R								C																								F							F							R	*A. ingens* Subzone c	0.65-1.07
22H-CC, 15-20	205.44	233.45	A	G	B	B	B	B	B				F			T												F																								F							F							C	*A. ingens* Subzone c	0.65-1.07
23H-CC, 24-29	215.80	245.25	A	G-M	T	B	B	B	B				C															F																								F							F							F	*A. ingens* Subzone c	0.65-1.07
24H-CC, 0-10	221.80	252.11	A	G	T	B	B	B	B				F															C																								T							F			R				C	*A. ingens* Subzone c	0.65-1.07
177-1093C-																																																																					
6H-CC, 17-22	52.17	68.01	A	G	B	B	B	B	B										F							R		D				R				R																		R					F			R				C	*T. lentiginosa* Subzone a + b	0.18-0.65
7H-CC, 0-10	64.59	78.40	A	G	B	B	B	B	B	R									R				R			R		D			R	R																						R					C			R				F	*T. lentiginosa* Subzone a + b	0.18-0.65
177-1093D-																																																																			
1H-CC, 0-4	142.88	159.37	A	G	R	B	B	B	B				R						R				R					A				R																											C			R				F	*T. lentiginosa* Subzone a + b	0.18-0.65
2H-CC, 20-25	147.68	163.69	A	G	R	B	B	B	B	R			R						R				F					A																R										R					C			R				C	*T. lentiginosa* Subzone a + b	0.18-0.65
3H-CC, 0-10	159.90	175.13	A	G	R	B	B	B	B				F						R							R		A			R	R																						R					F			R				F	*A. ingens* Subzone c	0.65-1.3
4H-CC, 14-19	173.37	190.68	A	G	R	B	B	B	B				C										R					C			R	R												R															F							R	*A. ingens* Subzone c	0.65-1.07
5H-CC, 0-10	182.73	200.96	A	G	F	B	B	B	B				F						R				R					D			T																												F			R				R	*A. ingens* Subzone c	0.65-1.07
6H-CC, 0-10	189.17	210.66	A	G	F	B	B	B	B				F						F				R					A				R												R															F			R				F	*A. ingens* Subzone c	0.65-1.07
7H-CC, 0-10	195.26	215.95	A	G	R	B	B	B	B				F							R						T		C				R												R								T							F			R				F	*A. ingens* Subzone c	0.65-1.07
8H-CC, 10-15	208.42	230.25	A	M	B	B	B	B	B				F							F			R			R		C																R								R							C							F	*A. ingens* Subzone c	0.65-1.07
10H-CC, 0-10	226.74	251.45	A	G	R	B	B	B	B				F															A																R								R							C			R				C	*A. ingens* Subzone c	0.65-1.07

Table T10 (continued).

Core, section, interval (cm)	Depth (mbsf)	Depth (mcd)	Diatom abundance	Diatom preservation	Silicoflagellate occurrence	Ebridian occurrence	*Actiniscus* occurrence	Sponge spicule occurrence	Opaline phytolith occurrence	*Actinocyclus actinochilus*	*Actinocyclus dimorphus*	*Actinocyclus fasciculatus*	*Actinocyclus ingens*	*Actinocyclus karstenii*	*Actinocyclus praeactinochilus*	*Asteromphalus hookeri*	*Asteromphalus parvulus*	*Azpeitia nodulifer*	*Azpeitia tabularis*	*Chaetoceros* spp.	*Coscinodiscus marginatus*	*Ethmodiscus rex*	*Eucampia antarctica*	*Fragilariopsis angulata*	*Fragilariopsis barronii*	*Fragilariopsis curta*	*Fragilariopsis interfrigidaria*	*Fragilariopsis kerguelensis*	*Fragilariopsis matuyamae*	*Fragilariopsis reinholdii*	*Fragilariopsis ritscheri*	*Fragilariopsis separanda*	*Fragilariopsis weaveri*	*Fragilariopsis* sp. A (Gersonde, 1991)	*Hemidiscus cuneiformis*	*Hemidiscus karstenii*	*Hemidiscus triangularus*	*Neobrunia mirabilis*	*Proboscia alata*	*Proboscia barboi*	*Rhizosolenia antennata* fo. *semispina*	*Rouxia antarctica*	*Rouxia heteropolara*	*Rouxia isopolica*	*Rouxia naviculoides*	*Stephanopyxis turris*	*Thalassionema nitzschioides*	*Thalassionema nitzschioides* var. *parva*	*Thalassiosira complicata*	*Thalassiosira convexa*	*Thalassiosira convexa* var. *aspinosa*	*Thalassiosira elliptipora*	*Thalassiosira fasciculata*	*Thalassiosira gracilis*	*Thalassiosira insigna*	Transition *T. insigna* / *T. oliverana*	*Thalassiosira inura*	*Thalassiosira kolbei*	*Thalassiosira lentiginosa*	*Thalassiosira lentiginosa* var. *obovatus*	*Thalassiosira oestrupii*	*Thalassiosira oliverana*	*Thalassiosira tetraoestrupii* var. *reimeri*	*Thalassiosira torokina*	*Thalassiosira vulnifica*	*Thallassiothrix antarctica-longissima* gr.	Diatom zone	Diatom age (Ma)
11H-CC, 0-10	237.67	259.78	A	G	T	B	B	B	B				F			T			R									F				R																											R			F				C-A	*A. ingens* Subzone c	0.65-1.07
12H-CC, 15-20	245.22	270.61	A	G	R	B	B	B	B				F									X						C																									R						F			R				C	*A. ingens* Subzone b	1.07-1.3
14H-CC, 0-10	259.98	286.08	A	G	B	B	B	B	B				C						R									F																															F							A	*A. ingens* Subzone b	1.07-1.3
15H-CC, 0-5	270.39	296.49	A	G	B	B	B	B	B				C						R									F																															F			R				A	*A. ingens* Subzone b	1.07-1.3
16H-CC, 0-5	278.50	304.60	A	G	B	B	B	B	B				A															C																															R			R				C	*A. ingens* Subzone b	1.07-1.3
17H-CC, 0-10	288.43	314.53	A	G	B	B	B	B	B				A															F																															R							C	*A. ingens* Subzone b	1.07-1.3
18H-CC, 0-2	297.50	323.60	A	G	T	B	B	B	B			R	C												R			C																															F			R				F	*A. ingens* Subzone b	1.07-1.3
21X-CC, 0-1	319.00	345.10	A	G	R	B	B	B	B			R	A									X			R			C																															C			R	R			F	*A. ingens* Subzone a	1.3-1.8
22H-CC, 0-5	329.75	355.85	A	G	B	B	B	B	B				D												R			R																							R												T			F	*A. ingens* Subzone a	1.3-1.8
27X-CC, 9-14	373.37	399.47	A	G	B	B	B	B	B				A															F																															C				T			R	*A. ingens* Subzone a	1.3-1.8
28X-CC, 5-15	378.78	404.88	A	G	B	B	B	B	B				C									X			F			F																															R			F				F	*A. ingens* Subzone a	1.3-1.8
29X-CC, 13-18	395.70	426.19	A	G	B	B	B	B	B				F												F			F																			A												R			R				F	*A. ingens* Subzone a	1.3-1.8
32X-CC, 20-24	415.30	441.40	A	G	B	B	B	B	B				A-D												C																						F															R				F	*A. ingens* Subzone a	1.3-1.8
33X-CC, 13-18	434.38	460.48	A	G	B	B	B	B	B				D												F																																					R	R			R	*A. ingens* Subzone a	1.3-1.8
34X-1, 0-1	434.43	460.40	A	G-M	B	B	B	B	B				A												F			F						F						T																		R	F			R				F	*T. kolbei/F. matuyamae*	2.0-2.5
34X-3, 0-1	437.30	463.40	A	G-M	T	B	B	B	B				F												C															F																		R-F	F			R	R			R	*T. kolbei/F. matuyamae*	2.0-2.5
34X-5, 0-1	440.30	466.40	A	M	B	B	B	B	B				F	T											F			F	R					F						F																		R	F				R			R	*T. kolbei/F. matuyamae*	2.0-2.5
34X-CC, 24-29	441.35	467.45	A	G	R	B	B	B	B				F	F	R										C				R					F						R													R			F		R				F	R			C	*T. kolbei/F. matuyamae*	2.0-2.5
35X-3, 0-1	446.90	473.00	A	M	B	B	B	B	B				F												F				F					R						F																		R	C			F	R			R	*T. kolbei/F. matuyamae*	2.0-2.5
35X-7, 0-1	452.50	478.60	A	G-M	B	B	B	B	B			R	C															F	R					R																								R	F							R	*T. kolbei/F. matuyamae*	2.0-2.5
35X-CC, 0-1	452.99	479.09	A	G	R	B	B	B	B			R	F	F	R							R			F																										R		R			R			F			F	R	F		C	*T. kolbei/F. matuyamae*	2.0-2.5
36X-CC, 24-29	462.96	489.06	A	G	R	B	B	B	B				F	R											C			R						R						R											R					F		F	A		R	F	R			R	*T. kolbei/F. matuyamae*	2.0-2.5
37X-3, 0-1	465.90	492.00	A	G-M	B	B	B	B	B												C				F																																	C	F			C					*T. kolbei/F. matuyamae*	2.0-2.5
37X-6, 0-1	470.40	496.50	A	M	B	B	B	B	B												C				F																																	A	F			F			R		*T. vulnifica*	2.5-2.6
37X-CC, 20-25	472.74	498.84	C	G	R	B	B	B	B				R	R							R				F									R																								F	C			C			C	R	*T. vulnifica*	2.5-2.6
38X-5, 0-1	478.50	504.60	C	M	B	B	B	B	B						T						F	X			F									R		T											T												F			C			R-F	R	*T. vulnifica*	2.5-2.6
38X-CC, 48-53	480.26	506.36	C	M	B	B	B	B	B				R	R							C				F									R																					R	R	R	R	R		R	C			C	R	*T. insigna*	2.6-3.3
39X-CC, 13-18	489.12	515.22	C	M	B	B	B	B	B		R														F								F										R												A		R	R	R			R				F	*T. insigna*	2.6-3.3
40X-1, 38-38	491.98	518.08	A	M	B	B	B	B	B												R												R																						C			R								C-A	*T. insigna*	2.6-3.3
40X-CC, 17-22	495.67	521.77	C-F	M	B	B	B	B	B		R				F				R				R				R						R																						A					R		R				R	*T. insigna*	2.6-3.3
41X-CC, 26-31	502.69	528.79	A	M	B	B	B	B	B																																															R										D	*T. insigna*	2.6-3.3
44X-CC, 20-25	531.31	557.41	A	M	B	B	B	B	B																		F															F			F	F			R						T		R	R	R			R				F	*F. interfrigidaria*	3.3-3.8
45X-CC, 0-10	545.28	571.38	A	G	R	B	B	B	B																		R						R																R								R	R								A	*F. interfrigidaria*	3.3-3.8
46X-CC, 11-16	552.51	578.61	A	G	B	B	B	B	B																C		F			R										R																										F	*F. interfrigidaria*	3.3-3.8
47X-CC, 0-10	559.40	585.50	A	M	B	B	B	B	B										T		R				R		F							R						R										T							R		R			R				F	*F. interfrigidaria*	3.3-3.8

Table T10 (continued).

Core, section, interval (cm)	Depth (mbsf)	Depth (mcd)	Diatom abundance	Diatom preservation	Silicoflagellate occurrence	Ebridian occurrence	*Actiniscus* occurrence	Sponge spicule occurrence	Opaline phytolith occurrence	*Actinocyclus actinochilus*	*Actinocyclus dimorphus*	*Actinocyclus fasciculatus*	*Actinocyclus ingens*	*Actinocyclus karstenii*	*Actinocyclus praeactinochilus*	*Asteromphalus hookeri*	*Asteromphalus parvulus*	*Azpeitia nodulifer*	*Azpeitia tabularis*	*Chaetoceros* spp.	*Coscinodiscus marginatus*	*Ethmodiscus rex*	*Eucampia antarctica*	*Fragilariopsis angulata*	*Fragilariopsis barronii*	*Fragilariopsis curta*	*Fragilariopsis interfrigidaria*	*Fragilariopsis kerguelensis*	*Fragilariopsis matuyamae*
48X-CC, 8-9	568.88	594.98	A	P	B	B	B	B	B				R																
50X-CC, 0-2	588.60	614.70	B			B	B	B	B																				
177-1093E-																													
1H-CC, 10-15	10.50	11.09	A	G-M	B	B	B	B	B	R			T							F			F			R		C	
2H-CC, 13-18	37.94	44.42	A	G	R	B	B	B	B										R				R					C	
177-1093F-																													
1H-CC, 13-18	40.06	43.11	A	G	R	B	B	B	B				T										F			R		A	

Core, section, interval (cm)	*Fragilariopsis reinholdii*	*Fragilariopsis ritscheri*	*Fragilariopsis separanda*	*Fragilariopsis weaveri*	*Fragilariopsis* sp. A (Gersonde, 1991)	*Hemidiscus cuneiformis*	*Hemidiscus karstenii*	*Hemidiscus triangularus*	*Neobrunia mirabilis*	*Proboscia alata*	*Proboscia barboi*	*Rhizosolenia antennata* fo. *semispina*	*Rouxia antarctica*	*Rouxia heteropolara*	*Rouxia isopolica*	*Rouxia naviculoides*	*Stephanopyxis turris*	*Thalassionema nitzschioides*	*Thalassionema nitzschioides* var. *parva*	*Thalassiosira complicata*	*Thalassiosira convexa*	*Thalassiosira convexa* var. *aspinosa*	*Thalassiosira elliptipora*	*Thalassiosira fasciculata*	*Thalassiosira gracilis*	*Thalassiosira insigna*	Transition *T. insigna* / *T. oliverana*	*Thalassiosira inura*	*Thalassiosira kolbei*	*Thalassiosira lentiginosa*	*Thalassiosira lentiginosa* var. *obovatus*	*Thalassiosira oestrupii*	*Thalassiosira oliverana*	*Thalassiosira tetraoestrupii* var. *reimeri*	*Thalassiosira torokina*	*Thalassiosira vulnifica*	*Thallassiothrix antarctica-longissima* gr.	Diatom zone	Diatom age (Ma)
48X-CC, 8-9						T		R	A																													*F. reinholdii*	5.6-6.4
50X-CC, 0-2																																						Unzoned	
177-1093E-																																							
1H-CC, 10-15																														C							R	*T. lentiginosa* Subzone c	0-0.18
2H-CC, 13-18																									R					F			F				R	*T. lentiginosa* Subzone c	0-0.18
177-1093F-																																							
1H-CC, 13-18							T					T																		F			R				F	*T. lentiginosa* Subzone c	0-0.18

Notes: Abundance abbreviations: D = dominant, A = abundant, C = common, F = few, R = rare, T = trace, X = present, B = barren, * = reworking of *A. ingens*. Preservation abbreviations: G = good, M = moderate, P = poor. For more specific definitions, refer to the **"Explanatory Notes"** chapter. This table is also available in ASCII format in the **TABLES** directory.

Table T11. Distribution of the main components of the radiolarian assemblage at Site 1093. (**See table note.** Continued on next two pages.)

Core, section, interval (cm)	Depth (mbsf)	Depth (mcd)	Abundance	Preservation	*Antarctissa denticulata*	*Antarctissa longa*	*Bortyostrobus aquilonalis*	*Calocycas* sp. cf. *C. sempoiita*	*Cycladophora davisiana*	*Cycladophora davisiana cornutoides*	*Cycladophora pliocenica*	*Cyrtocapsella longithorax*	*Cyrtocapsella tetrapera*	*Desmospyris spongiosa*	*Dictyocoryne crisiae*	*Eucyrtidium carvertense*	*Eucyrtidium spinosum*	*Helotholus vema*	*Lithelius nautiloides*	*Pharmacantha* sp.	*Pterocanium trilobum*	*Pterocorys* spp.	*Prunopyle antarctica*	*Prunopyle haysi*	*Prunopyle tetrapila*	*Prunopyle titan*	*Saccospyris antarctica*	*Saturnalis circularis*	*Siphocampe lineata*	*Spongaaiscus osculosus*	*Spongoplegma antarcticum*	*Spongotrochus glacialis*	*Spongurus pylomaticus*	*Stylatractus universus*	*Triceraspyris antarctica*
177-1093A-																																			
1H-CC, 12-17	8.49	8.49	C	E	C	C	C		C	F	R				F				F								F		F		F					
2H-CC, 12-17	18.09	18.27	C	E	A	C	C		F	F	F				F				F	F		F						F		F	F	F		F
3H-CC, 11-16	27.69	29.07	C	E	A	C	F		C	F	P				F				F			F					F					F			F
4H-CC, 10-15	37.49	41.47	A	E	A	C	F		F	F	R				F			R	F	F		F							F		F	F			
5H-CC, 15-20	46.86	50.22	C	E	A	F	C		F	F	R				F				F			F	F	F		F	F	F	F		F				
6H-CC, 0-10	56.01	61.35	C	E	A	C	F		C	F	R				F				F			F					F		F	F					F
7H-CC, 24-29	65.47	71.83	A	E	A	C	F		C	F	R				F				F			F	F				F		F	F					F
8H-CC, 0-10	75.09	82.62	A	E	A	C	F		C	F	R				F				F			F	F				F		F	F					F
9H-CC, 15-20	84.77	92.44																																	
10H-CC, 0-10	93.93	103.06	A	E	A	C	F		C	F	R				F				F	F		F					F		F	F					F
11H-CC, 16-21	103.76	114.11																																	
12H-CC, 0-10	113.06	124.69	A	E	A	C	F		F	F	R				F			R	F		F	F	F		F		F	F	F			F			
13H-4, 80-81	118.3	129.97	C	E	A	C	F		C	F	R				F				F			F	F				F		F	F					F
13H-5, 80-81	119.8	131.47	C	E	A	C			C	F	R				F				F			F	F		F		F		F	F	F	F	F	R	F
13H-CC, 15-20	122.43	134.1	C	E	C	C			F	F						R				F			F		F							F	F	F	F
14H-CC, 10-15	131.74	144.35	C	E	A	C	F		C	F	R				F				F			F	F		F		F		F	F	F	F	F	R	F
15H-CC, 11-16	141.86	154.39	C	E	C	C			C	F	R				F				F			F	F		F		F		F	F	F	F	F	R	F
16H-CC, 0-10	150.92	164.29	C	E	C	C			C	F	R				F				F			F	F		F		F		F	F	F	F	F	R	F
17H-CC, 24-29	160.88	173.99																																	
18H-CC, 10-15	170.37	184.66																																	
19H-CC, 17-22	179.85	196.94																																	
20H-CC, 17-22	189.28	208.33	C	E	A	C			C	F	R				R				F				F		F		F		F		F	F			
21H-CC, 48-53	198.48	219.03	C	E	A	C			C	F	R				R						R				F		F		F	F	F				F
22H-CC, 0-10	207.46	227.95	C	E	C	F			C		R								F				F				F			F		F			
23H-CC, 0-10	217.63	238.72			A	C			C	F	R								F	C	R						F			F	F		F		F
24H-CC, 35-40	227.11	249																																	
25H-CC, 25-30	235.16	256.2	A	E	A	C			C	F	R				R	R					R		F				F				F				
26H-CC, 19-24	243.69	263.96	C	E	A	C			C	F	R								F	F			F		F		F		F		F	F	F		F
28X-CC, 12-17	257.85	278.69	C	E	C	C			C		R									F							F		F						
29X-CC, 13-18	264.63	285.47	C	E	C	F			C	F	R								F	F			F		F		F			F	F				
30H-CC, 15-20	274.26	295.1	C	E	C	C			C	F	R				R						R		F				F				F				F
31X-CC, 0-2	275.4	296.24	C	E	A	C			C	F	R								F	F			F		F		F		F	F	F		F		
177-1093B-																																			
1H-CC, 8-13	7.1	12.38																																	
2H-CC, 0-10	16.16	23.1	R	G	A	A	F		C	F					F				F	F		F	F				F		F		F				F
3H-CC, 8-13	21.89	30.97																																	
4H-CC, 9-14	35.84	45.32																																	
5H-CC, 4-12	45.21	57.31																																	
6H-CC, 15-20	53.08	67.74	A	E	A	A	F		F						R							F					F		F		F	F			F
7H-CC, 10-15	63.89	77.66																																	
8H-CC, 7-12	73.39	87.86																																	
9H-CC, 10-15	83.24	99.33																																	
10H-CC, 17-22	91.91	108.38	C	E	C					F					F				F	F			F				F				F				
11H-CC, 12-17	102.29	121																																	
12H-CC, 18-23	110.68	130.23																																	
13H-CC, 16-21	121.43	140.14																																	
14H-CC, 11-16	130.23	149.88	C	E	C	C	F		C		R				F				F			R			C		F		F		F		F	R	F
15H-CC, 13-18	138.5	159.39																																	
16H-CC, 7-12	149.33	169.66																																	
17H-CC, 7-12	158.62	179.95																																	
18H-CC, 0-7	167.39	192.08	A	E	A	C			C						F				F				F		F		F		F		F		F	F	
19H-CC, 6-11	178.18	202.85																																	
20H-CC, 23-28	186.91	214.8																																	

Table T11 (continued).

Core, section, interval (cm)	Depth (mbsf)	Depth (mcd)	Abundance	Preservation	*Antarctissa denticulata*	*Antarctissa longa*	*Bortyostrobus aquilonalis*	*Calocyclas* sp. cf. *C. semipolita*	*Cycladophora davisiana*	*Cycladophora davisiana cornutoides*	*Cycladophora pliocenica*	*Cyrtocapsella longithorax*	*Cyrtocapsella tetrapera*	*Desmospyris spongiosa*	*Dictyocoryne crisiae*	*Eucyrtidium carvertense*	*Eucyrtidium spinosum*	*Helotholus vema*	*Lithelius nautiloides*	*Phormacantha* sp.	*Pterocanium trilobum*	*Pterocorys* spp.	*Prunopyle antarctica*	*Prunopyle haysi*	*Prunopyle tetrapila*	*Prunopyle titan*	*Saccospyris antarctica*	*Saturnalis circularis*	*Siphocampe lineata*	*Spongodiscus osculosus*	*Spongoplegma antrcticum*	*Spongotrochus glacialis*	*Spongrus pylomaticus*	*Stylatractus universus*	*Triceraspyris antarctica*
21H-CC, 14-19	195.34	224.19																																
22H-CC, 15-20	205.44	233.45	R	E	A	A									R				F									F							
23H-CC, 24-29	215.8	245.25																																	
24H-CC, 0-10	221.8	252.11	C	E	C	C			C	F																	F	F						R	F
177-1093C-																																			
1H-CC, 0-12	7.88	14.94	A	E	A				C		F								F								F								F
2H-CC, 0-10	13.76	23.3																																	
3H-CC, 14-19	25.14	35.28	A	E	A	F	C		F	F	R				F				F			F	F		F		F	F	F		F				
4H-CC, 11-16	36.6	48.06																																	
5H-CC, 11-16	44.5	58.92	C	E	A	C			C		R				F				F						F		F				F		F		
6H-CC, 17-22	52.17	68.01																																	
7H-CC, 0-10	64.59	78.4	A	E	A	C			C		F								F						F						F		F		
8H-CC, 24-29	74.05	89.3																																	
9H-CC, 15-20	83	100.01	A	E	C	C	F		C		F				F					F	R	R					F	F	F		F				
10H-CC, 8-15	91.06	108.55																																	
11H-CC, 13-18	101.06	120.02	A	E	C	C	F		C		F									R	R	R					F	F	F		F				
12H-CC, 6-11	111.34	131.39																																	
13H-CC, 13-18	114.37	138.42	C	E	A	C			C		R				F				F						F		F				F	F	F	R	
14H-CC, 15-20	128.12	147.35																																	
15H-CC, 9-14	136.86	161.37																																	
16H-CC, 0-7	144.12	167.71																																	
17H-CC, 9-14	155.49	180.5	C	E	C	F			F		R									F	R	R					F	F	F		F			F	
18H-CC, 11-16	162.19	189.12																																	
177-1093D-																																			
1H-CC, 0-4	142.88	159.37	A	E	A	A	F		C		R				F				F				F		F		F				F		F		
2H-CC, 20-25	147.68	163.69																																	
3H-CC, 0-10	159.9	175.13																																	
4H-CC, 14-19	173.37	190.68																																	
5H-CC, 0-10	182.73	200.96	C	E	A	A	C		C																										
6H-CC, 0-10	189.17	210.66																																	
8H-CC, 10-15	208.42	230.25																																	
10H-CC, 0-10	226.74	251.45	C	E	C	C			F						R						F				F						F	F		F	
11H-CC, 0-10	237.67	259.78																																	
12H-CC, 15-20	245.22	270.61																																	
14H-CC, 0-10	259.98	286.08	A	E	C	C	F		F												F		F		F		F	F			F				
15H-CC, 0-5	270.39	296.49																																	
16H-CC, 0-5	278.5	304.6																																	
17H-CC, 0-10	288.43	314.53	C	E	A	A	C	R	C	R		R				R	R				R						F	F			F				
18H-CC, 0-2	297.5	323.6	R	E	A				A																		F	F	C						
21X-CC, 0-1	319	345.1																																	
27X-CC, 9-14	373.37	399.47	C	G	A														F		R						F	F	F						
28X-CC, 5-15	378.78	404.88																																	
30X-CC, 13-18	398	424.1																																	
32X-CC, 20-24	415.3	441.4																																	
33X-CC, 13-18	434.38	460.48	C	G	A	A			A		R																F	F			F				
34X-CC, 24-29	441.35	467.45																																	
35X-CC, 0-1	452.99	479.09	C	G	A				A		R																		F		F				
36X-CC, 24-29	462.96	489.06	C	G	A	A			A		F					F												F		F				
37X-CC, 20-25	472.74	498.84	A	E	A	C		R	C		F		R			F											F	F	F		F				
38X-CC, 48-53	480.26	506.36																																	
39X-CC, 13-18	489.12	515.22																																	
40X-CC, 17-22	495.67	521.77	A	G	C	F					F			F		C		A										F	F					F	
41X-CC, 26-31	502.69	528.79	C	G	F						F			F		C		A																	
44X-CC, 20-25	531.31	557.41																																	

Table T11 (continued).

Core, section, interval (cm)	Depth (mbsf)	Depth (mcd)	Abundance	Preservation	*Antarctissa denticulata*	*Antarctissa longa*	*Bortyostrobus aquilonalis*	*Calocyclas* sp. cf. *C. semipolita*	*Cycladophora davisiana*	*Cycladophora dvisiana cornutoides*	*Cycladophora pliocenica*	*Cyrtocapsella longithorax*	*Cyrtocapsella tetrapera*	*Desmospyris spongiosa*	*Dictyocoryne crisiae*	*Eucyrtidium carvertense*	*Eucyrtidium spinosum*	*Helotholus vema*	*Lithelius nautiloides*	*Phormacantha* sp.	*Pterocanium trilobum*	*Pterocorys* spp.	*Prunopyle antarctica*	*Prunopyle haysi*	*Prunopyle tetrapila*	*Prunopyle titan*	*Saccospyris antarctica*	*Saturnalis circularis*	*Siphocampe lineata*	*Spongodiscus osculosus*	*Spongoplegma antrcticum*	*Spongotrochus glacialis*	*Spongrus pylomaticus*	*Stylatractus universus*	*Triceraspyris antarctica*
45X-CC, 0-10	545.28	571.38	C	G	F	F					C			F		C		A																	
46X-CC, 11-16	552.51	578.61																																	
47X-CC, 0-10	559.4	585.5	C	G	F						F			F		F		C							F			F							
48X-CC, 17-19	568.97	595.07																																	
49X-CC, 7-12	578.47	604.57																																	
50X-CC, 0-2	588.6	614.7	R	P																				A											
177-1093E-																																			
1H-CC, 10-15	10.5	11.09	A	E	A	A			C		R								F				F						F		F	F			
2H-CC, 13-18	37.94	44.42	A	E	A	A			C						R				F								F		F	F		F	C		F

Notes: Abundance abbreviations: A = abundant, C = common, F = few, R = rare. Preservation abbreviations: E = excellent, G = good, P = poor. For more specific definitions, refer to the **"Explanatory Notes"** chapter. This table is also available in ASCII format in the **TABLES** directory.

Table T12. Concentrations of methane obtained by the headspace technique at Site 1093.

Core, section, interval (cm)	Depth (mbsf)	C_1 (ppmv)
177-1093A-		
1H-4, 0-5	4.53	2
2H-5, 0-5	14.52	3
3H-5, 0-5	24.02	3
4H-5, 0-5	33.52	3
5H-5, 0-5	43.02	4
6H-5, 0-5	52.52	3
7H-5, 0-5	61.90	4
8H-5, 0-5	71.53	5
9H-5, 0-5	81.03	4
10H-5, 0-5	90.42	4
11H-5, 0-5	100.02	5
12H-5, 0-5	109.52	7
13H-5, 0-5	119.02	7
14H-5, 0-5	128.52	7
15H-5, 0-5	138.02	6
17H-5, 0-5	157.02	5
18H-5, 0-5	166.52	8
19H-5, 0-5	176.02	7
20H-5, 0-5	185.52	7
22H-5, 0-5	204.52	9
24H-5, 0-5	223.52	7
26H-5, 0-5	240.52	7
28X-4, 0-5	255.52	14
177-1093D-		
12H-3, 0-5	243.52	11
13H-4, 0-5	254.52	9
15H-1, 0-5	269.02	9
27X-3, 0-5	370.42	6
28X-2, 0-5	378.42	8
33X-5, 0-5	430.72	15
34X-4, 0-5	438.82	19
35X-5, 0-5	449.92	18
36X-5, 0-5	459.32	16
38X-5, 0-5	478.52	14
39X-4, 0-5	486.52	12

Note: C_1 = methane.

Table T13. Interstitial water chemistry from shipboard measurements at Site 1093. (Continued on next page.)

Core, section, interval (cm)	Depth (mbsf)	pH	Method	Alkalinity (mM)	Method	Salinity	Method	Cl (mM)	Method	SO_4 (mM)	Method	Na (mM)	Method	Mg (mM)	Method	Ca (mM)	Method
177-1093A-																	
1H-1, 145-150	1.48	7.97	ISE	3.659	T	35.0	R	553	T	28.4	I	465	CB	57.8	I	11.1	I
1H-2, 145-150	2.98	7.95	ISE	4.142	T	35.0	R	552	T	27.9	I	464	CB	57.2	I	10.9	I
1H-3, 145-150	4.48	8.02	ISE	3.980	T	35.0	R	552	T	28.1	I	464	CB	57.7	I	10.8	I
1H-4, 145-150	5.98	8.13	ISE	4.242	T	35.5	R	553	T	28.4	I	464	CB	57.7	I	11.6	I
1H-5, 145-150	7.48	8.08	ISE	4.487	T	35.0	R	557	T	27.9	I	469	CB	57.9	I	10.8	I
2H-1, 145-150	9.98	8.16	ISE	4.742	T	35.5	R	554	T	27.3	I	465	CB	58.0	I	10.6	I
2H-2, 145-150	11.48	8.13	ISE	4.795	T	35.5	R	556	T	27.9	I	469	CB	57.6	I	10.8	I
2H-3, 145-150	12.98	7.85	ISE	4.991	T	35.5	R	558	T	27.8	I	472	CB	57.0	I	10.7	I
2H-4, 145-150	14.48	7.84	ISE	5.933	T	35.0	R	558	T	27.6	I	474	CB	56.6	I	10.4	I
2H-5, 145-150	15.98	7.63	ISE	4.850	T	35.5	R	558	T	28.2	I	489	CB	50.7	I	9.4	I
2H-6, 145-150	17.48	7.32	ISE	4.613	T	35.5	R	559	T	27.6	I	476	CB	55.3	I	10.3	I
3H-1, 145-150	19.48	8.04	ISE	4.752	T	35.5	R	557	T	27.4	I	475	CB	55.8	I	9.8	I
3H-2, 145-150	20.98	7.58	ISE	4.004	T	35.5	R	560	T	27.6	I	477	CB	55.9	I	9.6	I
3H-3, 145-150	22.48	8.21	ISE	4.882	T	36.0	R	561	T	27.8	I	477	CB	56.8	I	10.0	I
3H-4, 145-150	23.98	7.87	ISE	5.284	T	36.0	R	562	T	28.4	I	479	CB	57.0	I	9.9	I
3H-5, 145-150	25.48	8.28	ISE	4.821	T	35.5	R	561	T	29.1	I	480	CB	56.8	I	9.7	I
3H-6, 145-150	26.98	8.13	ISE	4.770	T	35.5	R	564	T	28.7	I	479	CB	57.8	I	9.9	I
4H-1, 145-150	28.98	8.19	ISE	4.774	T	36.0	R	564	T	28.0	I	479	CB	57.8	I	9.7	I
4H-2, 145-150	30.48	8.06	ISE	4.886	T	35.5	R	565	T	28.8	I	482	CB	57.1	I	9.9	I
4H-3, 145-150	31.98	8.27	ISE	4.994	T	36.0	R	566	T	28.0	I	485	CB	56.2	I	9.4	I
4H-4, 145-150	33.48	7.95	ISE	4.883	T	36.0	R	565	T		I		CB		I		I
4H-5, 145-150	34.98	8.11	ISE	4.919	T	35.5	R		T	28.0	I		CB	56.5	I	9.7	I
4H-6, 145-150	36.48	8.21	ISE	5.061	T	35.5	R		T	28.4	I		CB	56.6	I	10.2	I
5H-1, 145-150	38.48	8.26	ISE	5.092	T	36.0	R	569	T	27.8	I	485	CB	56.6	I	10.2	I
5H-2, 145-150	39.98	8.00	ISE	5.127	T	36.0	R	567	T	28.1	I	484	CB	56.3	I	10.1	I
5H-3, 145-150	41.48	8.00	ISE	5.116	T	35.5	R	566	T	28.3	I	482	CB	56.7	I	10.4	I
5H-4, 145-150	42.98	8.00	ISE	5.127	T	36.0	R	567	T	28.6	I	482	CB	57.2	I	10.6	I
5H-5, 145-150	44.48	8.29	ISE	5.199	T	36.0	R	568	T	28.5	I	485	CB	57.2	I	10.2	I
5H-6, 145-150	45.98	8.08	ISE	5.238	T	36.0	R	569	T	28.9	I	489	CB	55.7	I	10.2	I
6H-1, 145-150	47.98	8.29	ISE	5.138	T	35.5	R	567	T	28.1	I	483	CB	56.4	I	10.5	I
6H-2, 145-150	49.48	8.27	ISE	5.296	T	36.0	R	566	T	29.3	I	488	CB	55.0	I	10.1	I
6H-3, 145-150	50.98	8.26	ISE	5.264	T	36.0	R	567	T	29.0	I	484	CB	56.6	I	10.7	I
6H-4, 145-150	52.48	8.04	ISE	5.374	T	36.0	R	567	T	28.0	I	486	CB	56.1	I	9.9	I
6H-5, 145-150	53.98	7.98	ISE	5.235	T	36.0	R	567	T	27.8	I	483	CB	56.4	I	10.1	I
6H-6, 145-150	55.48	7.91	ISE	5.283	T	36.0	R	568	T	29.3	I	486	CB	57.0	I	10.0	I
7H-3, 145-150	60.48	8.06	ISE	5.142	T	35.5	R	570	T	28.7	I	487	CB	56.8	I	10.5	I
7H-4, 145-150	61.98	8.12	ISE	5.355	T	35.0	R	569	T	28.2	I	488	CB	56.3	I	9.3	I
7H-5, 145-150	63.48	8.06	ISE	5.333	T	36.0	R	569	T	28.2	I	487	CB	56.5	I	10.0	I
8H-4, 145-150	71.48	8.14	ISE	5.629	T	35.5	R	569	T	27.8	I	488	CB	55.9	I	9.2	I
9H-4, 145-150	80.98	8.08	ISE	5.858	T	35.5	R	569	T	27.7	I	488	CB	56.0	I	9.6	I
10H-4, 145-150	90.38	7.98	ISE	6.148	T	35.5	R	567	T	28.7	I	487	CB	56.9	I	9.3	I
11H-4, 140-150	99.95	8.16	ISE	6.019	T	35.5	R	566	T	27.1	I	481	CB	57.6	I	9.3	I
12H-4, 145-150	109.48	8.51	ISE	6.030	T	35.5	R	565	T	27.3	I	482	CB	57.2	I	8.8	I
13H-4, 145-150	118.98	8.20	ISE	6.215	T	36.0	R	565	T	27.2	I	483	CB	56.7	I	9.2	I
14H-4, 145-150	128.48	7.92	ISE	6.558	T	35.5	R	567	T	26.9	I	484	CB	56.3	I	9.2	I
15H-4, 145-150	137.98	7.93	ISE	6.765	T	35.5	R	565	T	27.0	I	486	CB	55.7	I	8.8	I
16H-4, 145-150	147.48	8.21	ISE	6.436	T	35.5	R	566	T	26.0	I	483	CB	56.4	I	8.8	I
17H-4, 145-150	156.98	7.92	ISE	6.558	T	35.5	R	566	T	26.4	I	485	CB	56.2	I	8.7	I
18H-4, 145-150	166.48	8.19	ISE	6.243	T	35.5	R	567	T	26.3	I	488	CB	55.1	I	8.4	I
19H-4, 145-150	175.98	7.82	ISE	6.880	T	35.5	R	567	T	26.9	I	482	CB	57.8	I	9.5	I
20H-4, 145-150	185.48	8.02	ISE	6.757	T	35.5	R	567	T	26.4	I	473	CB	60.1	I	11.1	I
22H-4, 145-150	204.48	7.82	ISE	6.462	T	35.5	R	568	T	25.1	I	468	CB	60.2	I	13.1	I
24H-4, 145-150	223.48	8.18	ISE	6.067	T	35.5	R	568	T	24.4	I	460	CB	60.3	I	15.9	I
26H-4, 145-150	240.48	8.02	ISE	5.692	T	35.5	R	570	T	24.3	I	443	CB	65.4	I	19.7	I
28X-3, 145-150	255.48	8.04	ISE	5.653	T	35.0	R	564	T	25.1	I	447	CB	64.3	I	17.6	I
177-1093D-																	
12H-2, 145-150	243.48	7.75	ISE	5.426	T	35.5	R	573	T	25.2	I	495	CB	49.1	I	12.5	I
13H-3, 145-150	254.48	7.66	ISE	5.511	T	35.5	R	573	T	24.9	I	490	CB	50.0	I	13.5	I
27X-3, 145-150	371.88	7.75	ISE	4.391	T	35.0	R	563	T	26.0	I	488	CB	43.1	I	18.1	I
28X-1, 135-140	378.38	7.68	ISE	4.616	T	35.5	R	566	T	26.7	I	486	CB	45.3	I	19.3	I
33X-4, 140-150	430.65	7.55	ISE	4.318	T	34.0	R	554	T	20.9	I	484	CB	33.7	I	20.3	I
34X-3, 145-150	438.78	7.49	ISE	4.045	T	34.0	R	552	T	20.8	I	485	CB	31.7	I	20.3	I
36X-4, 145-150	459.28	7.61	ISE	4.566	T	33.5	R	553	T	18.0	I	490	CB	25.9	I	21.6	I
38X-4, 140-150	478.45	7.53	ISE	3.957	T	33.5	R	553	T	17.9	I	491	CB	25.7	I	21.7	I
39X-3, 140-150	486.45	7.73	ISE	4.354	T	33.5	R	547	T	19.4	I	488	CB	27.6	I	20.3	I

Note: Method abbreviations: ISE = ion selective electrode, T = titration, R = refractometer, I = ion chromatography, CB = charge balance calculation, S = spectrophotometry, AAS = atomic absorption spectrometry, AES = atomic emission spectrometry.

Table T13 (continued).

Core, section, interval (cm)	Depth (mbsf)	K (mM)	Method	H_4SiO_4 (µM)	Method	NH_4 (µM)	Method	HPO_4 (µM)	Method	Sr (µM)	Method	Fe (µM)	Method	Mn (µM)	Method	Li (µM)	Method
177-1093A-																	
1H-1, 145-150	1.48	11.3	I	823	S	96	S	29	S		AAS	1.4	AAS	24.4	AAS	25.4	AES
1H-2, 145-150	2.98	11.3	I	934	S	159	S	34	S	91	AAS		AAS		AAS		AES
1H-3, 145-150	4.48	11.4	I	932	S	193	S	39	S		AAS		AAS	20.8	AAS	23.5	AES
1H-4, 145-150	5.98	11.3	I	901	S	234	S	43	S	88	AAS	0.0	AAS		AAS		AES
1H-5, 145-150	7.48	11.3	I	869	S	262	S	49	S		AAS		AAS		AAS	22.2	AES
2H-1, 145-150	9.98	11.5	I	825	S	311	S	54	S	90	AAS	0.1	AAS		AAS		AES
2H-2, 145-150	11.48	11.3	I	873	S	332	S	54	S		AAS		AAS	24.0	AAS	20.7	AES
2H-3, 145-150	12.98	11.4	I	798	S	337	S	60	S	90	AAS	0.8	AAS		AAS		AES
2H-4, 145-150	14.48	11.1	I	795	S	344	S	57	S		AAS		AAS	20.7	AAS	20.3	AES
2H-5, 145-150	15.98	10.2	I	854	S	352	S	53	S	89	AAS	0.6	AAS		AAS		AES
2H-6, 145-150	17.48	11.4	I	909	S	368	S	54	S		AAS		AAS	16.6	AAS	20.0	AES
3H-1, 145-150	19.48	10.8	I	848	S	379	S	42	S	91	AAS	0.0	AAS		AAS		AES
3H-2, 145-150	20.98	11.2	I	983	S	417	S	44	S		AAS		AAS	7.6	AAS	19.7	AES
3H-3, 145-150	22.48	10.9	I	812	S	420	S	43	S	92	AAS		AAS	6.8	AAS		AES
3H-4, 145-150	23.98	11.0	I	926	S	430	S	38	S		AAS	0.0	AAS		AAS	19.6	AES
3H-5, 145-150	25.48	10.8	I	873	S	429	S	39	S	91	AAS		AAS	6.8	AAS		AES
3H-6, 145-150	26.98	11.7	I	909	S	461	S	38	S		AAS	0.0	AAS		AAS	19.6	AES
4H-1, 145-150	28.98	11.0	I	859	S	446	S	32	S	89	AAS		AAS	5.3	AAS		AES
4H-2, 145-150	30.48	11.1	I	873	S	450	S	34	S		AAS	-0.1	AAS		AAS	19.3	AES
4H-3, 145-150	31.98	10.8	I	722	S	453	S	34	S	90	AAS		AAS	6.9	AAS		AES
4H-4, 145-150	33.48		I	798	S	477	S	34	S		AAS	0.2	AAS		AAS	18.7	AES
4H-5, 145-150	34.98	11.6	I		S	462	S	28	S	91	AAS		AAS	7.5	AAS		AES
4H-6, 145-150	36.48	11.3	I		S	466	S	27	S		AAS	0.2	AAS		AAS	19.9	AES
5H-1, 145-150	38.48	11.1	I	884	S	481	S	35	S	91	AAS		AAS	7.9	AAS		AES
5H-2, 145-150	39.98	11.5	I	882	S	493	S	34	S		AAS	1.0	AAS		AAS	19.2	AES
5H-3, 145-150	41.48	10.9	I	869	S	477	S	35	S	91	AAS		AAS	7.8	AAS		AES
5H-4, 145-150	42.98	11.3	I	930	S	506	S	36	S		AAS	2.6	AAS		AAS	19.5	AES
5H-5, 145-150	44.48	10.7	I	901	S	509	S	34	S	92	AAS		AAS	7.4	AAS		AES
5H-6, 145-150	45.98	11.0	I	1032	S	501	S	32	S		AAS	1.8	AAS		AAS	19.7	AES
6H-1, 145-150	47.98	11.1	I	952	S	478	S	29	S	90	AAS		AAS	7.2	AAS		AES
6H-2, 145-150	49.48	11.1	I	1138	S	513	S	35	S		AAS	5.7	AAS		AAS	20.2	AES
6H-3, 145-150	50.98	11.4	I	1116	S	514	S	30	S	91	AAS	0.8	AAS	6.8	AAS		AES
6H-4, 145-150	52.48	10.9	I	970	S	515	S	31	S		AAS	1.5	AAS		AAS	20.4	AES
6H-5, 145-150	53.98	11.3	I	954	S	530	S	31	S	92	AAS		AAS	6.0	AAS		AES
6H-6, 145-150	55.48	11.4	I		S	533	S	33	S		AAS	2.6	AAS		AAS	20.5	AES
7H-3, 145-150	60.48	11.2	I	985	S	541	S	31	S	92	AAS		AAS	4.8	AAS		AES
7H-4, 145-150	61.98	11.1	I	905	S	545	S	30	S		AAS	2.1	AAS		AAS	20.8	AES
7H-5, 145-150	63.48	11.1	I	933	S	566	S	29	S	91	AAS	1.5	AAS		AAS		AES
8H-4, 145-150	71.48	11.3	I	974	S	618	S	30	S	93	AAS		AAS	3.8	AAS	21.2	AES
9H-4, 145-150	80.98	11.2	I	1032	S	652	S	29	S	92	AAS	1.2	AAS	4.1	AAS		AES
10H-4, 145-150	90.38	10.9	I	905	S	713	S	28	S	91	AAS		AAS	3.8	AAS	21.9	AES
11H-4, 140-150	99.95	11.0	I	1000	S	724	S	26	S		AAS	1.5	AAS	3.1	AAS	22.2	AES
12H-4, 145-150	109.48	11.2	I	1026	S	783	S	28	S	94	AAS		AAS	2.8	AAS	22.7	AES
13H-4, 145-150	118.98	10.9	I	1017	S	813	S	23	S	93	AAS	1.4	AAS	4.0	AAS	22.7	AES
14H-4, 145-150	128.48	11.7	I	1209	S	840	S	28	S	94	AAS	1.4	AAS	3.5	AAS	23.1	AES
15H-4, 145-150	137.98	10.9	I	1129	S	889	S	28	S	92	AAS	3.1	AAS	3.4	AAS	23.6	AES
16H-4, 145-150	147.48	10.6	I	970	S	894	S	21	S	92	AAS	1.8	AAS	3.0	AAS	23.6	AES
17H-4, 145-150	156.98	10.5	I	1127	S	966	S	18	S	91	AAS	1.4	AAS	2.1	AAS	24.1	AES
18H-4, 145-150	166.48	10.6	I	1226	S	999	S	23	S	95	AAS	4.8	AAS	2.5	AAS	24.6	AES
19H-4, 145-150	175.98	10.5	I	1185	S	1010	S	23	S	94	AAS	2.6	AAS	1.6	AAS	25.6	AES
20H-4, 145-150	185.48	10.8	I	1148	S	1040	S	19	S	94	AAS	4.2	AAS	1.4	AAS	26.5	AES
22H-4, 145-150	204.48	10.3	I	1178	S	1101	S	16	S	101	AAS	2.2	AAS	1.4	AAS	29.4	AES
24H-4, 145-150	223.48	10.3	I	1325	S	1177	S	11	S	106	AAS	1.8	AAS	1.2	AAS	31.0	AES
26H-4, 145-150	240.48	10.7	I	1424	S	1101	S	11	S	112	AAS	5.2	AAS	1.1	AAS	31.8	AES
28X-3, 145-150	255.48	9.1	I	1420	S	1052	S	8	S	109	AAS	2.5	AAS	1.5	AAS	32.1	AES
177-1093D-																	
12H-2, 145-150	243.48	10.5	I	1373	S	1252	S	6	S	110	AAS	6.4	AAS	1.0	AAS	32.8	AES
13H-3, 145-150	254.48	10.8	I	1424	S	1311	S	5	S	111	AAS	3.2	AAS	1.3	AAS		AES
27X-3, 145-150	371.88	9.2	I	1528	S	1206	S	3	S	136	AAS	9.6	AAS	1.9	AAS	37.7	AES
28X-1, 135-140	378.38	8.8	I	1508	S	1206	S	3	S	145	AAS	9.1	AAS	2.6	AAS	40.0	AES
33X-4, 140-150	430.65	8.3	I	1842	S	1444	S	1	S	280	AAS	5.2	AAS	8.8	AAS	67.2	AES
34X-3, 145-150	438.78	7.9	I	1697	S	1375	S	1	S	306	AAS	12.1	AAS	10.0	AAS	72.6	AES
36X-4, 145-150	459.28	8.0	I	1973	S	1582	S	1	S	363	AAS	4.7	AAS	14.8	AAS	88.5	AES
38X-4, 140-150	478.45	6.5	I	1631	S	1467	S	1	S	391	AAS	11.3	AAS	17.4	AAS	93.6	AES
39X-3, 140-150	486.45	6.6	I	1435	S	1357	S	1	S	375	AAS	6.6	AAS	19.7	AAS	85.0	AES

Table T14. Analytical results of inorganic carbon, calculated calcium carbonate, total carbon, total organic carbon, total nitrogen, total sulfur, and TOC/TN at Site 1093. (Continued on next page.)

Core, section, interval (cm)	Depth (mbsf)	IC (wt%)	$CaCO_3$ (wt%)	TC (wt%)	TOC (wt%)	TN (wt%)	TS (wt%)	TOC/TN
177-1093A-								
1H-1, 116-117	1.16	2.68	22.4	3.90	1.21	0.08	0.20	15.2
1H-3, 68-69	3.68	1.86	15.5					
1H-5, 68-69	6.68	0.96	8.0					
2H-1, 68-69	9.18	0.00	0.0	0.71	0.71	0.12	0.40	6.1
2H-3, 68-69	12.18	0.00	0.0					
2H-5, 68-69	15.18	0.33	2.7					
3H-1, 69-70	18.70	1.49	12.4	1.94	0.45	0.04	0.22	11.3
3H-3, 69-70	21.70	0.97	8.1					
3H-5, 69-70	24.70	0.81	6.7					
4H-1, 68-69	28.18	1.71	14.2	2.20	0.49	0.05	0.74	9.8
4H-3, 68-69	31.18	0.18	1.5					
4H-5, 68-69	34.18	0.02	0.1					
5H-1, 68-69	37.68	0.04	0.3	0.46	0.42	0.06	0.33	7.0
5H-3, 68-69	40.68	0.04	0.3					
5H-5, 68-69	43.68	0.04	0.3					
6H-1, 67-68	47.18	0.06	0.5	0.82	0.76	0.07	0.34	10.8
6H-3, 66-67	50.16	0.18	1.5					
6H-5, 66-67	53.16	0.47	4.0					
7H-1, 89-90	56.90	0.38	3.2	0.79	0.41	0.06	0.37	6.8
7H-3, 89-90	59.76	0.03	0.3					
7H-5, 87-88	62.74	0.16	1.3					
8H-2, 33-34	67.34	6.05	50.4	6.97	0.92	0.05	0.16	18.5
8H-4, 64-65	70.64	0.11	0.9					
8H-5, 35-36	71.86	0.01	0.1					
9H-2, 90-91	77.40	0.04	0.4	0.76	0.72	0.07	0.34	10.3
9H-4, 91-92	80.42	0.19	1.6					
9H-6, 104-105	83.54	0.03	0.3					
10H-2, 29-30	86.20	0.05	0.4	0.49	0.44	0.07	1.04	6.3
10H-4, 39-40	89.30	0.02	0.2					
10H-6, 30-31	92.26	0.26	2.1					
11H-1, 69-70	94.70	1.15	9.5	1.98	0.84	0.07	0.29	11.9
11H-3, 69-70	97.70	0.03	0.2					
11H-5, 69-70	100.70	0.02	0.2					
12H-1, 69-70	104.20	0.02	0.1	0.44	0.43	0.08	0.34	5.4
12H-3, 69-70	107.20	0.02	0.2					
12H-5, 69-70	110.20	0.83	6.9					
12H-7, 38-39	112.88	6.29	52.4					
13H-1, 69-70	113.70	5.75	47.9	6.90	1.14	0.05	0.14	22.9
13H-3, 69-70	116.70	0.56	4.6					
13H-5, 69-70	119.70	0.51	4.3					
14H-1, 69-70	123.20	0.04	0.4	0.63	0.59	0.09	0.69	6.6
14H-3, 69-70	126.20	0.03	0.2					
14H-5, 69-70	129.20	0.19	1.6					
15H-2, 104-105	134.55	0.13	1.1	0.95	0.82	0.08	0.24	10.3
15H-4, 108-109	137.58	0.09	0.8					
15H-6, 107-108	140.58	0.10	0.8					
16H-1, 108-109	142.58	0.19	1.6	0.92	0.73	0.07	0.20	10.5
16H-3, 106-107	145.56	0.51	4.2					
16H-5, 107-108	148.58	0.22	1.8					
17H-1, 110-111	152.10	0.19	1.6	0.84	0.65	0.06	0.25	10.8
17H-3, 110-111	155.10	1.07	8.9					
17H-6, 110-111	159.60	1.12	9.3					
18H-1, 98-99	161.49	0.58	4.9	0.93	0.34	0.05	0.15	6.8
18H-3, 98-99	164.48	0.55	4.6					
18H-5, 98-99	167.48	2.62	21.9					
19H-1, 69-70	170.70	0.22	1.8	1.16	0.94	0.09	0.30	10.4
19H-3, 69-70	173.70	0.08	0.7					
19H-6, 69-70	178.20	0.29	2.4					
20H-1, 69-70	180.20	1.83	15.2	2.72	0.89	0.06	0.19	14.9
20H-3, 69-70	183.20	1.61	13.4					
20H-5, 69-70	186.20	0.08	0.7					
21H-1, 69-70	189.70	0.98	8.2	1.81	0.83	0.07	0.29	11.9
21H-3, 70-71	192.70	1.56	13.0					
21H-5, 69-70	195.70	0.02	0.2					

Table T14 (continued).

Core, section, interval (cm)	Depth (mbsf)	IC (wt%)	$CaCO_3$ (wt%)	TC (wt%)	TOC (wt%)	TN (wt%)	TS (wt%)	TOC/TN
23H-2, 70-71	210.20	0.03	0.3	1.12	1.09	0.11	0.63	9.9
23H-4, 59-60	213.10	0.04	0.3					
23H-6, 101-102	216.52	1.94	16.2					
24H-1, 71-72	218.22	0.93	7.8	1.75	0.82	0.05	0.00	16.4
24H-3, 35-36	220.86	0.62	5.1					
24H-6, 20-21	225.20	3.40	28.3					
25H-2, 70-71	228.12	1.75	14.6	2.69	0.94	0.06	0.14	15.6
25H-4, 64-65	231.06	0.39	3.2					
25H-6, 70-71	234.12	1.07	8.9					
26H-1, 70-71	235.20	1.80	15.0	2.53	0.73	0.06	0.16	12.2
26H-3, 70-71	238.20	3.46	28.8					
26H-6, 70-71	242.70	2.18	18.2					
28X-1, 69-71	251.70	0.15	1.2	1.20	1.04	0.10	0.59	10.0
28X-3, 69-71	254.70	1.78	14.8					
29X-1, 60-61	261.30	1.68	14.0	2.48	0.81	0.06	0.10	13.5
29X-3, 60-61	264.30	1.11	9.2					
30H-1, 81-82	271.22	2.97	24.7	3.78	0.81	0.06	0.12	13.5
30H-2, 81-82	272.52	1.57	13.1					
177-1093D-								
15H-1, 67-68	269.68	0.91	7.6	1.64	0.72	0.02	0.26	42.6
27X-1, 99-100	368.40	1.22	10.2	2.20	0.98	0.02	0.11	48.8
27X-3, 106-107	371.46	2.96	24.7					
28X-1, 98-99	377.98	0.39	3.2	1.20	0.82	0.04	0.56	20.4
30X-1, 89-90	396.80	0.47	4.0					
33X-1, 63-64	425.34	4.63	38.6	5.32	0.70	0.01	0.39	53.5
33X-3, 89-90	428.60	1.23	10.2					
33X-5, 69-70	431.40	3.46	28.8					
34X-2, 59-60	436.40	1.54	12.8	2.24	0.70	0.03	0.26	23.4
34X-4, 69-70	439.50	2.94	24.5					
35X-2, 127-128	446.68	0.90	7.5	1.90	1.00	0.03	0.25	33.2
35X-4, 35-36	448.76	2.43	20.2					
36X-2, 59-60	455.40	0.21	1.8	0.84	0.63	0.04	0.00	15.8
36X-4, 69-70	458.50	2.25	18.7					
36X-6, 50-51	461.30	5.21	43.4					
37X-2, 62-63	465.02	1.57	13.1	2.51	0.94	0.03	0.00	31.5
37X-5, 98-99	469.88	1.20	10.0					
38X-2, 68-69	474.68	0.00	0.0	0.73	0.73	0.04	0.38	18.3
38X-4, 98-99	477.98	0.79	6.6					
39X-1, 69-70	482.70	0.00	0.0	0.73	0.73	0.02	0.00	29.1
39X-3, 69-70	485.70	0.00	0.0					
39X-5, 69-70	488.70	0.59	4.9					
40X-1, 130-131	492.90	3.08	25.7	4.12	1.04	0.03	0.00	37.1
40X-2, 133-134	494.44	0.00	0.0					
40X-CC, 9-10	495.60	6.83	56.9					
41X-1, 49-50	501.80	0.88	7.3	1.70	0.82	0.03	0.00	27.3
44X-1, 90-91	531.10	0.13	1.1	0.92	0.79	0.03	0.00	30.3
45X-1, 73-74	540.64	0.00	0.0	0.84	0.84	0.04	0.24	21.0
45X-3, 73-74	543.64	2.78	23.2					
46X-2, 34-35	551.34	0.00	0.0	0.84	0.84	0.03	0.00	28.0

Note: IC = inorganic carbon, $CaCO_3$ = calcium carbonate, TC = total carbon, TOC = total organic carbon, TN = total nitrogen, TS = total sulfur.

Table T15. Summary of physical properties measurements conducted at Site 1093.

Measurement	Core 177-1093A-	Core 177-1093B-	Core 177-1093C-	Core 177-1093D-	Core 177-1093E-	Core 177-1093F-
GRA sample spacing	1H-30H: 2 cm	1H-24H: 2 cm	2H-1H: 4 cm	1H-47X: 2 cm	1H-2H: 2 cm	1H: 2 cm
MS sample spacing	1H-30H: 2 cm	1H-24H: 2 cm	2H-18H: 2 cm	1H-47X: 2 cm	1H-2H: 2 cm	1H: 2 cm
NGR sample spacing	1H-3H5: 2 cm, 3H6-25H, 28X-30H: 4 cm	2H-24H: 4 cm	2H-18H: 4 cm	1H-47X: 4 cm	1H-2H: 4 cm	1H: 4 cm
PWL sample spacing	1H-25H, 28X-30H: 2 cm	1H-24H: 2 cm	2H-18H: 2 cm	1H-47X: 2 cm	1H-2H: 2 cm	1H: 2 cm
OSU-SCAT sample spacing	1H-26H, 28X-30H: 4 cm	1H-24H: 4 cm	1H-12H, 14H-18H: 4 cm	1H-17H: 4 cm	1H-2H: 4 cm	1H: 4 cm
CM2002 sample spacing	—	—	—	—	1H-2H: 4 cm	1H: 4 cm
PWS3	*N* = 335	*N* = 169	*N* = 126	*N* = 120	—	—
MAD	*N* = 150	*N* = 5	*N* = 51	—	—	—
TC	*N* = 26	*N* = 20	*N* = 16	*N* = 17	—	—

Notes: GRA = gamma-ray attenuation, MS = magnetic susceptibility, NGR = natural gamma radiation, PWL = *P*-wave logger, OSU-SCAT = Oregon State University Split Core Analysis Track, PWS3 = *P*-wave velocity sensor 3 for split cores, MAD = moisture and density, TC = thermal conductivity.

Table T16. Thermal conductivity measurements at Site 1093. (See table note. Continued on next two pages.)

Core, section, interval (cm)	Depth (mbsf)	Depth (mcd)	TC (W/[m·K])	Start (s)	Length (s)	End (s)
177-1093A-						
1H-3, 75	3.75	3.75	0.647	112.0	27.5	139.5
1H-3, 75	3.75	3.75	0.632	106.5	36.0	142.5
2H-3, 75	12.25	12.43	0.658	78.0	25.0	103.0
4H-3, 75	31.25	35.23	0.648	114.0	25.0	139.0
4H-3, 75	31.25	35.23	0.646	115.5	26.0	141.5
6H-3, 75	50.25	55.59	0.714	43.5	29.5	73.0
6H-3, 75	50.25	55.59	0.708	36.0	25.0	61.0
7H-3, 60	59.47	65.83	0.675	68.0	28.0	96.0
7H-3, 60	59.47	65.83	0.679	47.5	25.0	72.5
8H-3, 75	69.25	76.78	0.652	124.0	25.5	149.5
8H-3, 75	69.25	76.78	0.697	45.5	25.0	70.5
9H-3, 75	78.75	86.42	0.651	77.5	25.0	102.5
9H-3, 75	78.75	86.42	0.626	107.5	26.5	134.0
11H-3, 75	97.75	108.10	0.672	64.0	25.0	89.0
11H-3, 75	97.75	108.10	0.657	96.0	25.0	121.0
10H-3, 75	88.15	97.28	0.662	75.0	25.0	100.0
10H-3, 75	88.15	97.28	0.659	63.5	25.0	88.5
12H-3, 75	107.25	118.88	0.675	41.5	25.0	66.5
12H-3, 75	107.25	118.88	0.665	48.5	25.0	73.5
13H-3, 75	116.75	128.42	0.628	109.0	25.0	134.0
13H-3, 75	116.75	128.42	0.628	112.5	25.0	137.5
13H-2, 75	115.25	126.92	0.678	117.0	25.0	142.0
13H-2, 75	115.25	126.92	0.698	90.5	25.0	115.5
14H-3, 75	126.25	138.86	0.775	118.0	25.0	143.0
14H-3, 75	126.25	138.86	0.774	43.0	25.0	68.0
15H-3, 75	135.75	148.28	0.684	118.0	25.0	143.0
15H-3, 75	135.75	148.28	0.712	42.0	25.0	67.0
16H-3, 75	145.25	158.62	0.638	74.5	25.0	99.5
16H-3, 75	145.25	158.62	0.630	111.0	25.0	136.0
17H-3, 75	154.75	167.86	0.632	101.0	26.0	127.0
18H-3, 75	164.25	178.54	0.619	72.5	25.0	97.5
18H-3, 75	164.25	178.54	0.615	117.5	25.0	142.5
19H-3, 75	173.75	190.84	0.709	92.5	31.0	123.5
19H-3, 75	173.75	190.84	0.726	49.5	25.0	74.5
20H-3, 75	183.25	202.30	0.698	101.5	28.5	130.0
20H-3, 75	183.25	202.30	0.675	109.5	31.0	140.5
21H-2, 75	191.25	210.78	0.682	99.0	25.0	124.0
21H-2, 75	191.25	210.78	0.680	99.0	32.5	131.5
22H-3, 75	202.25	221.68	0.639	102.5	25.0	127.5
22H-3, 75	202.25	221.68	0.635	111.0	25.0	136.0
23H-3, 75	211.75	231.98	0.696	56.5	27.0	83.5
24H-3, 75	221.25	244.34	0.777	67.0	25.0	92.0
24H-3, 75	221.25	244.34	0.766	69.0	25.0	94.0
25H-3, 75	229.66	254.60	0.746	83.0	25.0	108.0
25H-3, 75	229.66	254.60	0.753	28.0	25.0	53.0
26H-3, 75	238.25	262.57	0.732	41.5	25.0	66.5
26H-3, 75	238.25	262.57	0.715	68.5	25.5	94.0
29X-2, 75	262.95	287.84	0.739	55.5	26.0	81.5
177-1093B-						
11H-3, 75	96.35	115.06	0.625	93.0	27.5	120.5
12H-3, 75	105.85	125.40	0.709	100.0	27.5	127.5
14H-3, 75	124.85	144.50	0.710	27.0	25.0	52.0
15H-4, 50	135.60	156.49	0.650	45.0	26.0	71.0
16H-3, 75	143.85	164.18	0.640	104.0	25.0	129.0
17H-3, 75	153.35	174.68	0.593	44.5	26.5	71.0
18H-3, 75	162.85	187.54	0.729	115.5	26.5	142.0
18H-3, 75	162.85	187.54	0.744	63.0	28.5	91.5
19H-3, 75	172.35	197.02	0.626	116.0	25.0	141.0
19H-3, 75	172.35	197.02	0.614	96.0	25.0	121.0
20H-3, 90	182.00	206.75	0.686	87.5	38.0	125.5
20H-3, 90	182.00	206.75	0.689	93.5	25.0	118.5
21H-3, 75	191.35	219.20	0.716	120.0	25.0	145.0
21H-3, 75	191.35	219.20	0.712	91.5	26.5	118.0
22H-3, 75	200.85	227.82	0.681	67.5	25.0	92.5
24H-3, 75	219.85	251.36	0.726	36.5	25.0	61.5

Table T16 (continued).

Core, section, interval (cm)	Depth (mbsf)	Depth (mcd)	TC (W/[m·K])	Start (s)	Length (s)	End (s)
24H-3, 75	219.85	251.36	0.685	118.0	25.0	143.0
2H-3, 75	10.85	17.79	0.720	25.0	25.0	50.0
2H-3, 75	10.85	17.79	0.704	36.5	28.0	64.5
23H-3, 75	210.35	240.82	0.687	86.5	25.0	111.5
23H-3, 75	210.35	240.82	0.679	87.5	25.0	112.5
4H-3, 50	29.60	41.08	0.824	92.0	29.5	121.5
5H-3, 75	39.35	51.45	0.696	84.0	25.0	109.0
5H-3, 75	39.35	51.45	0.677	120.0	25.5	145.5
6H-3, 75	48.85	63.51	0.662	104.5	26.5	131.0
6H-3, 75	48.85	63.51	0.686	47.0	25.0	72.0
7H-3, 75	58.35	72.12	0.543	119.5	26.0	145.5
7H-3, 75	58.35	72.12	0.554	76.5	27.5	104.0
8H-3, 75	67.85	82.32	0.698	55.5	26.0	81.5
8H-3, 75	67.85	82.32	0.681	81.5	29.0	110.5
9H-3, 75	77.35	93.44	0.694	68.5	25.0	93.5
9H-3, 75	77.35	93.44	0.703	33.5	25.0	58.5
177-1093C-						
1H-3, 75	3.75	10.81	0.694	26.0	25.0	51.0
1H-3, 75	3.75	10.81	0.674	44.0	27.0	71.0
2H-3, 60	11.60	21.14	0.640	40.0	25.5	65.5
2H-3, 60	11.60	21.14	0.641	100.5	25.0	125.5
3H-3, 60	21.10	31.24	0.720	92.0	25.0	117.0
3H-3, 60	21.10	31.24	0.710	85.5	25.0	110.5
4H-3, 60	30.60	42.06	0.714	80.0	26.0	106.0
4H-3, 60	30.60	42.06	0.717	41.0	25.0	66.0
5H-3, 75	40.25	54.67	0.700	51.5	26.5	78.0
5H-3, 75	40.25	54.67	0.684	74.0	28.0	102.0
6H-3, 75	49.75	65.59	0.668	93.0	28.5	121.5
6H-3, 75	49.75	65.59	0.670	70.0	25.0	95.0
7H-3, 75	59.25	73.06	0.646	46.5	25.0	71.5
7H-3, 75	59.25	73.06	0.635	113.5	25.0	138.5
8H-3, 75	68.75	84.00	0.690	53.5	25.0	78.5
8H-3, 75	68.75	84.00	0.668	121.5	26.0	147.5
9H-3, 75	78.25	95.26	0.678	46.0	25.0	71.0
11H-5, 75	100.25	119.21	0.717	39.5	25.0	64.5
11H-5, 75	100.25	119.21	0.674	124.0	25.0	149.0
10H-3, 75	87.75	105.24	0.690	121.0	25.0	146.0
10H-3, 75	87.75	105.24	0.705	68.5	25.0	93.5
12H-3, 75	106.75	126.80	0.745	116.5	25.0	141.5
12H-3, 75	106.75	126.80	0.735	77.5	25.0	102.5
14H-3, 75	125.75	144.98	0.709	68.0	31.5	99.5
14H-3, 75	125.75	144.98	0.710	90.0	25.0	115.0
15H-3, 75	135.25	159.76	0.669	102.5	27.5	130.0
15H-3, 75	135.25	159.76	0.689	62.5	25.0	87.5
16H-2, 75	143.25	166.84	0.673	50.0	26.0	76.0
16H-2, 75	143.25	166.84	0.649	117.5	25.5	143.0
17H-3, 75	154.25	179.26	0.663	100.5	25.0	125.5
177-1093D-						
1H-3, 75	139.75	156.24	0.724	39.0	25.0	64.0
1H-3, 75	139.75	156.24	0.687	90.5	25.0	115.5
2H-1, 75	146.25	162.26	0.723	82.0	25.0	107.0
3H-3, 75	158.75	173.98	0.715	43.5	25.5	69.0
3H-3, 75	158.75	173.98	0.709	42.0	25.0	67.0
4H-3, 75	168.25	185.56	0.665	124.0	25.5	149.5
4H-3, 75	168.25	185.56	0.663	116.5	25.0	141.5
5H-3, 75	177.75	195.98	0.724	65.0	26.5	91.5
5H-3, 75	177.75	195.98	0.734	45.5	25.0	70.5
6H-3, 75	187.25	208.14	0.740	43.5	25.5	69.0
6H-3, 75	187.25	208.14	0.723	57.0	25.0	82.0
7H-1, 75	193.75	213.44	0.725	47.0	25.0	72.0
7H-1, 75	193.75	213.44	0.698	89.5	27.0	116.5
8H-3, 75	206.25	227.04	0.664	73.5	25.5	99.0
8H-3, 75	206.25	227.04	0.662	90.5	25.0	115.5
10H-2, 75	223.75	249.66	0.659	115.0	29.0	144.0
11H-3, 75	234.75	260.88	0.738	64.5	25.0	89.5
11H-3, 75	234.75	260.88	0.746	46.0	25.0	71.0
12H-3, 75	244.25	274.03	0.700	48.0	25.0	73.0
12H-3, 75	244.25	274.03	0.706	34.0	25.0	59.0
13H-3, 75	253.75	279.77	0.697	58.0	28.5	86.5

Table T16 (continued).

Core, section, interval (cm)	Depth (mbsf)	Depth (mcd)	TC (W/[m·K])	Start (s)	Length (s)	End (s)
13H-3, 75	253.75	279.77	0.708	36.0	25.0	61.0
27X-4, 75	372.65	403.14	0.787	34.5	25.0	59.5
27X-4, 75	372.65	403.14	0.750	95.5	25.0	120.5
30X-1, 75	396.65	427.14	0.648	122.0	25.0	147.0
30X-1, 75	396.65	427.14	0.646	109.0	32.0	141.0
33X-3, 75	428.45	458.94	0.763	42.5	25.0	67.5
33X-3, 75	428.45	458.94	0.754	46.5	30.0	76.5
34X-3, 75	438.05	468.54	0.753	112.5	27.5	140.0
34X-3, 75	438.05	468.54	0.769	72.0	25.0	97.0
35X-3, 90	447.80	478.29	0.712	93.5	28.0	121.5
35X-3, 90	447.80	478.29	0.708	101.0	30.5	131.5

Notes: TC = thermal conductivity. Start, Length, and End refer to the interval of the time-temperature series used for the determination of thermal conductivity. This table is also available in ASCII format in the **TABLES** directory.